1-1-2012

The Effect of Steel Fibers Type and Content on the Development of Fresh and Hardened Properties and Durability of Selfconsolidating Concrete

Nirmal Tamrakar
Ryerson University

THE EFFECT OF STEEL FIBERS TYPE AND CONTENT ON THE DEVELOPMENT OF FRESH AND HARDENED PROPERTIES AND DURABILITY OF SELF-CONSOLIDATING CONCRETE

By

NIRMAL TAMRAKAR, B.Eng.

Tribhuvan University, Kathmmandu, Nepal, 2001.

A thesis

presented to

Ryerson University

in partial fulfillment of the

requirements for the degree of

Master of Applied Science

in the program of

Civil Engineering

Toronto, Ontario, Canada, 2012

Author's Declaration

I hereby declare that I am the sole author of this thesis. This is a true copy of the thesis, including any required final revisions, as accepted by my examiners.

I authorize Ryerson University to lend this thesis or dissertation to other institutions or individuals for the purpose of scholarly research.

I further authorize Ryerson University to reproduce this thesis or dissertation or by photocopying or by other means, in total or in part, at the request of other institutions or individuals for the purpose of scholarly research.

I understand that my thesis may be made electronically available to the public.

Author's signature, _____ Date _____

ABSTRACT

THE EFFECT OF STEEL FIBERS TYPE AND CONTENT ON THE DEVELOPMENT OF FRESH AND HARDENED PROPERTIES AND DURABILITY OF SELF-CONSOLIDATING CONCRETE

Master of Applied Science 2012

By

Nirmal Tamrakar

Department of Civil Engineering, Ryerson University, Toronto, Canada

Steel fiber reinforced self-consolidated concrete (SFRSCC) has the advantages of both self-consolidated concrete and fiber reinforced concrete. Thirteen concrete mixtures (with short and long steel fiber) were prepared including control mix. The steel fiber volume fraction varied from 0 to 2.4% by the volume of concrete. The fresh properties of SCC were evaluated using slump flow test, J-ring test, V-funnel test and L-Box test. Bond strength, compressive strength and flexural tests were performed in order to investigate mechanical properties. Water sorptivity, water absorption and porosity, rapid chloride permeability test (RCPT), corrosion and freeze-thaw cycles tests were performed in order to investigate the durability properties. Bond strength gain of 244% with respect to control mix was observed. Moreover, the compressive strength and MOR gained 45% and 127%, respectively. There was no significant weight loss of the concrete specimen after freeze-thaw cycles for concrete mixture with steel fibers. However, flexural toughness was reduced after freeze-thaw cycles.

Acknowledgements

I would like to express my sincere gratitude to my supervisor Dr. Mohamed Lachemi for providing guidance and patience during the steps of this research. Many thanks to Dr. Mohamed Lachemi for accepting me as a M.A.sc student at Ryerson University and for providing moral and financial support during steps of this research. His invaluable time, creative thinking, encouragement and motivation helped to develop this thesis writing within time frame.

I would like to thank Dr. Aly Emam on his continuous moral support and guidance during thesis writing. His countless motivation and technical support during writing made this document possible.

Also, I would like to thank visiting scholars Dr. Erdogan Ozabay and Dr. Okan Karahan for supporting me during lab work. Their continuous support and help in lab give me opportunity to learn experimental program of this thesis.

I address my sincere thanks to Nidal Jaalouk, Mohamed Aldardari, Domenic Valle and all Ryerson's civil technicians for providing valuable information regarding equipment handling and safety requirement for lab work.

I address my special thanks to Nycon Company for providing steel fibers and also to Lafarge Inc. for providing cement and slag for my experiment.

Finally, special gratitude goes to my beloved wife, Shradha Kansakar. Without her constant love and sacrifice, my success would not be possible. I would also like to thank all my friends who had helped me throughout my thesis writing.

Dedications

To My Wife

And

To those who supported me towards success

Table of Contents

List of Figures

List of Tables

Chapter 1

Introduction

1.1 General

Self-consolidating concrete (SCC) is a concrete which has the ability to flow by its own weight and achieve good consolidation without external vibration. In addition, SCC has good resistance to segregation and bleeding because of its cohesive properties. SCC was developed in the mid-1980s in Japan. With the advent of SCC, the Japanese were able to produce durable concrete as well as provide proper filling of the concrete for highly congested steel bar reinforced concrete structures (Khayat, 1999; Okamura & Ouchi, 2003).

Self-consolidating concrete can be achieved by combining either a mineral admixture such as slag, fly ash (FA) or a viscous-modifying admixture (VMA) (Lachemi et al.,2005). The use of super plasticizer (SP) also helps in the flowability of SCC. In the last two decades, extensive research has been done on SCC, and it has gained popularity in various parts of the world including Canada (Lachemi et al., 2004). Because of its unique features, SCC has potential for future improvement of concrete structures as well as the development of material sciences and modified construction techniques.

Concrete is known to be brittle and can easily crack under low levels of tensile force. Therefore there are limitations on the use of conventional concrete within impact loading and earthquake prone zones. Fiber reinforced concrete (FRC), developed in the late 1960s, has been used in various construction applications in order to overcome the weakness of conventional concrete (Vondran, 1991). For the past three decades, however, different types of commercially available fibers such as steel fiber, glass fiber, polypropylene fiber,… etc. have been used. Incorporating these fibers into concrete improves the engineering properties of structural and non-structural concrete including fracture toughness, impact strength, durability and abrasion (Khayat & Roussel, 2000; Nawy, 2008). Steel fiber is one of the most popular fibers to be studied with

consideration of different aspects such as concrete grade, concrete type, curing time, steel fiber geometry, aspect ratio and volume fraction, etc. (Xu & Shi, 2009).

Merging steel fibers with SCC to produce steel fiber reinforced self-consolidating concrete (SFRSCC) is therefore highly desirable and carries a lot of potential for the concrete industry. In SFRCC, the uniform dispersion of steel fibers can be achieved through self compaction, which is beneficial over conventional steel fiber reinforced concrete (SFRC). The compactness of the SFRSCC matrix occurs due to the high content of fine materials, which improve the properties of the aggregate-matrix interface as well as the fiber-matrix bond and lead to enhanced post-cracking toughness and energy absorption capacity (Shah et al., 2010; Guetti et al., 2010).

In recent years, only a few researchers have investigated the integration of steel fiber with SCC, and very limited data is available concerning the testing, proportioning and performance of SFRSCC (Khayat & Roussel, 2000). Therefore, further research on FRSCC is strongly recommended in order to evaluate the restricted deformability of SFRSCC using the workability test methods used for regular SCC and the quality control procedure for proper dispersion of fibers (Shah et al., 2010).

1.2 Scope and objectives of research

The early deterioration and expensive maintenance costs of conventional concrete are major issues in the construction industry. The main scope of this research includes a comprehensive experimental investigation on the fresh properties of SFRSCC, and the mechanical and durability aspects of SFRSCC using various volume fractions of two different types of steel fibers (long steel fibers with hooked end and short steel fibers). In this research, a rapid chloride permeability test and corrosion test were performed to investigate the durability of SFRSCC in terms of chloride ion penetration. The freeze-thaw resistance test and the flexural test before and after freeze-thaw cycles were performed to evaluate the strength loss. Durability testing related to the sorptivity test and water absorption and porosity tests were also performed. Mechanical properties tests including compressive strength, bond strength (between steel reinforcing bar and concrete) and flexural strength were also conducted.

The use of SFRSCC not only increases the overall economic efficiency of the construction process by reducing the workforce required, but also minimizes future maintenance costs by

increasing the durability of concrete. The main focus of this research is to understand the synergy between self-consolidating and steel fiber-reinforced technologies incorporating two different types of steel fiber, as well as different percentages of fiber content. The objectives of this thesis are to:

- Develop SFRSCC using two different types of steel fiber and different fiber volume fractions by the volume of the concrete.
- Investigate the fresh properties of SFRSCC as well as hardened properties such as mechanical and durability.
- Examine the behavior of the two different types of steel fiber in different volume fractions in fresh and hardened properties of SFRSCC.
- Explore accelerated corrosion and freeze and thaw behavior of SFRSCC.
- Recommend a suitable SFRSCC for future development of the concrete industry.

1.3 Thesis outline

Chapter 2 provides a literature review of SCC, FRC and SFRSCC included materials, mix design methodology, application, and mechanical and durability properties.

Chapter 3 provides details of experimental programs regarding materials used and their properties. Mix design methodology of SFRSCC, the test methods applied to fresh properties and workability, and mechanical and durability properties are all presented.

Chapter 4 provides detailed discussion of the results related to the influence of steel fiber type and fiber volume fractions on the development of SCC. This chapter also provides in-depth analyses of fresh, mechanical and durability properties of SFRSCC.

Chapter 5 presents the summary and conclusion of the present study. It also outlines possible implementations and recommendations for further research on SFRSCC.

Chapter 2

Literature Review

2.1 Introduction

According to ASTM C125-11a: " Concrete is a composite material that consists essentially of binding medium within which are embedded particles or fragments of aggregate; in hydraulic-cement concrete, the binder is formed from a mixture of hydraulic cement and water." Concrete is undoubtedly a simple and fascinating building material; anyone can mix water, cement and aggregates, cast it in moulds of almost any shape and finally obtain an artificial stone with some strength (Schutter et al., 2008). Because of its complex nature, care should be taken for both fresh and hardened properties. The structural behaviour and durability of hardened concrete depend on the workability and compactness of fresh concrete. Traditionally, an internal vibrator is used to consolidate concrete to the desired compactness. However, the growing use of heavy reinforcement in structural elements, especially in seismic zones, has created the need for flowable concrete to ensure proper filling in congested reinforcement areas. Also, excessive vibration can cause undesirable segregation and bleeding of the concrete.

Self-consolidating concrete (SCC), also called self-compacting concrete (SCC), is a highly flowable high-performance concrete (HPC) with the capability of self-consolidation under its own weight without internal or external vibration and without exhibiting defects due to segregation and bleeding (Dhonde et al., 2007; Lachemi et al., 2005; Lachemi et al., 2004). The advent of SCC in the construction industry has achieved economic benefits by reducing the workforce and providing proper compaction of the concrete in congested reinforcing areas. In addition, because of its flowability, SCC can be cast in a non-congested structural area in less time, which reduces the overall construction cost. Hence, the development of SCC technology has a positive impact within the construction industries.

Concrete is weak in tension and is significantly brittle when compared to other building materials such as steel and polymer. Concrete cracks easily and loses durability because it is prone to deteriorating agents such as sulfate attack, steel corrosion, discoloration, and freeze and thaw damage (Banthia, 1994). Therefore, the inclusion of fibers in concrete is a good option to

improve tensile strength as well as durability. The concept of fiber reinforcement has been used since an ancient times. Since 1900, asbestos-cement was successfully used as FRC (Johnston, 2001). However, the use of asbestos fiber has been banned since 1970 because of its health hazards. Since then, effort had been put into a search for alternative fibers such as steel, polyproylene, polyester, carbon, nylon bundles, alkali-resistant (AR) glass strands, fibrillated polypropylene tapes, etc. (Johnston, 2001). The nature of the fiber matrix with fresh concrete depends on the type and form of fiber and the proportion of fiber used. Hence, FRC is defined as concrete containing hydraulic cement, aggregate, water and a uniform dispersion of fibers. It may also contain other fine mineral admixtures such as silica fume, slag and fly ash as well as other chemical admixtures. Steel fiber is one of the most popular and widely used fibers. The integration of steel fibers into conventional concrete improves the performance of structural and non-structural concrete for better crack resistance, ductility and toughness, as well as greater tensile strength, fatigue resistance, impact, blast loading and abrasion (Khayat & Roussel, 2000).

The incorporation of steel fibers in SCC has a tremendous potential for high-performance concrete. SFRSCC exhibits both SCC and FRC qualities that will be beneficial to the congested reinforcement areas in seismic-prone zones. The practicality of SFRSCC has been investigated in recent research, however limited data are available concerning the testing, proportioning and performance of such concrete (Khayat and Roussel, 2000; Dhonde et al., 2007; Yildirim et al., 2010). The literature review in this chapter focuses on the current state of the SCC technologies and SFRSCC by summarizing the fresh, mechanical and durability properties.

2.2 Self-consolidated concrete (SCC)

2.2.1. Definition of SCC

According to ACI 237R-27, “SCC is highly flowable, non-segregating concrete that can spread into space, fill the formwork, and enscapsulate the reinforcement without any mechanical consolidation.” Therefore, it provides three fundamental fresh properties of concrete: filling ability, passing ability and segregation resistance (Khayat, 1999; Liu, 2010). Generally, SCC is made from conventional concrete materials with a higher percentage of fine mineral admixture including cement such as slag, silica fume and fly ash, and in some cases viscosity-modifying

admixture (VMA). The fine mineral admixture as well as VMA increase the viscosity of the SCC. The amount of coarse aggregate is much lower than in conventional concrete.

2.2.2. Brief History of SCC

The durability of concrete was a major concern during the post war era in Japan. The concept of SCC was first proposed by Hajime Okamura, University of Tokyo, in 1986 as a major solution to concrete deterioration (Ashtiani et al., 2011). The project team, led by H. Okamura and including K. Maekawa, K. Ozawa and M. Ouchi, soon indicated that inadequate compaction was the most common cause of concrete deterioration (Schutter et al., 2008). Modern SCC was first developed around the late 1980s. The first few publications on modern SCC were thought to be from University of Tokyo by Ozawa et. al in 1992 (Goodier, 2003). However, the term used for SCC was "high-performance concrete with special properties."

After the development of first prototype SCC, extensive research was done in different parts of Japan, especially within the research institutes of the large construction companies (Goodier, 2003). With the advent of VMA and superplasticizer, further development of SCC was posssible. SCC was introduced to Europe and North America in the second half of the 1990s, when Germany and the United States showed considerable interest in the "washout-resistance" of fresh SCC for underwater construction (Mehta & Monteiro, 2006).

2.2.3 Characteristics of SCC

Basically, SCC is different from traditional conventional concrete in terms of workability of the fresh concrete and the durability of the hardened concrete, both of which are driven by different material components and mix proportions. Generally, in SCC, the proportion of coarse aggregate is much lower than in traditional conventional concrete. On the other hand, it contains a high amount of fine material such as slag, silica fume, fly ash and/or additives to increase viscosity (Vejmelkova et al., 2011). In addition, the water-binder ratio is also much lower. Lower water content in SCC can be obtained either by using a fine mineral admixture or by incorporating VMA (Lachemi et al., 2005). Therefore, SCC is defined as a fresh concrete having better flowability and stability. It has the following characteristics: (Ashtiani et al., 2011).

- Flowing ability: filling all areas and reaching nooks and corners into which it is placed.

- Passingy ability: passing through a congested reinforcing area.
- Resistance to segregation: uniform distribution of coarse components of the mix.

2.2.4.Advantages and Applications of SCC

SCC exhibits many advantages over traditional conventional concrete. Some of these are as follows: (Okamura and Ouchi, 2003; Khatib, 2008; Boukendakdji et al., 2009)

- The working environment is significantly improved without vibration-related damage and with significant noise reduction during casting.
- Allows the pumping of concrete to a great height and flow through the congested reinforcing steel bars.
- Reduced work force for transportation and placement of concrete.
- Reuse of the form work for longer periods of time.
- In the hardened state it shows a lower permeability and absorption by capillary action, which contribute to the improved durability of concrete.

The use of SCC in actual structures gradually increased after the development of the prototype SCC in 1988. Currently, the volume of precast SCC factory products is increasing in comparison to the on-site placement of SCC. According to the report prepared by Nagataki et al. 2010 for the 6th International RILEM Symposium on Self-Compacting Concrete, "The share of SCC placed in situ is approximately 0.1%-0.2% of total produced amount of ready-mixed concrete in Japan and that of factory product is about 2-3%." The volume of the SCC application in Japan since 1992 is shown in Figure 2.1 (Nagataki et al., 2010).

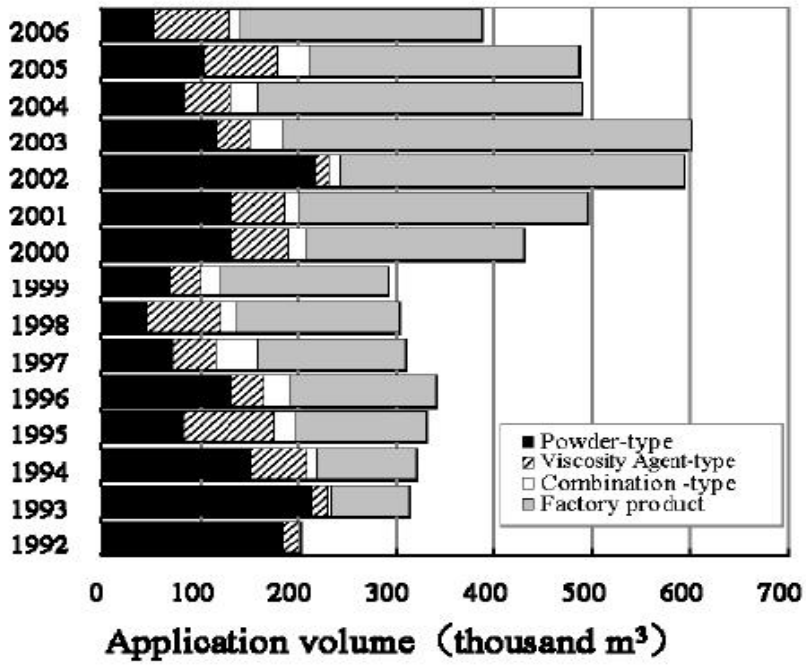

Figure 2.1: Volume of SCC application in Japan

Here are two examples of practical applications of the SCC in large scale projects.

- Akashi-Kaikyo Ohashi Bridge, Japan: SCC was used in the construction of two massive anchorages of the Akashi-Kaiko Bridge, a suspension bridge with the longest span in the world (1,991 meters) (Okamura & Ouchi, 2003), opened in April 1998. A total volume of 290,000m^3 of SCC was cast in the two anchorages (1A and 4A) as shown in Figures 2.2 and 2.3 (Nagataki et al., 2010). The cable anchor frame and reinforcing steel members in the two anchorages (1A and 4A) were heavily reinforced. For proper compaction, vibration of the fresh normal concrete was impossible. Hence, three types of SCC, depending on the percentage of viscosity modifying agent (VMA) and superplasticizer, were adopted. In one day, a total volume of 1900m^3 was poured (Nagataki et al., 2010). Anchorage 4A is shown in Figure 2.2 (Okamura & Ouchi, 2003).

Figure 2.2: Anchorage of Akashi-Kaikyo Ohashi Bridge

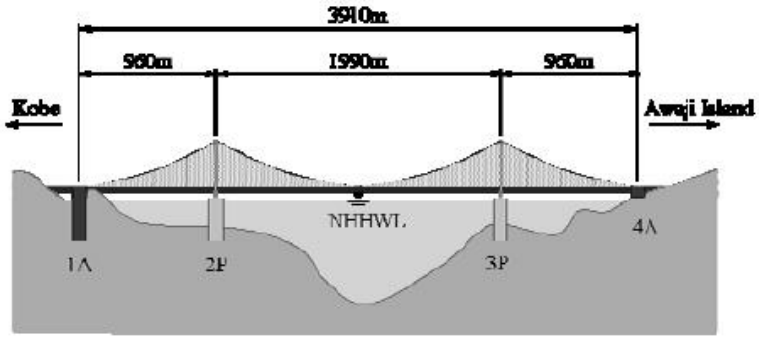

Figure 2.3: Outline of Akashi-Kaikyo Ohashi Bridge

- Tunnel Anchorage at Kurushima Ohashi Bridge: SCC was successfully implemented in a tunnel anchorage of the Kurushima Ohashi Bridge (cross-sectional area 80m^2), which was installed into the earth at a 40-degree inclination, as shown in Figure 2.4**: Placement of SCC at tunnel anchorage**Anchor frames and reinforced steel members were installed in a complicated manner, which caused difficulty in compaction. A total volume of SCC concrete of around 13000m^3 was used for two tunnels (Nagataki et al., 2010).

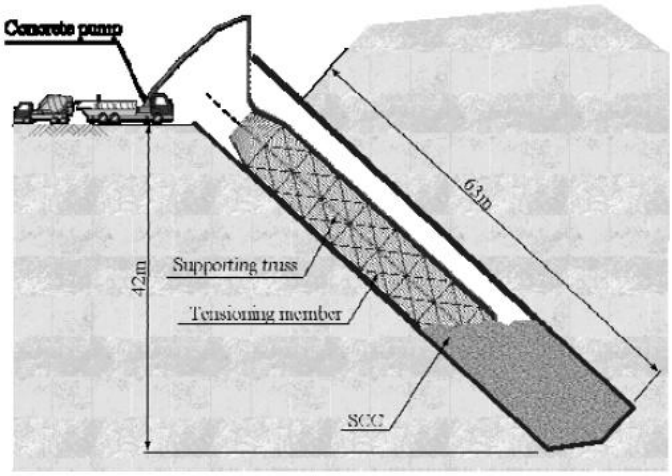

Figure 2.4: Placement of SCC at tunnel anchorage

2.3 Mix Design Methodology of SCC

Since the advent of SCC in the early 1990s, various researchers (Okamura and Ouchi, 2003; Lachemi et al., 2005; Felekoglu et al., 2007; Khatib, 2008; Ozbay et al., 2009; Boukendakdji et al., 2009; Liu, 2010; Ashtiani et al., 2011; Vejmelkova et al., 2011) have worked on different methodologies of mix design. For concrete to behave as SCC, it has to fulfill three basic characteristics: passing ability, filling ability and resistance to segregation (Billberg, 2010). Over the last two decades, a wide variety of materials and mixture design parameters have been proposed based on production processes and application requirements. SCC can be achieved by increasing the sufficient amount of fine materials or mineral admixtures such as silica fume, fly ash, ground granulated blast furnace slag (GGBFS), powder limestones, and volcanic ash, without changing water cement ratio to that of conventional concrete (Lachemi M. et al., 2003; European SCC Guidelines, 2005). The use of mineral admixtures improved the homogenity of the concrete, offered excellent surface quality, lowered the cost of the mix by replacing costly cement, lowered the heat of hydration, and resulted in higher sulphate and acid resistance, better workability, lower permeability and higher corrosion resistance (Khatib, 2008; Boukendakdji et al., 2009; Ashtiani et al., 2011). Below are the properties of some of the mineral admixtures:

GGBFS is a mineral addition that has a similar chemical composition to cement and helps to increase the fluidity of concrete (Boukendakdji et al., 2009). GGBFS is finer than portland cement, which in turn provides more surface area than cement and therefore reduces the bleeding

of concrete (Nawy, 2008). In addition, GGBFS has other advantages such as lower heat of hydration, resistance to sulphate and acid reaction, better workability, lower permeability and higher corrosion resistance (Boukendakdji et al., 2009). However, slower setting of concrete incorporating GGBFS can also increase the risk of segregation (European SCC Guidelines, 2005). Fly ash is pozzolanic in nature and cementitious even in the absence of cement. It increases the workability of SCC and contributes to its long-term strength (Khatib, 2008). Also, the use of fly ash as an addition in SCC increases cohesion and reduces the sensitivity to change in water content. Therefore, a high level of fly ash may produce a paste fraction which is so cohesive that it can resist the flow and hinder the filling ability (European SCC Guidelines, 2005). Silica fume is also pozzolanic in nature and is finer with more surface area than cement. It is spherical in shape and results in good cohesion with improved resistance to segregation when used in SCC (European SCC Guidelines, 2005). Also, silica fume is very effective in reducing bleeding and shrinkage cracking, especially in curing conditions of elevated temperature, low humidity and high winds, all of which allow rapid evaporation of water from the fresh placed concrete (Nawy, 2008).

Simple mixture proportions were proposed by Okamura and Ozawa (1999). In this method, coarse to fine aggregate ratios are kept constant and SCC can be achieved by adjusting water/cement ratio and super plasticizerdosage only (Felekoglu et al., 2007). However, using super plasticizeralone not only increases the fluidity of SCC but also increases segregation and bleeding. Therefore, in order to avoid segregation, SCC utilizes a lower aggregate content, lower water/cement ratio and the use of super plasticizer(Okamura & Ouchi, 2003). At the same time, mineral admixtures such as slag, fly ash and silica fume can be used to avoid bleeding and segregation. Okamura and Ouchi (2003) employed the method shown in Figure 2.5 in order to achieve SCC.

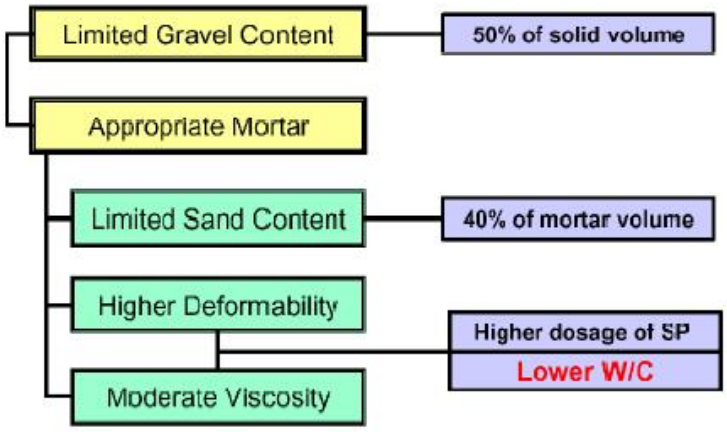

Figure 2.5: Method of achieving SCC

Previous studies have shown that the use of blast furnace slag and fly ash are effective in reducing the dosage of super plasticizer needed to obtain similar slump flow to concrete made with portland cement only (Bouzoubaa & Lachemi, 2001).

One alternative approach to producing SCC is incorporating a VMA (Lachemi et al., 2004). The use of VMA along with the appropriate proportion of super plasticizercan ensure high deformability and adequate workability, leading to good segregation resistance (Lachemi et al., 2004). In addition, an appropriate proportion of mineral admixture can also be used in order to minimize bleeding and segregation due to the presence of superplasticizer. In addition to that, SCC performance is highly affected by ingredient characteristics such as size, shape, surface area and grain size distribution of the aggregate (Saak et al., 2002). Therefore, SCC can be classified into three types: powder type, viscosity agent type and combination type (EFNARC, 2006).

- In powder type, SCC is recognized by a high proportion of fine materials such as slag, fly ash, silica fume, etc., usually in the range of 550 to 650 kg/m^3. These fine materials produce the necessary mortar volume to increase plastic viscosity and hence the segregation resistance of the mix. The other rheological property (yield stress) is controlled by the addition of SP.
- In viscosity agent type SCC, fine material content is lower (350 to 450 kg/m^3). The viscosity required to restrain segregation is mainly controlled by a VMA and yield stress by the addition of superplasticizer.

- In combination type SCC, the fine materials content varies from 450 to 550 kg/m^3, and includes small amounts of VMA as well as an appropirate dosage of superplasticizer in order to control rhelogical property. The purpose of adding VMA is to limit the addition of fine materials, thus making the fresh concrete more cohesive.

No standard method for SCC concrete mixture design has been universally approved, and different procedures to achieve SCC depend on the workability parameters as well as on the availability of material type and admixture. In addition, no single method has been found which characterizes all the significant workability aspects. Therefore each mixture design should be tested according to workability parameters (Felekoglu et al., 2007). According to the report prepared by Domone (2006), 68 case studies of an application of SCC have been analyzed (from 1993 to 2003 in different countries). Of those cases, about 70% used maximum aggregate size in the range of 16-20mm. A limestone powder was the mineral admixture used most often, at almost 41% overall (Domone, 2006). Approximately half the cases used a VMA including super plasticizerand could therefore be considered a combined type SCC (Domone, 2006). Median values of the key mix proportions were: (Domone, 2006)

- Coarse aggregate content: 31.2% by volume
- Paste content: 34.8% by volume
- Powder content: 500 kg/m^3
- Water/powder ratio: 0.34 by weight
- Fine aggregate/mortar ratio: 47.5% by volume

Almost 90% of the cases used slump flow in the range of 600-750mm, with 80% of the mixtures having strength in excess of 40MPa (Domone, 2006). These case studies done by Domone (2006) also showed that SCC is a wide family of concrete mixtures, and there is no unique mixture for a given application or a set of requirements (Domone, 2006). Table 2.1 gives an indication of the typical range of constituents in SCC by weight and volume (European SCC Guidelines, 2005)

Table 2.1: Typical range of SCC mix composition (European SCC Guidelines, 2005).

Constituent	Typical range by mass (kg/m^3)	Typical range by volume ($litres/m^3$)
Powder	380 - 600	
Paste		300 - 380
Water	150 - 210	150 - 210
Coarse aggregate	750 - 1000	270 - 360
Fine aggregate (sand)	Content balances the volume of the other constituents, typically 48 – 55% of total aggregate weight.	
Water/Powder ratio by Vol		0.85 – 1.10

2.3.1 Fresh Properties of SCC

The fresh properties of SCC are characterized by uniform flow without segregation between ingredients or bleeding resistance. Achieving SCC involves not only the deformability and stability of paste and mortar, but also resistance to segregation between coarse aggregate and mortar when flowing through the congested reinforcing area (Okamura & Ouchi, 2003). Hence, there are three key properties of fresh SCC:

- Filling ability
- Passing ability
- Segregation resistance or stability

2.3.1.1 Filling ability

Filling ability or flowability is the ability of the fresh mixture to flow under its own weight in any direction and completely fill all the spaces in the formwork without external vibration. Therefore filling ability reflects the deformability of SCC, which can change shape under its own weight (Khayat, 1999). There are two aspects of deformability: one is deformation capacity, which is the maximum ability to deform (that is, how far concrete can flow), and another is deformation velocity, which refers to the time it takes for concrete to finish flowing (RILEM Technical Committe 174-SCC, 2000). In 1940, Kennedy proposed “Excess paste theory,” which is crucial to understanding workability of fresh concrete (Oh, Noguchi, & Tomosawa, 1999). Excess paste theory explains that there must be enough paste to cover the surface area of the aggregate in order to achieve the workability of concrete and reduce friction between aggregates (Figure 2.6).

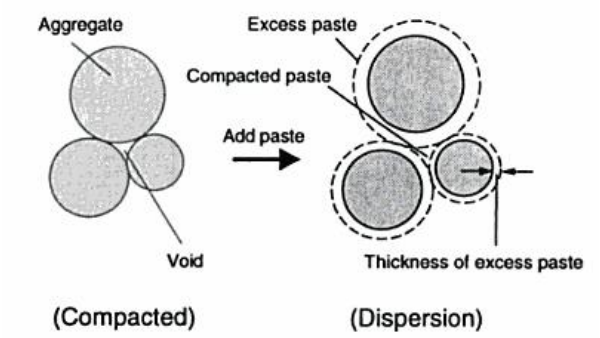

Figure 2.6: Excess paste theory (Oh et al., 1999)

Khayat (1999) also mentioned that the inter-particle friction between coarse aggregate, sand and powder material increases internal resistance to flow. Moreover, the speed probability of such friction is high even when concrete flows through the restricted area, because of the greater chance of collision between the coarse aggregates. Thus, the deformability of SCC can be increased by increasing water binder ratio (W/B), adding the appropriate dosage of super plasticizerand by increasing the fine mineral admixture (Khayat, 1999). However, increasing W/B may affect the durability and mechanical properties of concrete in the long run due to reduction in strength and excessive porosity. In addition, it also creates segregation problems and reduces cohesiveness.

Therefore, in order to achieve an adequate filling ability, the following actions should be considered: (RILEM Technical Committee 174-SCC, 2000)

(i) Increase the deformability of the paste through:

- Use of superplasticizing admixture
- Balanced W/B ratio

(ii) Reduce inter-particle friction by using:

- Low coarse aggregate volume (high paste content)
- Optimum graded powder relative to aggregates and cement used

2.3.1.2 Passing ability

Passing ability is the ability of a fresh mix to flow through confined and tight spaces as well as through the opening between reinforcing bars; it is governed by the size and amount of coarse

aggregate. The L-Box test is a common method used to determine the passing ability of fresh concrete mixtures. Blocking results when the frequency of collision and contact between aggregates increases as relative distance between the aggregates increases (Okamura & Ouchi, 2003; Khayat, 1999). Internal stress also increases when the concrete mixture flows through the narrow opening. When the concrete mixtures approach a narrow space, the aggregates close to the narrow opening tend to slow down, and a difference in the flow velocity of the mortar paste and aggregates is created (Oh, Noguchi, & Tomosawa, 1999; Okamura & Ouchi, 2003). This leads to the formation of an aggregate bridge or arch at the narrow opening, which blocks the rest of the concrete, as shown in Figure 2.7 (RILEM Technical Committe 174-SCC, 2000).

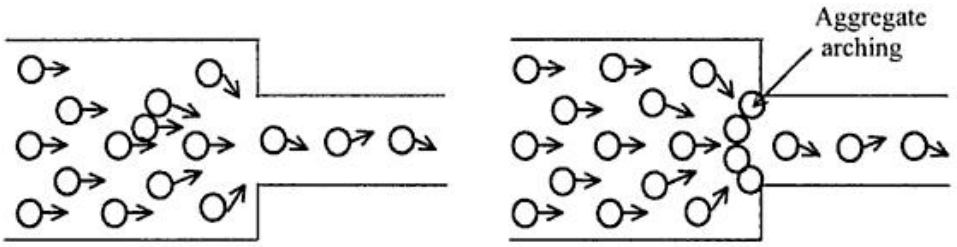

Figure 2.7: Mechanism of blocking of the concrete mixtures approaching a narrrow space

Therefore, inter-particle interaction can be reduced by reducing coarse aggregate content. Research has shown that the energy required to flow a concrete mixture is often consumed by internal stresses between the coarse aggregates. According to Okamura, the blocking of the aggregate particles can be reduced by limiting coarse aggregate content (Okamura & Ouchi, 2003).

Therefore, in order to achieve adequate passing ability, the following action should be considered: (RILEM Technical Committe 174-SCC, 2000)

(i) Enhance cohesiveness to reduce aggregate segregation by using:

- Low water-to-powder ratio
- Viscosity agent

(ii) Ensure compatible clear spacing and coarse aggregate characteristics by using:

- Low coarse aggregate volume
- Low maximum size of aggregate

2.3.1.3 Segregation resistance or stability

Segregation resistance is also called stability, which is the ability of the fresh concrete mixture to maintain uniform distribution of mortar paste and aggregates during the construction process (mixing, transportation, placing and compaction) (Schutter et al., 2008). Two different kinds of segregation occur in a fresh mixture: the bleeding of water from the concrete mixture after placing in the form work, and segregation between the mortar paste and aggregate due to lower cohesiveness.

Bleeding is a special form of segregation in which water moves upward from the horizontal surface of the cast element, where a thin layer of paste with a very high water cement ratio is formed (Schutter et.al 2008). Some bleeding is normal for concrete, but excessive bleeding leads to reduced strength and durability as well as excessive porosity. Bleeding usually happens after placement of the concrete mixture, therefore it is also referred to as a static segregation.

Segregation between the mortar paste and aggregate is due to excess movable water in the mixture. The stability or segregation resistance largely depends on the cohesiveness and viscosity of the fresh concrete mixture during the construction process, which can be obtained by reducing the excess movable water and increasing the mineral admixture. Incorporating a lower water-to-powder ratio and increasing the fine materials improves the stability of the fresh concrete mixture and decreases inter-particle friction among the solid particles around the narrow opening (Khayat et al., 1999).

Therefore, in order to achieve adequate stability, the following actions should be considered: (RILEM Technical Committe 174-SCC, 2000).

(i) Reduce separation of solids by using:

- Limited aggregate content
- Reduced maximum size of aggregate
- Low water-to-powder ratio
- Viscosity modifying agent (VMA)

(ii) Minimise bleeding (free water) through:

- Low water content
- Low water-to-powder ratio
- Powders with high surface area
- Incorporating VMA

2.3.2 Test Procedure for Fresh Properties of SCC

There are several tests available to define the fresh properties of SCC, which have been primarily developed by EFNARC (European Guidelines of Self-compacting Concrete), ASTM (American Standard for Testing Material), PCI (Precast/ Prestressed Concrete Institute) and JSCE (Japenese Society of Civil Engineering). Considerable progress has been achieved in the last two decades, but the lack of a standardised and universally established testing method is an obstacle to the wider use of SCC in Europe and other countries (Schutter et al., 2008). Therefore, it is important that standardised testing be implemented to identify the fresh properties of SCC. Based on EFNARC, some of the important tests are discussed briefly as follows:

Slump flow: The slump flow value describes the flowability and deformability of the fresh mixture of SCC in the absence of obstruction (unconfined condition) (European SCC Guidelines, 2005). Most of the fresh properties of SCC can be determined from the slump flow test. It is one of the most popular tests because of its simplicity, low cost and availability. The familarity of the basic equipment is also a factor, such as the use of Abram's cone in slump testing of conventional concrete. Slump flow test results show the average diameter of SCC measured in two perpendicular directions, and the recorded time when the flow of fresh concrete stops. The typical range of slump flow values is 600-800mm (Schutter et.al 2008). According to Domone (2006), out of 68 case studies of an application of SCC, almost 50% of the applications show slump flow values in the range of 650-700mm, and nearly 90% in the range of 600-750mm, as shown in Figure 2.8. Usually a slump flow value of less than 600mm is practically unsuitable for SCC applications (Schutter et al., 2008). The time required to reach a diameter of 500mm is measured as T50 or T500. A visual observation and T50 data can give additional information about the segregation resistance and uniformity of the fresh mix of SCC (European SCC Guidelines, 2005).

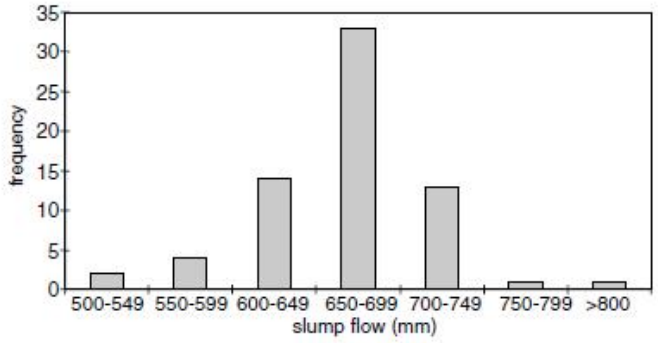

Figure 2.8: Slump flows values and frequencies

The classes of filling ability based on slump flow value as given by European SCC Guidelines (2005) are presented in Table 2.2.

Table 2.2: Classes of filling ability by slump flow diameter of SCC

SF1 (550-650mm) is suitable for: Low filling ability • Unreinforced or slightly reinforced concrete structures that are cast from the top with free displacement from the delivery point (e.g. housing slabs). • Casting by a pump injection system (e.g. tunnel linings). • Sections that are small enough to prevent long horizontal flow (e.g. piles and some deep foundations).
SF2 (660 – 750mm) is suitable for many normal applications (e.g. walls, columns). SF2 has good filling ability.
SF3 (760 – 850mm) is typically produced with a small maximum size of aggregates (less than 16mm) and is used for vertical applications in very congested structures, structures with complex shapes, or for filling under formwork. SF3 will often give better surface finish than SF2 for normal vertical applications, but segregation resistance is more difficult to control. SF3 has high filling ability.

V-funnel: A V-funnel test was first introduced in Japan and used by Ozawa (Ozawa et.al., 1995). It is used to measure the deformability or flowability of fresh SCC by determining the V-funnel time (TVF). In this test, a V-shaped funnel is filled completely with fresh SCC using manual consolidation, and the bottom outlet is open for concrete to flow using gravity. The time required for the gravitational flow of concrete is observed until all the fresh concrete has passed from the small opening at the bottom of the V-funnel. Basically, TVF measures the deformability and flow-rate of a fresh mix of SCC (Schutter et al., 2008). The flow time is directly proportional to the plastic viscosity of the fresh mix. A higher value of TVF indicates a partial blocking of the concrete at the bottom of the opening due to a higher concentration of coarse aggregate.

Therefore, the flow time value is also used as an observation of the static segregation of the mix. According to Domone (2006), the average flow time TVF for V-funnel is from 3 to 15 seconds. The typical value range of flow time TVF is 5 to12 seconds (Schutter et al., 2008).

The flow time value TVF of the V-funnel test and/or T50 of slump flow time are incorporated in viscosity classes in the European guidelines (European SCC Guidelines, 2005) (Table 2.3).

Table 2.3: Classes of filling ability based on V-funnel flow time TVF and/or slump flow time T50

Class	T50, sec	V-Funnel time in Sec (TVF)
VS1/VF1	≤ 2	≤ 8
VS2/VF2	>2	9 to 25
VS1/VF1 has good filling ability even with congested reinforcement. It is capable of self-levelling and generally has the best surface finish. However, it is more likely to suffer from bleeding and segregation.		
VS2/VF2 has no upper class limit but with increased flow time it is more likely to exhibit thixotropic effects, which may be helpful in limiting the formwork pressure or improving segregation resistance. Negative effects may be experienced regarding surface finish (blow holes) and sensitivity to stoppages or delays between successive lifts.		

J-ring: The exact origin of the J-ring principal is still unknown, but the practical form of the test was developed by Bartos et al. at the ACM center at the University of Paisley (Scotland) (RILEM Technical Committee TC 145-WSM, 2002). The equipment consists of a circular ring with re-bars around its circumference, with a width based on bar size, base board and Abram's cone. The sample of fresh SCC is allowed to flow in all directions, as in slump flow, but the flow in this instance is blocked by the circular arrangement of bars which replicate reinforcement. The primary purpose is to obtain the passing ability or blocking characteristic of the fresh mix of SCC. The filling ability and flow time (as in slump flow) are also measured. In addition, segregation can be visualized by looking at the dispersion of aggregate. According to Domone (2006), the J-ring test has been less widely used to determine fresh properties of SCC because slump flow is sufficient for the filling ability test and the L-box test provides adequate data on the passing ability of fresh concrete. Filling ability is similar to the slump flow diameter; classes are shown in Table 2.4 (European SCC Guidelines, 2005).

Table 2.4: Classes of filling ability based on flow spread on J-ring test

Classes	Slump Flow Diameters (mm)	Comments
SFJ1	550-650	Low filling ability
SFJ2	660-750	Good filling ability
SFJ3	760-850	High filling ability

The passing ability of J-ring is classified through blocking step BJ, which provides a measure of the degree of risk regarding the fresh mix of SCC when passing through reinforcement. The typical range of blocking step BJ is 3-20mm (Schutter et al., 2008). The classes of passing ability based on BJ are shown in Table 2.5 (RILEM Technical Committe TC 145-WSM, 2002).

Table 2.5: Classes of passing ability based on blocking step BJ

Classes	Blocking step (mm)	Comments
BJ1	≤10	0 to low risk of blocking. Suitable for structural elements with dense reinforcement.
BJ2	>10≤20	Moderate to high risk of blocking. Widely spaced or no reinforcement, few obstacles to flow.

Note: BJ1 to BJ2: Passing ability classes expressed by blocking step (J-ring test)

L-box test: The L-box test apparatus consists of a vertical box section and a horizontal trough. This test was first developed in order to assess the fluidity of fresh underwater concrete mixtures by measuring the distance it could flow under its own weight, without passing through any bars (Schutter et al., 2008). The main objective is to measure the consistency of the fresh concrete mixture. It has now been extended to measure the passing ability of the fresh mix of SCC with the reinforcing bars placed in between the vertical section and the horizontal trough. In addition, the flowability and visual segregation can be observed during the test. The height of concrete left in the vertical section (H1) and the height of the concrete at the end of the trough (H2) are measured (See Figure 3.6 in chapter 3). The ratio of H2/H1 is calculated and considered as a passing ratio (PR), which is the ability of the fresh mix of SCC to flow around the obstruction. The typical range of PR measured by the L-box is 0.85 – 0.95 (Schutter et al., 2008). The classes

of passing ability based on the L-box test are shown in Table 2.6 (European SCC Guidelines, 2005; Schutter et al., 2008).

Table 2.6: Classes of passing ability based on the L-box test

PA1≥0.8 with 2 rebars structures with a gap of 80 to 100mm: adequate passing ability for general purpose application with light or no reinforcement (e.g. housing, vertical structures)
PA2≥0.8 with 3 rebars structure with a gap of 60 to 80mm: suitable for placing into formwork with congested reinforcement (e.g. civil engineering structures)

- **Note**: Symbols and abbreviation SF1 to SF3: Consistent classes expressed by slump-flow diameter
- VS1 to VS2: Viscosity classes expressed by T50 of slump-flow time
- VF1 to VF2: Vicosity classes expressed by V-Funnel time
- PA1 to PA2: Passing ability classes expressed by Passing ratio (PR) of L-Box Test

Conclusion on SCC Fresh Properties Testing

The slump flow test has been used universally as a measure for flow capacity. Flow rate or deformability rate values are expressed as T50 (slump flow time). V-Funnel time is measured to calculate the filling ability and viscosity of the fresh concrete mixture. According to Domone, nearly 90% of slump flow measurements were from 600-750mm (Domone, 2006). According to Grdic et al. (2010), the highest permissible value for SCC is 850mm and the lowest value required is 650mm. Domone (2006) studied 68 cases of SCC properties from 1993 to 2003, and mentioned a considerable variation of T50 time and V-funnel time. T50 ranged from 1.8 to more than 12 seconds, and V-funnel times ranged from 3 to 15 seconds. There was no destinctive pattern of higher flow diameter associated with lower flow rates, which signifies the independence of these properties (Domone, 2006). J-ring was less widely used, and only 17 cases were reported the value from L-Box passing ability (Domone, 2006).

Table 2.7: PCI guidelines for using SCC (Lanier, et al., 2003)

			Slump flow (mm)			T50 Time (Sec)			L-Box (%)			V-Funnel (Sec)			J-Ring Passing Ability		
			<558	558-660	>660	<3	3-5	5	<75	75-90	>90	6	6-10	>10	Excellent [<15]	Good [10-15]	Poor[>10]
Member Characteristics	Reinforcement Level	Low															
		Med	■			■			■			■					■
		High	■			■			■			■				■	■
	Element Shape Intricacy	Low															
		Med	■					■						■			
		High	■	■				■						■		■	■
	Element Depth	Low															
		Med															■
		High				■						■				■	■
	Surface Finish Importance	Low															
		Med	■					■						■			
		High	■	■				■						■			
	Element Length	Low															
		Med	■						■								■
		High	■	■		■			■	■		■				■	■
	Wall Thickness	Low	■	■				■	■					■			
		Med	■														
		High															
	Coarse Aggregate Content	Low															
		Med															■
		High									■			■		■	■
	Placement Energy	Low	■	■					■					■		■	■
		Med	■														■
		High				■						■					

Dark blocks represent potential problems areas.

Table 2.7 provides the Precast/Prestressed Concrete Institute (PCI) guidelines for SCC application in North American practice. These interim guidelines have been prepared in response to the wide use of SCC in the prestressed and precast industries in the North American market (Lanier et al., 2003). The European Guidelines of self-compacting concrete (EFNARC) are easy to understandmost past research papers have also been based on it. Hence, EFNARC is used as a reference in this thesis.

2.4 Fiber Reinforced Concrete (FRC)

According to ACI 116R (cement and concrete terminology), the term Fiber Reinforced Concrete (FRC) is defined as: "concrete containing dispersed randomly oriented fiber." The report, entitled "State-of-the-art on fiber reinforced concrete" and published by ACI Committee 544.1R-96, defines FRC as "concrete made primarily with hydraulic cement, aggregates, and discrete reinforcing fibers." In the last four decades, significant development and abundant research have been carried out on FRC as a means of strengthening the tension weakness of concrete.

The use of various types of fibers such as glass, steel and synthetic fibers had been researched and developed since the 1920s and 1930s. It was in the early 1960s when Romaldi and Batson published the first report on the use steel fibers in FRC, which caught the attention of academics and industry research scientists around the world (Keer, 1984; Zollo, 1997).

Concrete is weak in tension and exhibits brittleness of character when forces are applied. In addition, micro-cracks can develop before external load is applied due to thermal and shrinkage strains, plastic settlement and bleeding. These cracks create easy access routes for other harmful agents, leading to chlorine ingression, freeze-thaw damage and steel corrosion in reinforcing steel concrete. Recent research has shown that the addition of mineral admixtures such as silica fumes, fly ash, slag, etc. to concrete help increase compressive strength and durability. However, at the same time, high compressive strength concrete becomes more brittle with catastrophic failure potential. Therefore, by incorporating random distributed fibers, brittleness behavior of concrete can be overcome because fibers bridge micro-cracks and restrain widening, thus delaying post cracks (Wang et al., 2011). This result is referred to as toughness or the energy-absorbing capacity of the hardened FRC. Fibers also help protect the early-age cracking of concrete by restraining drying shrinkage (Corinaldesi & Morconi, 2011).

According to ACI 544.1R-96, there are basically four categories of FRC based on material used. These are as follows:

SFRC: for steel fiber FRC
GFRC: for glass fiber FRC
SNFRC: for synthetic fiber FRC
NFRC: for natural fiber FRC

Steel fiber is the most popular and commonly used fiber in both research and commercial applications. Recent research has shown that the use of steel fiber helps in the mechanical behavior of hardened concrete especially in terms of tensile strength and fracture toughness (Xu & Shi, 2009). An effective dispersion of steel fibers can be controlled during mix design of SFRC. The fresh properties of SFRC are governed by the aspect ratio of the fiber, fiber geometry, the volume fraction of the fiber and the fiber-matrix interfacial bond characteristic (ACI Committee 544.1R-96, 2001). Among them, the most important parameters affecting both fresh and hardened properties are the aspect ratio (ratio of length to diameter of fibers) and volume fraction of the fiber. According to ACI Committee 544.4R-88, the steel volume fraction used ranges from 0.5% to 1.5% by volume of concrete, whereas the aspect ratio of the steel fibers used is between 50 and 100. The higher volume fraction of steel fiber (higher than 1.5%) usually decreases the workability of SFRC due to clumping of the fibers. However, a higher percentage of fibers up to 20% can be achieved with a special fiber addition technique and placement procedure such as slurry infiltration process using steel fibers (Lankard, 1986). On the basis of tensile strength of the composite matrix of SFRC, the higher the aspect ratio, the higher the interfacial surface area, which is directly proportional to the pullout resistance. Therefore, the pullout resistance increases with an increase in fiber length, which improves post cracking behavior of SFRC. However, in practice, the greater length of the steel fiber with a high aspect ratio greater than 100 hinders the workability of concrete mixtures and effective dispersion of the steel fibers may not be achieved. Therefore, in order to promote the wider use of SFRC as a proper structural component, effective control of the fiber dispersion must be exercised during fresh mix design. The incorporation of steel fibers in SCC is one method of achieving effective control of the fiber dispersion, along with the self-compacting nature of SCC, which leads to the elimination of compaction by vibration. In order to control the effective dispersion of steel fibers,

adding a mineral admixture along with the cement, plus the higher ratio of fine to coarse aggregate in SCC helps form a compact matrix. This also improves the interface-zone properties and, consequently, the fiber matrix bond, leading to enhanced post-cracking toughness and energy absorption capacity (Shah et al., 2010).

There are limited data available concerning the use of fiber in SCC. Further research is required to determine the potential of using the test methods employed for SCC to evaluate the restricted flowability of SFRSCC (Khayat & Roussel, 2000). Hence, the synergy between self-consolidating concrete and SFRC in developing SFRSCC may create enhanced concrete properties. SFRSCC is discussed in detail in next section.

2.5 Steel Fiber Reinforced Self-Consolidating Concrete (SFRSCC)

According to Khayat and Russel (2000), "A truly fiber-reinforced SCC (FRSCC) should spread into a place under its own weight and achieve consolidation without internal or external vibration, ensure proper dispersion of fibers, and undergo minimum entrapment of air voids and loss of homogeneity until hardening." A significant amount of research has been done in the last two decades to establish proper guidlines for SCC mixes. In addition, FRC is also widely recognized and has been used in different applications of civil engineering structures such as highway pavements, slabs and floors, bridge deck and tunnel lining. Therefore, combining SCC and FRC to develop FRSCC has promising advantages including improved mechanical characteristics such as toughness, ductility and energy abosrbing capacity. In the last decade, various researchers have conducted valuable tests and aided in further development of FRSCC (Khayat and Roussel, 2000; Corinaldesi and Morconi, 2011; Greenough and Nehdi, 2008; Dhonde et al., 2007;Ozbay et al., 2010).

Researchers have studied FRSCC with different kinds of fibers including steel fibers, poly-vinyl-alcohol (PVA) fibers, poly-propylene (PPHT), glass fibers, nylon bundles, and carbon fibers. The use of steel fibers in FRC is widely used around the world because it improves the post-peak ductility and the energy absorption capacity of the concrete. SCC has shown a densified matrix with better bonding between steel and concrete (Hossain & Lachemi, 2008). Therefore, taking the advantage of SCC properties by including steel fibers should provide a positive new feature and a new dimension in concrete technology, which could lead to better behaviour in

mechanical performance of SFRSCC in the hardened state. A study done by Corinaldesi and Moriconi (2011) with three different types of fibers (Steel, PVA and PPHT) in SCC showed the increased effectiveness of steel fibers in improving flexure behaviour over PVA and PPHT.

2.5.1 Mix Design and Methodology of SFRSCC

The inclusion of fibers in SCC is possible. However, there is only limited data regarding the proportioning of the standard FRSCC mix design. Resistance to bleeding and segregation are essential in the production of SCC, especially when steel fibers are used (Khayat & Roussel, 2000). Past research on FRSCC has shown that the workability of SCC decreases with increased inter-particle collision among the aggregate particles and fibers. Therefore, the proper ratio of VMA and water reducing admixture should be incorporated to get the desired slump flow for SCC. The proper design and control of fibers in SCC depend on the careful selection of materials for proper workability, sufficient consolidation and improved uniformity of fiber distribution.

SFRSCC mixtures can be developed by increasing the fine mineral admixture and reducing the coarse aggregate. Khayat and Russel (2000) studied the feasibility of SFRSCC with characteristics similar to SCC. Sixteen concrete mixtures were made with steel fibers, measuring 38mm in length and with a steel fiber volume fraction range of 0%-1% (Khayat & Roussel, 2000). The concrete mixtures were designed in a similar manner to high-performance SCC, with various types of binary and ternary cementitious materials and water to cementitious ratio (w/cm) of 0.37 to 0.45. SFRSCC with 0.5% volume fraction of steel fibers had behavior almost identical to normal SCC, whereas an increase in steel fiber volume from a fraction to 1% resulted in considerable limitation of restricted flow. Moreover, the high-range water reducing agent (HRWR) was slightly increased for 0.5% fiber volume fraction. The higher demand of HRWR was recorded for the SFRSCC with 1% steel fiber volume fraction.

Torrijos et al. (2008) successfully used SFRSCC on slender elements of considerable height (slender columns), avoiding the use of conventional reinforcing bars. An experiment conducted by Torrijos et al. (2008) used prototype columns filled with SCC and two SFRSCC obtained from same batch, incorporating 25 and 50 kg/m^3 of fibers with super plasticizer. The result showed that the SFRSCC with 25 kg/m^3 of steel fiber had SCC properties almost similar to the plain SCC. However, the self-compacting capacity of SFRSCC with 50kg/m^3 of steel fiber were significantly reduced. This result showed that SFRSCC can be successfully applied in the

construction of slender columns. However, the use of a higher percentage of fibers is not recommended in highly congested reinforcement areas.

Grunewald and Walraven (2001) studied the effect of four types of steel fibers with different contents on the workability of two series of SCCs with different composition. The sand content was kept constant at 40% by volume of mortar. In order to maintain the SCC properties, water and super plasticizer content were adjusted to obtain the desired slump flow for SCC. In the mixture design, the addition of fibers depended on the fiber aspect ratio and fiber length. The coarse aggregate was reduced as fibers were added in the mix proportion. The study showed that with the decreasing aspect ratio of the fiber, more fibers can be added to SCC without problematic loss of workability. It also showed that maximum fiber content is not a single value and depends on the mixture composition as well.

Pereira et al. (2005) studied economical SFRSCC for pre-cast industrial applications. The mixture design was similar to high-performance SCC with limestone filler (LF), super plasticizer (SP), three types of aggregates (fine river sand, coarse river sand and crushed granite 5-12mm) and hooked-end steel fiber. According to the study, the mix design was developed with three main steps: (Pereira et al., 2005)

1. The proportions of constituent materials of binder paste with the optimum percentage of LF addition in the final composition were defined.
2. The proportions of each aggregate on the final solid skeleton were determined in order to optimize aggregate mix, which was assumed to be the heaviest one.
3. The binder paste and solid skeleton were mixed in different proportions until the self-compacting requirements of flow ability, correct flow velocity, filling ability, blockage and segregation resistance were assured.

Hence, the mixture design methodology of SFRSCC depends not only on the fiber volume percentage but also on fiber type and aspect ratio. A different mineral admixture composition and chemical admixture also play a vital role. As different researchers have adopted different methodologies to satisfy SCC conditions, further development and robust methodology must be well defined for future improvement in SFRSCC.

2.5.2 Fresh Properties of SFRSCC

Grunewald and Walraven (2001) found that the workability of fresh SFRSCC is directly proportional to the fiber content and aspect ratio. The increment in fiber volume percentage increases internal resistance to flow, as observed by several studies (Grunewald and Walraven, 2001; Sahmaran et al., 2005; Dhonde et al., 2007). The passing and filling ability of SFRSCC mixes with long fibers might be unsatisfactory, especially in congested reinforcing areas. Dhonde et al. (2007) also studied the concept of fiber factor, with V_f* L/d_f , where V_f as the percentage of fiber volume and L/d_f as fiber aspect ratio, L as length of the fiber and d_f as diameter of fiber. A combination of short fibers with large fiber factor has a higher passing ability of SFRSCC than long fibers with a low fiber factor (Dhonde et al. 2007). Therefore, the passing ability is more sensitive to the length of the fiber than to the fiber factor.. In general, the greater the aspect ratio, and the lower the fiber content in the concrete mixture, the harder it is to reach the critical fiber volume essential for the hardened properties of SFRSCC (Liao et al., 2006).

Grunewald (2004) outlined the relationships between different parameters such as maximum aggregate size, fiber volume, fiber type and mixing process in order to optimize fiber content. These are important parameters to achieving the desired workability of SFRSCC. At the higher fiber volume fraction, the balance between deformability and stability became especially important parameters (Grunewald, 2004) .

Experiments conducted by Torijos et al., (2008) on slender columns with plain and SFRSCC showed that the physical and the mechanical properties did not vary significantly along the height of the column. However, aggregate distribution was slightly more homogeneous in the case of fiber SCC, which implies that the fibers may provide stability or resistance against segregation of SCC.

2.5.3 Mechanical Properties of SFRSCC

In the last two to three decades, the compressive strength of concrete has reached up to 100 MPa. At the same time, however, brittle characteristics of the concrete have increased along with the compressive strength. The inclusion of fibers in concrete improves ductility, which represent the internal confinement of the concrete. Other mechanical properties such as crack control, toughness, impact resistance and durability can also be enhanced. The effect of fibers depends on

several parameters including type, size, geometry, aspect ratio, volume fraction, tensile strength, stiffness, surface properties and fiber matrix bond (Yildirim et al., 2010; European SCC Guidelines, 2005).

An investigation of mechanical properties of SFRSCC was conducted by Dhonde et al. (2007) on two different types of steel fibers and variable amounts of hooked steel fiber. They used Dramix RC 80/60 BN (60mm in length), which has a "trough" shape with hooked end steel fiber, and ZP305 (30mm in length), a short steel fiber with a hooked end as well. The aspect ratios of Dramix RC 80/60 BN and ZP305 were 80 and 50, respectively. Three different types of SFRSCC in total were prepared with 0.5% and 1% by volume of concrete. Only one mix of SFRSCC with Dramix RC 80/60 BN at 0.5% by volume, and the other two mixes of SFRSCC with ZP305 at 0.5% and 1% by volume were prepared. The control SCC was prepared with the same basic proportion as the SFRSCC mixes. Slightly higher amounts of cement and fine aggregate were used in SFRSCC mixes to offset the influence of the addition of fibers on fresh properties of SCC. The result of the compression study showed that the non-fibrous mixture exhibited sudden failure with brittle characteristics, while the fibrous concrete cylinders were quite ductile. The study showed that the cylinders with short fibers had slightly higher 28-day compressive strengths than those with the longer fibers, depsite having the same exact fiber volume percentage. The study also showed that there were only marginal increases in compressive strengthe after the increase of fiber volume fraction from 0.5% to 1%. Another study done by Yildirim et al. (2010) showed a slight increase in 28-day compressive strength after the increment of fiber volume percentage was increased from 0.3% to 1.2%. Overall, the short fiber samples had higher 28-days compressive strength than those with longer fibers.

The study done by Dhonde et al. (2007) showed a higher modulus of rupture (MOR) in fibrous concrete mixtures compared with non-fibrous concrete. The MOR of cylinders with longer fibers was higher than those with short fibers, despite having an equal volume fraction of fibers. Also, an increase in MOR for short fiber mixtures was observed after the increment of fiber volume fraction decreased from 0.5% to 1%. Average residual strength (ARS) (also referred to as flexural toughness or fracture energy value) increased along with fiber volume fraction (Dhonde et al., 2007; Yildirim et al., 2010; Nataraja et al., 2000). Similarly, the ARS values for samples with longer fibers were higher as compared to those with shorter fibers having equal volume

percentages of fiber. The study done by Yildirim et al. (2010) also reported an increase in flexure strength or MOR with the increment of fiber volume fraction.

ARS or flexural toughness is an important parameter when dealing with fibrous concrete, specially that with steel fibers. The main contribution of use of steel fibers is to increase the strength after the cracking of concrete matrix during loading. The bridging mechanism of the steel fibers, after first crack formation, delays further crack formation and limits crack propagation (Balaguru et al., 1992). Hence, fiber debonding and the pulling out mechanisms of fibers require more energy, which is recorded as the area under a load-deflection curve in flexure. The typical load deflection curve shown below is from ASTM 1018, which illustrates the area under load deflection curve as a flexural toughness or ARS (ACI Committee 544.1R-96, 2001).

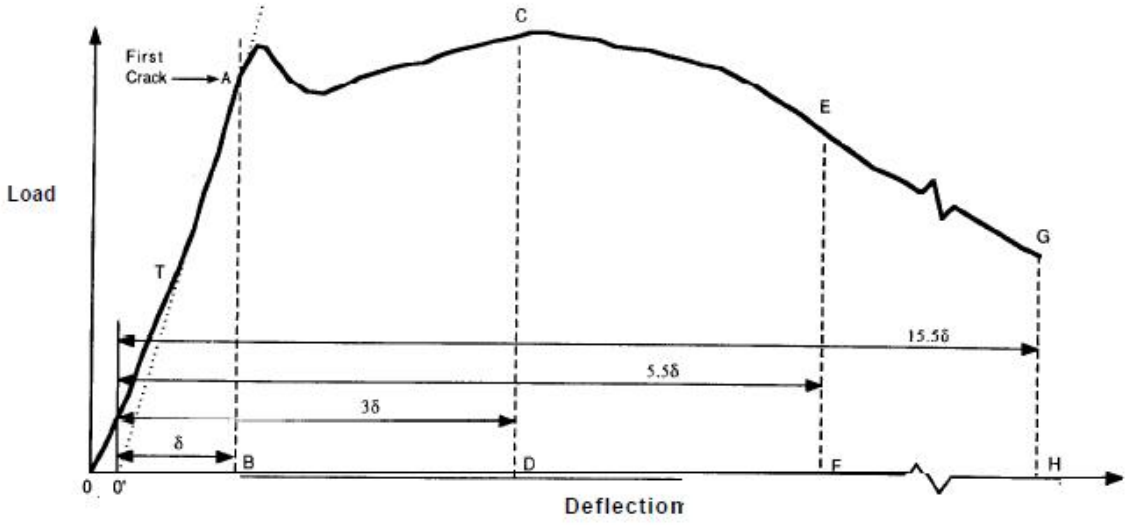

Figure 2.9: Typical load deflection curve

Experimental data shows little improvement in the bond strength of SCC compared to normal concrete due to its filling ability (Almeida Filho et al., 2005; Domone, 2007). The study done by Haraji and Salloukh (1997) showed that bond strength went up by 55% after increasing the steel fiber volume fraction by 2%. Similarly, Krstulovic-Opara et al. (1994) found a 10-20% increase in the bond strength after adding a 1% steel fiber volume fraction. Also, bond strength was increased by 2 to 3 times when the steel fiber volume fraction went up 3% to 7% (Krstulovic-Opara et al., 1994).

2.5.4 Durability properties of SFRSCC

Steel fibers have gained popularity in recent decades due to low fiber volume fraction, which enhances toughness, flexure strength and resistance to shrinkage-induced cracking (Miloud, 2005). However, there is little information available regarding the effect of steel fiber on the durability performance of concrete (Miloud, 2005).

A durability test of high-performance steel fiber reinforced concrete done by Ramodoss and Nagamani (2008) showed that water absorption and porosity do not change significantly compared to the control mixture without steel fibers (Shah & Ribakov, 2011; Ramadoss & Nagamani, 2008). Water absorption and porosity ranged from 1.86 – 1.91% (with W/CM ratio 0.4) and 4.43 – 4.50% (with W/CM ratio 0.4), respectively. Water absorption by immersion provides information related to the pore volume of concrete, but gives no information related to concrete permeability. Experimental water absorption is in the range of 3 to 6.5%, as per Belgian Standard NBN B15-215 (Schutter & Audenaert, 2004). Concrete is regarded as good quality if saturated water absorption is around 3%, according to The Concrete Society, United Kingdom (Ramadoss & Nagamani, 2008). Study done by Ramadoss and Nagamani (2008) also show that water absorption and porosity decrease when water to cementitious ratio decreases. Miloud (2005) found that the addition of 30mm long steel fibers did not affect porosity when fiber volume fraction increased from 0.5% to 1%. Addition of 20mm steel fiber showed exactly the same results. As per existing literature, it is important to mention that fiber addition generally did not significantly increase the number of pores as compared to conventional concrete (concrete without fibers) (Miloud, 2005).

Sorptivity is a material's ability to absorb and transmit water through capillary suction. Sorptivity is also related to absorption and is sometimes used as an indicator of the volume of capillary pore space or open porosity (Sabir et al., 1998). Study done by Ramadoss and Nagamani (2008) found that the Sorptivity was in the range of 0.0893 – 0.0914 mm/√min (with W/CM ratio 0.4) (Ramadoss & Nagamani, 2008). The study done by Ramodoss and Nagamani (2008) showed that the sorptivity value decreased with an increase in the steel fiber volume fraction. A sorptivity value of less than 0.77 mm/√min is considered good quality in terms of durability performance (Nawy, 1997). According to Taywood Engineering Limited, good quality concrete has a sorptivity value of less than 0.1 mm/√min. According to a study done by El-Dieb

(2009), in ultra-high strength concrete incorporating steel fibers, the sorptivity value did not change significantly for a fiber volume fraction range from 0.08 – 0.52%; its values ranged from 0.0353 – 0.0385 mm/√min, respectively. The study also found that sorptivity value decreases with age.

The rapid chloride permeability (RCPT) test assesses the ability of concrete to resist chloride ion penetration. The RCPT test conducted by Tsai et Al. (2009) and El-Dieb (2009) showed that the total charge passes and the electrical conductivity increases with an increase in the steel fiber content of SFRSCC. El-Dieb also found that the increment of steel fiber volume fraction by 1% in SFRSCC has a good ability to resist chloride ion penetration.

The corrosion of steel bars is a major problem for the durability of concrete. Whenever concrete is exposed to a chloride environment, chloride ion can penetrate and diffuse through the body of the concrete. Research has shown that the obstruction of chloride diffusion is minimal for low permeability and dense concrete. Mihashi et al. (2011) performed a corrosion test on reinforcing steel bars in hybrid fiber-reinforced cementitious composites (HFRCC) containing polyethylene (PE) and steel cord (SC) fibers. The beam specimens were subjected to accelerated corrosion for one year by applying the reinforcing steel bar as anode and steel wire mesh as cathode. As the wire mesh was connected to negative terminal of DC (direct current) supply, electrons were forced to go to the wire mesh. These electrons combined with the water and oxygen available near the vicinity of the beam's bottom surface and converted to hydroxial ions (OH^-) and chloride ions (Cl^-). These ions moved towards the Fe^{++} ion in the steel bar (anode) and caused a corrosion reaction, as shown in Figure 2.10. Mihashi et al. (2011) found the theoretical mass loss of the steel bar using Faraday's law was higher than the experimental mass loss. The figure also shows the random distribution of steel fibers in the cover zone of the beam specimen and their connectivity to the steel reinforcing bar. Therefore, some of the SC fibers connected to the steel bar considered the anode and corroded first as they were in close proximity to the cathodic region. This explains why the experimental mass loss differed from the theoretical mass loss by Faraday's law. However, all SC fibers were not corroded as they were randomly distributed (Mangat & Gurusamy, 1988). Mihashi et al. (2011) also found that corrosion of the steel bar in HFRCC was less than in the control mortar (without steel fiber) after the experiment. According to Mihashi et al. (2011), some of the SC fibers connected to the steel reinforcing bar acted as

anodes, hence a galvanic couple formed and corrosion began. This reduced the corrosion of the steel reinforcing bar. The formation of galvanized steel fibrous matrix as protection shield is also mentioned by Someh et al. (1997) as a way to inhibit corrosion of reinforced concrete members. Mihashi et al. (2011) also mentioned resistance to corrosion in HFRCC due to bridging of cracks by fibers and self healing of some of the cracks.

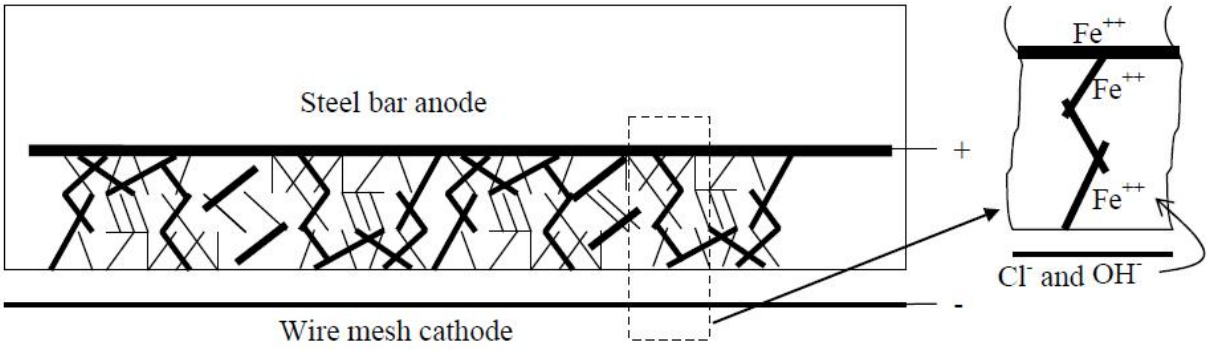

Figure 2.10: Schematic of distribution of SC fibers (▬▬) and PE fibers (——) in the specimen and formation of sacrificial SC fibers (Mihashi et al., 2011)

The surface corrosion of steel fibers in the SFRC was studied by Granju and Balouch (2005). It has been found that steel fibers were less vunerable to corrosion than steel bars when exposed to marine saline fog for one year. With different dimensions of crack mouth opening (CMO) less than 0.1mm a light corrosion of fibers was observed with no reduction of the section (Granju & Balouch, 2005). However, only the CMO exceeding 2-3mm on the external face of the specimen showed extensive corrosion. According to ACI 544.1R-96, "If a concrete has a 28 days compressive strength over 3000psi (21Mpa), is well compacted, and complies with ACI 318 recommendations for water cement ratio, then corrosion of fibers will be limited to the surface skin of the concrete". There is limited surface corrosion even in a highly saturated chloride ion solution (ACI Committee 544.1R-96, 2001). The use of galvanized steels in concrete has been suggested by ACI 549 (ACI Committee 544.1R-96, 2001). The corrosion of steel bars in SFRSCC and SFRC is still a hot research topic in the future development of durable concrete technology.

Freeze resistance of concrete is a physical function which reflects the important parameter of concrete durability. Most studies have already proven that the pore structure of concrete plays an

important role in concrete antifreezing. In most cases, the deterioration of concrete due to freeze-thaw consists of two parts:

a) When pore water turns to ice due to negative temperature changes, volume increases about 9%. Due to the increment of volume, concrete begins to expand and causes tensile stress. This will disintegrate the concrete when stress exceeds the tensile strength of the concrete.
b) Migration of pore water towards the super cold water in the gel pore occurs as a result of the osmosis process. This generates osmotic pressure on the pore walls, which will disintegrate the concrete when the stress exceeds the tensile strength of concrete.

According to ACI 544.4R-88, "Steel fibers do not significantly affect the freeze-thaw resistance of concrete, although they may reduce the severity of visible cracking and spalling as a result of freeze in concrete with an inadequate air void system." The study conducted by Atis and Karahan (2009) into steel fiber-reinforced fly ash concrete showed that the freeze-thaw resistance of steel fiber concrete increased slightly compared to concrete without fibers. The tensile strength of steel fiber-reinforced concrete resists the tensile stress generated during the freeze-thaw cycles. Khaloo and Molaee (2003) also found an improvement in freeze-thaw resistance in the SFRC over the control concrete mixture without steel fiber. Fa-ming and Chuan-qing (2011) tested the influence of freeze-thaw cycles on SFRC with different fly ash contents. A decrease in compressed strength was observed in concrete without fly ash after 75 freeze-thaw cycles. However, when fly ash content increased beyond 30%, there was no significant compressive strength loss. This shows that the fly ash gained strength as time passed and aslo steel fibers helped with good bonding of the concrete matrix.

2.5.5. Summary

Extensive research had been done on the fresh and mechanical properties of SFRSCC. Previous studies have talked about the limitations of the workabiilty of fresh properties beyond 1% steel fiber volume fraction because higher fiber volume fraction causes greater hindrance in the spreading of fresh concrete. The incorporation of steel fiber in concrete improved bond strength between the steel reinforcing bar and concrete matrix, and increased compressive strength and

flexural strength of the concrete. The durability performance of SFRSCC is major focus in the research done for this thesis.

Chapter 3

Experimental Program

3.1 Introduction

All experiments to develop SFRSCC concrete mixtures were performed in concrete and structural laboratories at Ryerson University. A total of 13 SFRSCC concrete mixtures with different percentages of fiber volume and two different fiber lengths were used, including the control SCC (0% fiber). The experimental program was made up of two phases. In the first phase, the fresh properties tests were performed on the SFRSCC concrete mixtures, including slump flow, slump flow time T50, L-box, V-funnel and J-ring. In the second phase of the experimental program, hardened properties such as mechanical properties (compressive test, pullout test and flexure test) and durability properties tests (water absorption and porosity, sorptivity, RCPT test, corrosion test, and freeze-thaw resistance test) were performed.

3.2 Materials

Cement

A type GU (General Use) hydraulic cement as per CSA A3001-03 was used. The physical and chemical properties are illustrated in Table 3.1.

Slag

A type S-ground granulated blast furnace slag (GGBFS) as per CSA A23.5 was used. The physical and chemical properties of slag are illustrated in Table 3.1.

Binder

The binder for the 13 SFRSCC concrete mixtures consists of 70% cement and 30% GGBFS by weight. The total binder content was 500 kg/m^3, with 350 kg/m^3 of cement and 150 kg/m^3 of GGBFS respectively.

Water

Clean drinkable water was used for all 13 SFRSCC concrete mixtures. The temperature of the water ranged from 19 to 22 degrees Celsius.

Aggregate

The grading of coarse and fine aggregate was performed according to ASTM C 136 -06 (2005). The grain size distributions of coarse and fine aggregate are illustrated in Table 3.3 and Figures 3.1 and 3.2. The average diameter of the coarse aggregate is 10mm.

Table 3.1: Chemical and physical properties of cement and slag (Source: Lafarge Inc.)

Chemical Analysis (%)		**Cement**	**Slag**
Silicon dioxide	Sio_2	21.72	38.40
Aluminum Oxide	Al_2O_3	5.96	10.64
Ferric Oxide	Fe_2O_3	3.60	0.79
Calcium Oxide	CaO	60.78	34.2
Magnesium Oxide	MgO	2.64	6.94
Potassium Oxide	K_2O	0.75	0.84
Sodium Oxide	Na_2O	0.17	0.16
Sulphur Trioxide	SO_3	2.17	1.48
Phosphorus Pentoxide	P_2O_5	0.04	0.07
Titanium dioxide	TiO_2	0.36	0.71
Chromium Oxide	Cr_2O_3	0.0455	0.01
Manganese(III) Oxide	Mn_2O_3	0.1496	1.84
Loss of ignition (LoI)		2.0	3.09
Tri-calcium silicate	C_3S	52.26	
Di-calcium silicate	C_2S	16.83	
Tetra Calcium aluminoferitte	C_4AF	7.57	
Total Alkali		1.00	
Free Lime	CaO	0.79	
Physical Analysis		Cement	Slag
Residue 45 micron (%)		4.5	1.0
Blaine fineness (cm^2/g)		3500	4300
Density (g/cm^3)		3.18	2.87
Air Content (%)		7.78	
Initial set (min)		113	
Compressive Strength (MPa)			
1 Day		19.23	
3 Days		30.35	
7 Days		33.82	
28 Days		41.45	

Physical tests of coarse and fine aggregates were done according to the ASTM standard; properties are shown in Table 3.3.

Table 3.2: Physical test of coarse and fine aggregate

Test	Coarse Aggregate	Fine Aggregate
Bulk specific gravity (dry)	2.59	2.56
Bulk specific gravity (SSD)	2.63	2.58
Fineness Modulus		3.34
Absorption (%)	1.51	0.64

Steel Fiber

Two different geometric shapes and lengths of steel fibers from Nycon Company were used. These are cold drawn wire low-carbon steel fibers. One has a hooked end (length = 25mm, diameter = 0.5mm) and the other is a straight shaft configuration (length = 13mm, diameter = 0.2mm). These are type I Nycon Steel Fibers as specified by ASTM A820-06. Characteristics of Type I steel fibers are illustrated in Table 3.4. The steel fibers are shown in Figure 3.3.

Chemical Admixture

ADVA CAST 530 from Grace Canada Inc. was used as a super plasticizer. It is a polycarboxylic-either type high range water reducing admixture (HRWR) with a solid content of approximately 30%. The properties of ADVA CAST 530 are provided in Table 3.5.

Rebar

A deformed rebar with nominal bar size of 15M was used in the concrete specimen for accelerated corrosion and pullout testing. The diameter of the bar is 16mm and specified yield strength is 400 MPa.

Table 3.3: Grading of coarse and fine aggregate

Coarse Aggregate						
Sieve Size (mm)	Inches	No	Fractional mass retained (gm)	Fractional % retained	Cumulative % retained	Cumulative % passing
19	0.75	3/4"	0.00	0.00	0.00	100.00
12.7	0.50	1/2"	97.47	9.76	9.76	90.24
9.5	0.37	3/8"	490.47	49.09	58.84	41.16
6.3	0.25	1/4"	331.14	33.14	91.99	8.01
4.75	0.19	4	41.50	4.15	96.14	3.86
2.36	0.09	8	33.50	3.35	99.49	0.51
Pan			5.08	0.51	100.00	0.00
Total:			999.16	100.00		
Fine Aggregate						
12.70	0.50	1/2"	0.00	0.00	0.00	100.00
9.50	0.37	3/8"	0.00	0.00	0.00	100.00
6.30	0.25	1/4"	6.42	1.29	1.29	98.71
4.75	0.19	4.00	14.65	2.93	4.22	95.78
2.36	0.09	8.00	41.80	8.37	12.59	87.41
1.18	0.05	16.00	61.51	12.31	24.90	75.10
0.60	0.02	30.00	92.00	18.42	43.32	56.68
0.42	0.02	40.00	68.24	13.66	56.98	43.02
0.18	0.01	80.00	167.10	33.45	90.44	9.56
Pan			47.77	9.56	100.00	0.00
Total:			499.49	100.00	333.73	

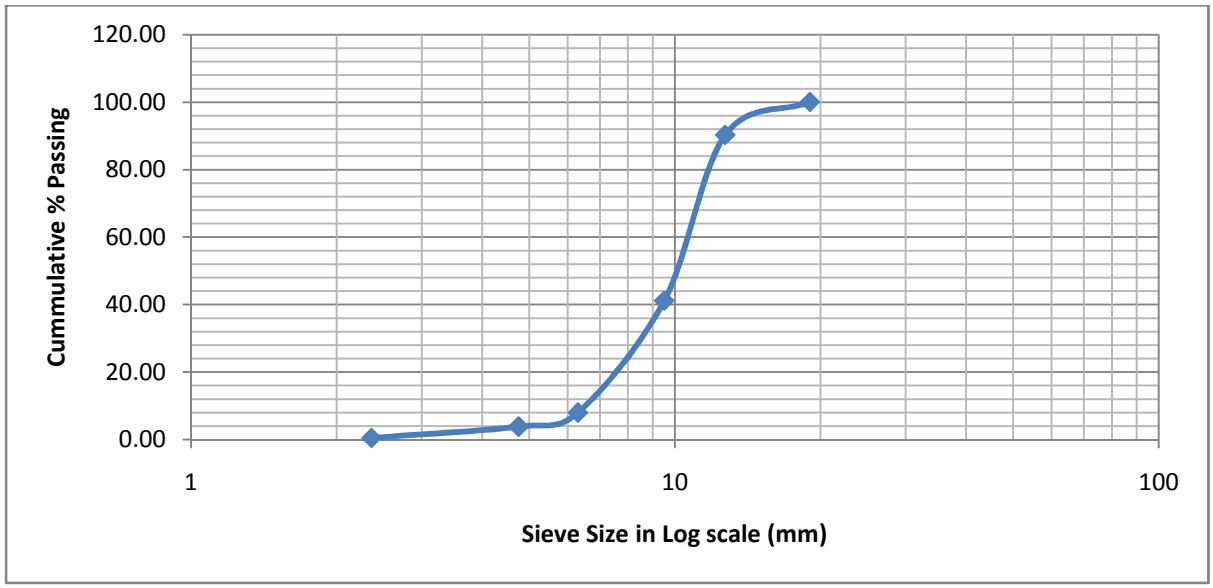

Figure 3.1: Grading of coarse aggregate

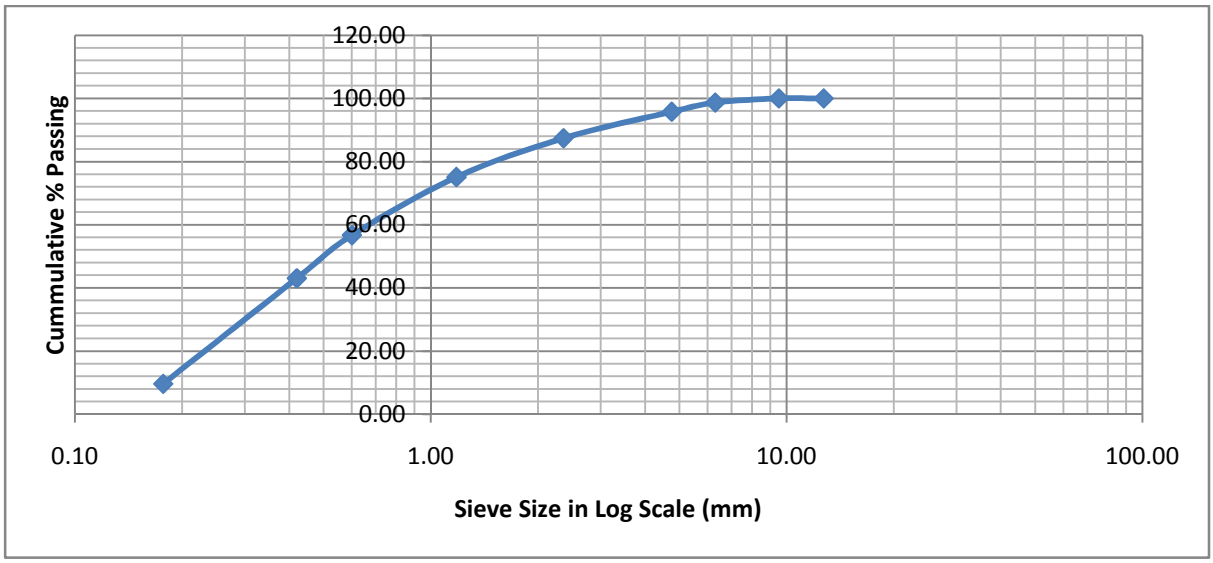

Figure 3.2: Grading of fine aggregate

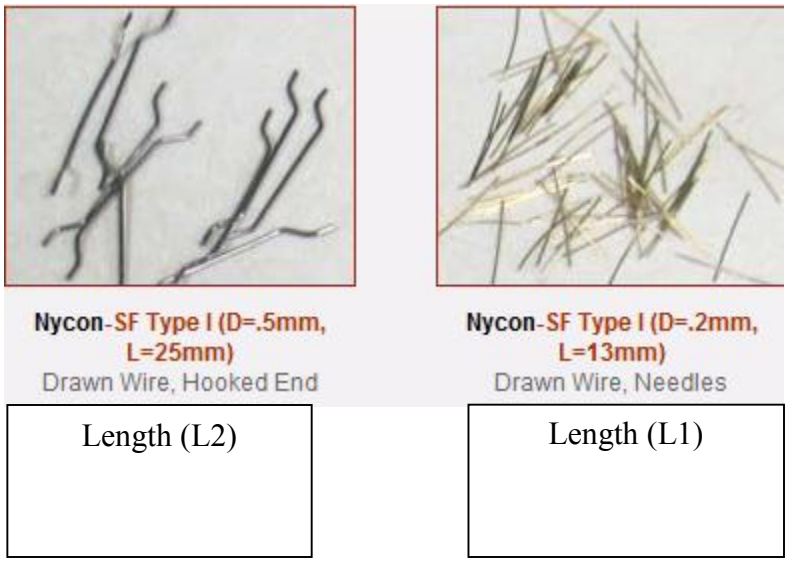

Figure 3.3: Steel fibers used for study

Table 3.4: Characteristics of steel fiber

Type	**Hooked End**	**Straight Shaft**
Diameter (mm)	0.5	0.2
Length (mm)	25	13
Aspect Ratio (L/D)	50	65
Tensile Strength (MPa)	≥1000	≥1000
Modulus of Elasticity (Psi)	29000000	29000000
Melting Point	1516 degrees Celsius	
Bending	Meet requirement of ASTM A820	
Surface Condition	Meet requirement of ASTM A820, sec 11.1 and 11.2 for bright and clean	

Table 3.5: Physical and chemical properties of ADVA CAST 530

Physical State:	Liquid
Appearance/Odour:	Clear yellow brown with a mild odour.
Odour Threshold: (ppm)	Not Determined
pH:	5 - 7
Vapour Pressure: (Mm Hg)	Unknown
Vapour Density: (Air = 1)	>1
Solubility in Water:	Miscible
Specific Gravity: (Water = 1)	Approximately 1.1
Evaporation Rate: (Butyl Acetate = 1)	Not Applicable
Boiling Point:	>212^{o}F/100^{o}C
Viscosity:	Unknown
Bulk Density: (Pounds/Cubic Foot) (Pcf)	Not Applicable
% Volatiles (gm/L): (70^{o}F) (21^{o}C)	70% (As Water)

3.3 Methodology

3.3.1 Mix design

After the development of SCC in late 1980s, it has been proven that SCC can be made with local material. A simple mixture proportion has been proposed by Okamura and Ozawa (1999). In this method, coarse to fine aggregate ratios are kept constant and SCC can be achieved by adjusting the water/cement ratio and the super plasticizerdosage only (Felekoglu et.al 2007). However, super plasticizeralone can only increase the fluidity and has a negative impact on bleeding and segregation. Therefore, in order to avoid segregation, SCC utilizes a lower aggregate content, water/cement ratio and use of super plasticizer(Okamura & Ouchi, 2003). The mixture proportions were based on Okamura's method for the optimization of coarse and fine aggregate content.

Thirteen SFRSCC concrete mixtures were developed with 50% coarse aggregate and 50% fine aggregate by volume of concrete. In addition, a constant water/cementitious ratio was adopted. The average coarse aggregate size was 10mm and the SFRSCC mixtures were developed based on a control SCC mixture. The control SCC was tested first in order to optimize the super plasticizerdosages for required slump flow. As the steel fiber percentage by volume of concrete increases, the workability of SCC decreased and the dosage of superplastizer adjusted

accordingly in order to get the required flowability of SFRSCC. Table 3.6 shows all 13 SFRSCC mixtures including the control SCC mixture (Mix 08/01) with zero fiber percentage by volume of concrete.

Table 3.6: Mix design of SFRSCC mixtures

Mix No.	FC %	Mix ID	LF mm	Water Kg/m^3	Cement Kg/m^3	Slag Kg/m^3	Steel fiber Kg/m^3	SP Kg/m^3	FA Kg/m^3	CA Kg/m^3
M02	0.4	4L1	13	180	350	150	28.68	1.75	807	819
M03	0.8	8L1	13	180	350	150	57.36	2.00	801	813
M04	1.2	12L1	13	180	350	150	86.04	2.25	796	808
M05	1.6	16L1	13	180	350	150	114.72	3.75	791	802
M06	2.0	20L1	13	180	350	150	143.40	4.25	785	797
M07	2.4	24L1	13	180	350	150	172.08	4.50	780	792
M08/ M01	0.0	0Fiber		180	350	150	0.00	1.75	812	824
M09	0.4	4L2	25	180	350	150	28.68	1.75	807	819
M10	0.8	8L2	25	180	350	150	57.36	2.15	801	813
M11	1.2	12L2	25	180	350	150	86.04	2.25	796	808
M12	1.6	16L2	25	180	350	150	114.72	2.50	791	802
M13	2.0	20L2	25	180	350	150	143.40	2.65	785	797
M14	2.4	24L2	25	180	350	150	172.08	3.05	780	792

Note: symbols used in the above table are:

FC: Fiber Content

LF: Length of Fiber

SP: Super Plasticizer

FA: Fine Aggregate

CA: Coarse Aggregate

3.3.2 Preparation of Mix

- After calculating the design mix for 1m^3 of concrete, the 20 liter batches prepared for each design mixture were adjusted. All materials required for the concrete mixture were prepared and weighed as per batch requirements. A small electrical scale was used in order to weigh the super plasticizer and the fiber amount. All the testing equipment required for fresh properties was prepared such as L-Box, V-Funnel, J-ring and slump

flow. The cylinders and prism moulds for hardened properties test were also prepared. 16mm diameter deformed bars were weighed on the small electrical scale and prepared for the corrosion test and bond strength test.

3.3.3 Mixing Procedure

The mixing procedure involved the following steps:

1. Coarse and fine aggregate were put into the drum and mixed for 15 seconds.
2. 20% of the water was added and mixed again for 30 seconds in order to homogenize coarse aggregate and fine aggregate.
3. Cement and slag were added within 10 seconds of stoppage time and 60% of the water was added.
4. Mixing was continued for another 30 seconds.
5. Steel fibers were added uniformly within 10 seconds of stoppage time and all remaining water was added along with the super plasticizer.
6. The concrete was properly mixed for another 60 seconds.
7. The mixing continued for another 2 minutes and then was stopped.

The total mixing time was approximately 300 seconds before testing the fresh properties of the mixture.

3.3.4 Specimen preparation

Immediately after mixing, a slump flow test was conducted, followed by J-ring, V-funnel and L-Box tests. A cylinder (100mm diameter x 200mm height) and a prism (410mm length x 100mm width x 75mm height) were also cast without external vibration. In addition, two cylinders of the same size with a 16mm diameter reinforcing bar inside were cast for the bond strength test. After casting was done, the cylinders and prisms were well covered by wet burlap and transferred to a 95% humidity room at 24±2^{o}C for curing. Cylinders and prisms were demoulded after 24 hours and shifted to a plastic drum filled with water until the specified testing time.

3.4 Fresh Property Test

There are different tests for the workability of fresh concrete SCC such as slump flow test, J-ring, L-Box test and V-funnel test.

3.4.1 Slump flow test

This is the most commonly used and readily available test for evaluating SCC. This test is expensive and is a modified version of the slump test (ASTM C143). It was first developed in Japan in order to test underwater concrete. The testing apparatus consists of an Abrams cone with a base diameter of 200mm, a top diameter of 100mm and a height of 300mm and a 900x900mm square steel plate as shown in Figure 3.4. The square steel plate has a 500mm diameter circular marking. The cone was placed at the center of the square steel plate and filled with the concrete without vibration. The stop watch was started as soon as the cone had been lifted vertically upwards and the time was measured when the flow reached 500 mm mark line. This time is considered as T50 time in seconds. T50 is recorded as an indicator of concrete flowability. The stop of the concrete flow was also recorded. The horizontal spread of the concrete sample was measured in two perpendicular directions and the average distance measured is the slump flow.

As stated in EFNARC (2002), segregation tendency of concrete can be determined through a visual observation of the spread. Slump flow is only used as an indication of flowability; other properties like filling ability cannot be sufficiently evaluated by using the slump flow test. For filling ability, another test like L-box should be used.

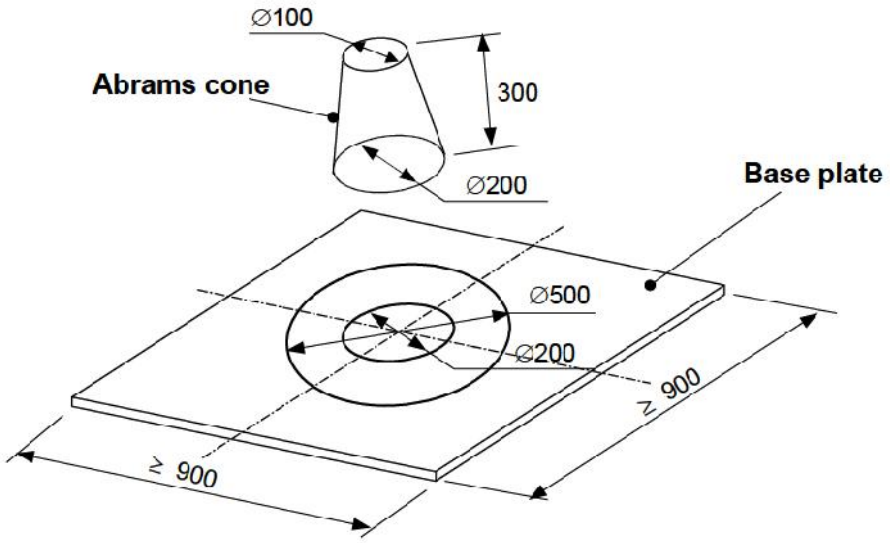

Figure 3.4: SCC slump cone and square steel plate

3.4.2 J-ring Test

This test is helpful in defining the passing ability of concrete. The J-ring apparatus consists of a steel ring measuring 300mm in diameter at the centre of the ring and 25mm in thickness (ASTM C1612, 2009). Smooth 16mm diameter, 100 high smooth rods are evenly spaced around the ring (ASTM C1612, 2009). The test setup is similar to the slump flow test including the J-ring, as shown in Figure 3.5.

The Abrams cone and the J-ring were placed concentrically onto the centre of the square steel plate. The concrete was poured into the cone without external vibration. The stop watch was started as soon as cone was lifted vertically upwards and the concrete was allowed to flow through the ring. The time was recorded as soon as the flow reached the 500mm mark on the plate and was considered as T50 in seconds. The time when the flow of concrete stopped was also recorded. The following measurement was done using a straight edge and measuring tape: (Schutter et al., 2008)

- Centre of the ring (h_o)
- Two opposite points at the outside edge of the ring are considered as h_{x1} and h_{x2}
- Two other points perpendicular to the previous points are considered as h_{y1} and h_{y2}

In addition, the slump flow for the J-ring was calculated to be the mean of the horizontal spread of the fresh concrete sample in two perpendicular directions.

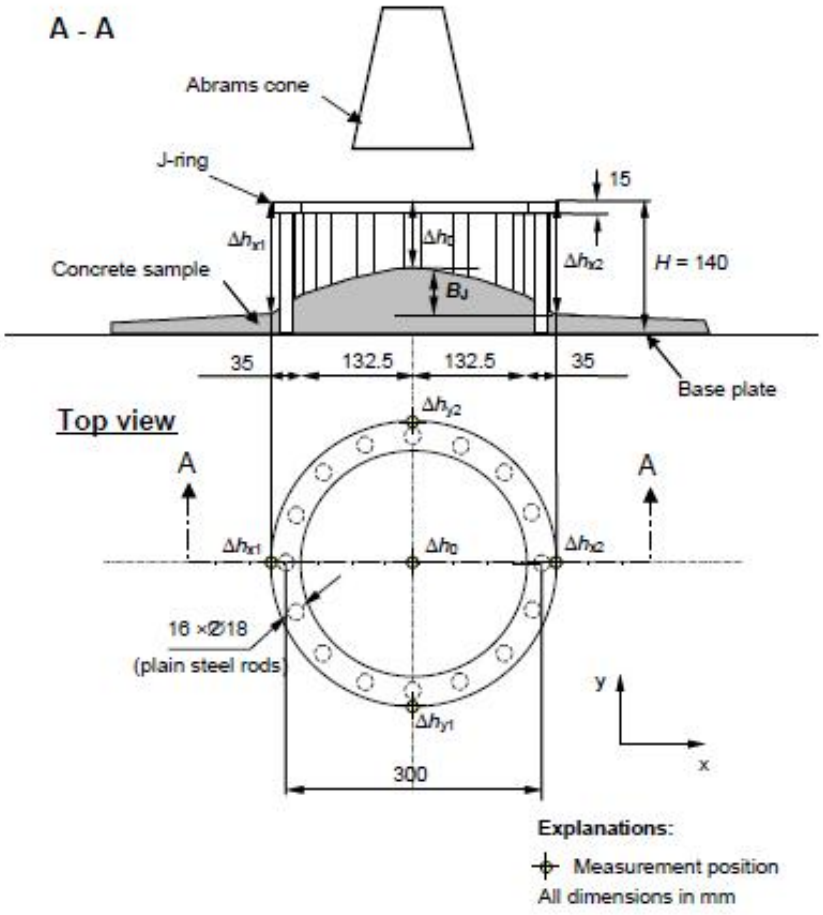

Figure 3.5: J-ring test setup

3.4.3 L-Box Test

This test was first developed to assess the flowability of a fresh underwater concrete mixture by measuring the distance it could flow under its own weight (Schutter et al. 2008). However, no reinforcement was used those days. Currently, the L-Box test is used with reinforcement as blocking the flowable concrete in order to check passing ability of SCC. This test is currently a primary application within the industry.

The L-box apparatus consists of the vertical hollow column of a rectangular cross-section connected to a horizontal trough attached at the bottom. A vertical sliding door separates the horizontal trough from the vertical hollow column. Three 12mm diameter bars were placed immediately behind the separating gate and used as a passing gate, as shown in Figure 3.6.

During the L-Box test, the vertical sliding door was closed and concrete was poured up to the top of the vertical hollow column. The vertical sliding door was lifted gradually and the concrete was allowed to pass through the reinforcing bars before flowing from the column to the horizontal trough. The stop watch was started as soon as the vertical sliding door was lifted, and the time of flow of concrete at T_{20} (20cm from reinforcing bar) and T_{40} (40cm from the reinforcing bar) were recorded. T_{20} and T_{40} are representative of the speed of flow of the fresh concrete. As it stopped flowing, the heights of "H1" and "H2" were measured, as shown in Figure 3.6. The passing ability was calculated as the ratio of H2/H1.

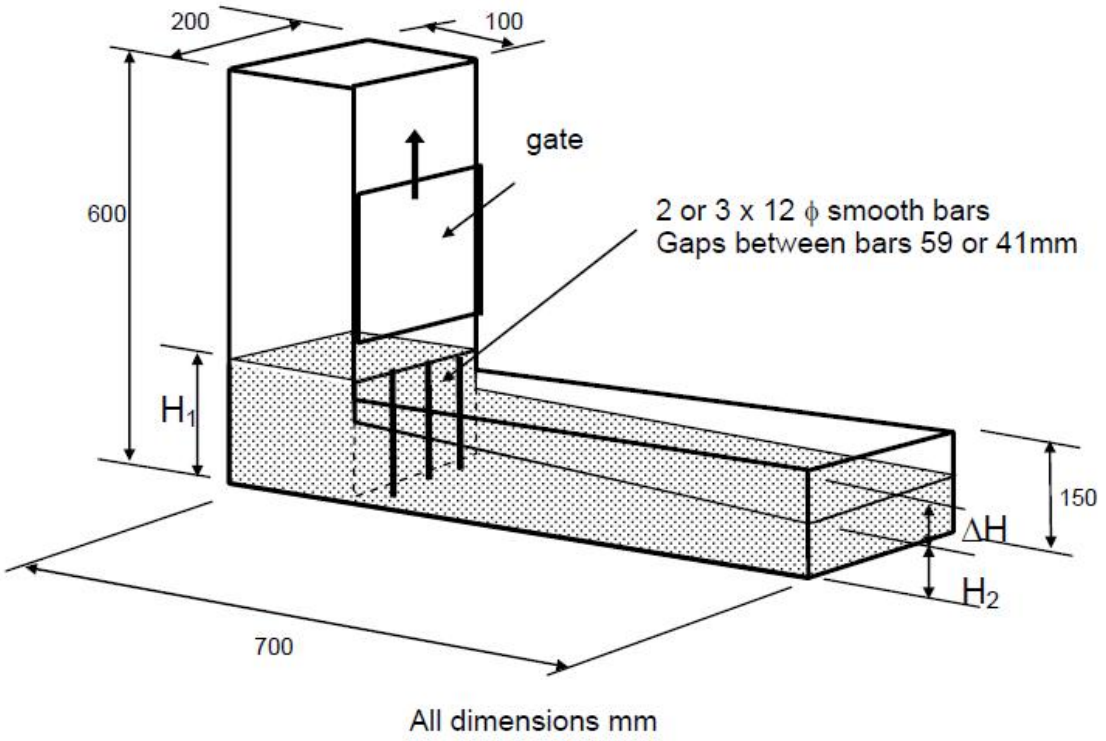

Figure 3.6: General assembly of L-Box test

3.4.4 V-Funnel Test

A V-funnel flow time is used to measure the viscosity and the filling ability of SCC (European SCC Guidelines, 2005). The V-funnel is a container which tapers all the way from top to bottom and is connected to a short length of rectangular pipe, as shown in Figure 3.7. There is also a closing gate attached to the end of the rectangular pipe.

The cleaned V-Funnel was placed on stable, flat ground. Before the test was started, the interior wall of the V-funnel was moistened with a wet towel and an empty bucket was placed underneath. With the gate closed, \ approximately 12 liters of concrete were poured into the V-funnel without compaction. The stop watch was started as soon as the gate opened at the end of the rectangular pipe, and was stopped once daylight showed through the narrow gate of the rectangular pipe from the top. The V-funnel time was recorded as TVF in the nearest 0.1 second.

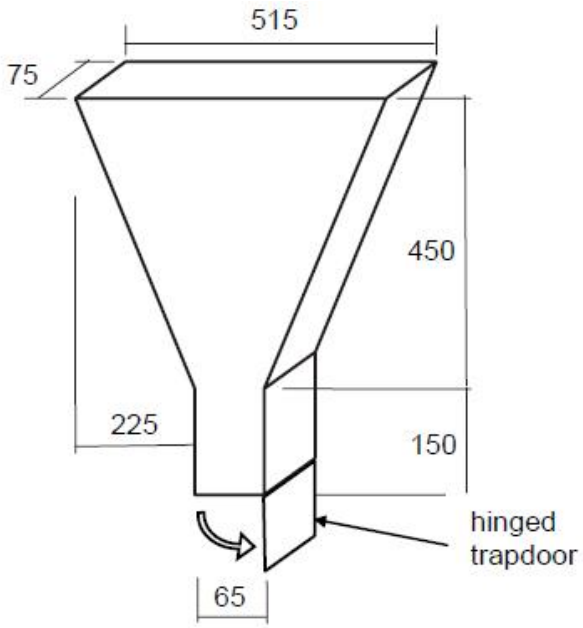

Figure 3.7: V-Funnel apparatus made of steel (dimensions in mm)

3.5 Hardened Properties of Concrete Tests

3.5.1 Mechanical Properties Test

3.5.1.1 Compressive Test

Compressive strength testing was performed after 28 days of curing according to ASTM C39. The capping of concrete cylinders (100mm diameter x 200mm height) was done according to ASTM C617. The compressive machine used in the lab had a capacity of 400,000 lb. For all compressive tests, a medium failure load of range 3 (up to 80,000 lb) was used. Three specimens were tested for each mix and an average of three tests were used to get results.

Figure 3.8: Compressive test on cylinder [Mix ID: 24L2]

3.5.1.2 Flexural Strength Test

An MTS Series 494 machine was used to test the flexural strength of the prism. The test was conducted according to ASTM C78-10, which covers the determination of the flexural strength of concrete by third point loading. The MTS controlled loading rate and load-deformation curve were recorded in the computer system. Beams were 410mm in length, 100mm wide and 75mm long; the test was done as shown in the Figure 3.10 (ASTM C78-10, 2009).

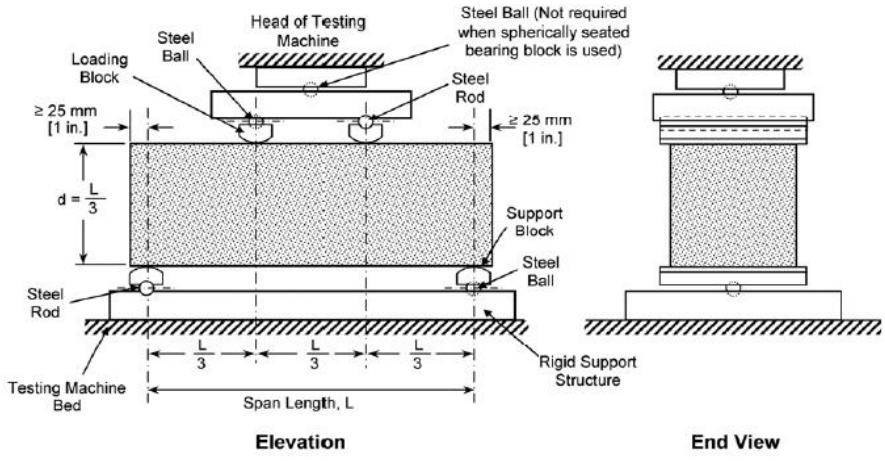

Figure 3.9: Schematic of a suitable apparatus for flexure test of concrete by third-point loading method

Figure 3.10: Test setup for flexural strength test

During testing, all cracks were initiated in the tension surface within the middle third of the span. The modulus of rupture was calculated accordingly using equation 3.1 (ASTM C78-10, 2009).

$$R = (PL)/(bd\text{^}2) \qquad 3.1$$

Where R is the modulus of rupture in MPa, P is the maximum applied load indicated by testing machine in N (Newton), L is the span length in mm, b is the width of specimen in mm and d is the depth of the specimen in mm.

Toughness is an important parameter when dealing with fibrous concrete. According to ACI 544.4R-88, toughness may be defined as the area under the load-deflection curve in the flexural test, which is considered as total energy absorption prior to complete separation of the specimen (ACI Committe 544.4R-88, 1999). The load-deflection curves were recorded in the computer system assembled with the MTS machine and analyzed using ASTM C1018 (American Standard Code), JSCE-SF4 (Japanese Standard Code) and the recently developed post-crack strength (PCS) method.

- ***ASTM C1018***

  The ASTM C1018 standard defines two parameters for the area under the load-deflection curve. First is toughness index [I], which defines the ratio of the area under the load deflection curve (absorbed energy) up to the given deflection and the area under the load deflection curve (absorbed energy) up to first crack. The standard toughness indices are I_5,I_{10}, and I_{20}, as shown in Figure 3.11 (ACI Committee 544.1R-96, 2001). The second

parameter is residual strength, which defines the average post cracking load that the specimen may carry over the specified deflection interval. Residual strengths $R_{5,10}$ and $R_{10,20}$ are calculated using equation 3.2 (Mindess et al., 2003).

$$R_{5,10}=20\,(I_{10}-I_5) \text{ and } R_{10,20}=10\,(I_{20}-I_{10}) \qquad 3.2$$

By definition, toughness indices I_5, I_{10} and I_{20} represent deflection of 3δ, 5.5δ and 10.5δ respectively, as shown in Figure 3.11, where δ is the deflection at the first crack.

For perfectly elasto-plastic behaviour, the values of the toughness indices are: I_5=5, I_{10}=10 and I_{20}=20. These values for fibrous concrete will give the comparative value of toughness, which is related to energy absorbing capacity after the first crack.

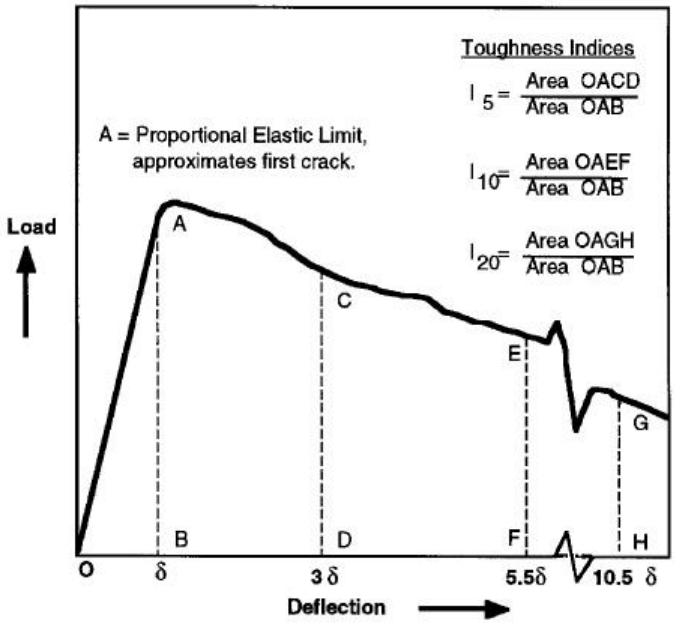

Figure 3.11: Flexural toughness as per ASTM C1018

- ***JSCE-SF4***

JSCE-SF4 was first published in 1984 by the Japanese Concrete Institute (as described in ACI Committee 544.1R-96, 2001 and Banthia and Sappakittipakorn, 2007), and suggests a simple approach to calculate the area under the load-deflection curve up to the specified deflection (δ_{tb} = L/150). The area is referred to toughness (T_b) (Figure 3.12) (ACI Committee 544.1R-96, 2001). The toughness factor or JSCE flexural toughness factor (σ_b) is calculated using Equation 3.3.

$\sigma_b = (T_b \times L) / (bh^2 \times \delta_{tb})$ 3.3

where,

T_b (Toughness) = Area under load-deflection curve [N.mm]

L = length of the span between two supports [mm]

b = breadth of specimen [mm]

h = Height of specimen [mm]

δ_{tb} = End point deflection (L/150) [mm]

The equivalent JSCE flexural strength can be used directly for design purposes, as it reflects the strength at an acceptable deflection (Papworth, 1997).

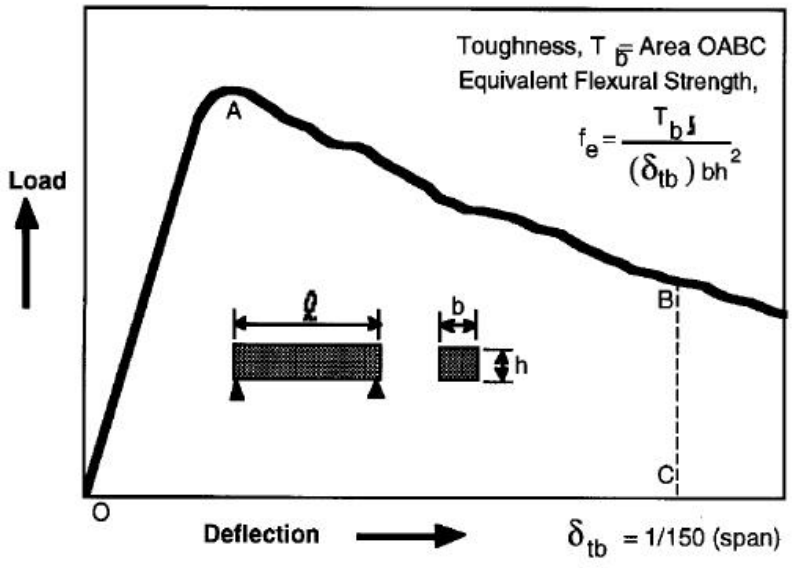

Figure 3.12: Toughness as per JSCE-SF4

- ***PCS Method***

Load-deflection curves are also analyzed using a recently developed post-crack strength (PCS) method, as mentioned by various researchers (Banthia and Sappakittipakorn, 2007; Singh et al., 2010). In the PCS method, the load-deflection curve is translated into the equivalent flexural strength curve. This method is shown in Figure 3.13 below, which divides the curve into two parts from peak load deflection. They are designated as pre-peak energy (E_{pre}) and post-peak energy (E_{post}).

For the beam with a width of B and depth of H, PCS at L/m is expressed as in Eq. 3.4 (Banthia & Sappakittipakorn, 2007).

$$PCS = E_{post,m} / (L / m - \delta_{peak}) \times L / (BH^2) \quad 3.4$$

L/m is referred to as a fraction of the span where 'L' is the beam span from support to support and 'm' has different values ranging from 150 to 3000 (Banthia & Sappakittipakorn, 2007). In this study, PCS strength has been calculated using 10 different points ranging from 0.4 to 2.4mm (L/m). PCS value at peak-load deflection would coincide with a modulus of rupture (MOR) value, as MOR is calculated based on peak load.

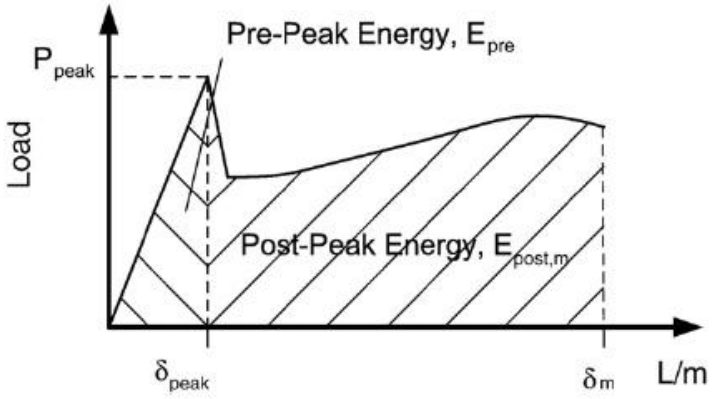

Figure 3.13: PCS method on fibrous concrete beam

3.5.1.3 Bond strength test

A bond strength test was carried out with a pullout test of a reinforcing steel bar embedded in a concrete cylinder. Two specimens of each mix were prepared for the pullout test using a 15M steel bar embedded in a concrete cylinder, with a diameter of 100mm and a height of 200mm. The details of the pullout test setup are shown in Figures 3.14 and 3.15.

A tensile force was applied to the end of the protruding bar and each load increment was recorded by a data acquisition program through a load cell connected to the computer. The ultimate bond stress τ_{avg} is calculated as per equation 3.5 (Abrishami & Mitchell, 1992):

$$\tau_{avg} = T / (\pi \times l_d \times d_b) \quad 3.5$$

where,

T= tension force in the steel [N]

l_d = length of the rebar embedded in concrete [mm]

d_b = diameter of rebar [mm]

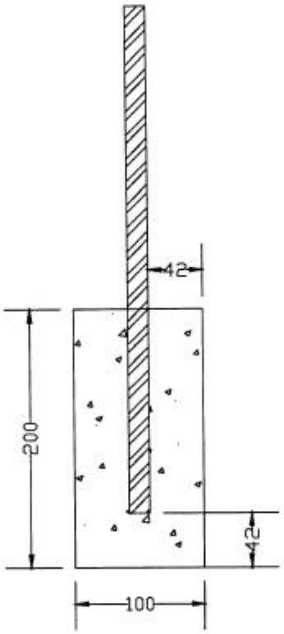

Figure 3.14: Typical pullout test specimen

Figure 3.15: Pullout test setup [Mix ID: 20L2]

3.5.2 Durability Test

3.5.2.1 Rapid Chloride Permeability Test (RCPT)

Low permeability of concrete is a very important parameter regarding the ingression of harmful and aggressive substances such as sulphates, chloride ions, etc. RCPT is one of the most popular tests used to determine the permeability of concrete. The main purpose of the RCPT test is to measure the electrical conductivity of concrete to present a rapid indication of its resistance to chloride ion penetration as per ASTM C1202-10.

In this study, concrete specimen setup and classification of permeability resistance were followed as per ASTM C1202-10 (Figure 3.16 and Table 3.7). Two specimens of each mixture were cut in the middle portion with 51±3mm height and 100mm diameter.

Special attention was taken before starting the RCPT test. First, specimens were placed in a sealed dessicator and vacuumed for three hours. After the three hours, with the vacuum pump still running, the distilled water was allowed to run inside the dessicator by turning the stopcock on until the specimens were fully submerged in the distilled water. After the addition of the distilled water, the vacuum pump was allowed to run for one more hour, then air was allowed to enter the dessicator. The specimens were left submerged inside the dessicator for another 18±2 hours.

The specimens were then removed from the dessicator; excess water was removed with a paper towel, a rubber gasket was mounted on both side of each specimen and each unit was fixed within the test chamber. Each test chamber has two cells. One cell was filled with 3% NaCl solution and other with a sodium hydroxide (0.3N NaOH) solution. A DC power source with 60V was applied in the chamber, with the negative terminal connected to the NaCl and the positive terminal connected to the NaOH solution, providing a path for the negatively charged chloride ions to migrate towards the positive terminal. The total charge migrated at six hours was measured automatically by a computerized measuring system. Based on the total charge passed in six hours, measured in Coulombs, chloride ion permeability was determined.

Table 3.7: Chloride ion penetrability based on charged passed in Coulombs

Charged Passed (Coulombs)	**Chloride Ion Penetrability**
>4000	High
2000-4000	Moderate
1000-2000	Low
100-1000	Very Low
<100	Negligible

Figure 3.16: RCPT test setup showing specimen in dessicator and during testing

3.5.2.2 Freezing and Thawing Resistance

Resistance through freezing and thawing is an important parameter for the durability of concrete, especially in cold climates. Therefore, studying the durability of concrete in the laboratory using rapid freezing and thawing cycles provides important information regarding the deterioration of concrete in cold climates. ASTM C666-03 is the most common test procedure for evaluating the basic deterioration mechanism for internal damage following repeated exposure to freezing and thawing cycles. There are different parameters related to concrete deterioration, such as water/cement ratio, cement content, type of cement, mineral admixture, freezing temperature, rate of freezing, and air entrainment (Schutter et al., 2008). Although this test (ASTM C666-03) provides valuable information on frost resistance, the complex behaviour of concrete exposed to severe cold climates cannot be entirely understood using this test.

Two 410 x 100 x 75mm concrete prisms from each mix were used. The freezing and thawing apparatus used for this test was a special chamber in which specimens were subjected to specified freezing and thawing cycles. Prior to the test, concrete prisms were fully saturated in the water tank. The initial weights of saturated prisms in surface dried (SSD) condition were measured before starting the test. The prisms were then placed in steel boxes and completely soaked with water. A low temperature was generated through a box placed underneath the steel box, and thawing was generated using electrical elements in the middle of the steel box (Figure 3.17).

According to ASTM C666, “The nominal freezing and thawing cycle shall consist of alternately lowering the temperature of the specimens from 40 to 0^{o}F (4 to -18^{o}C) and raising it from 0 to

40°F (-18 to 4°C) in not less than 2 hours and not more than 5 hours." Total cycles must be set to 300.

In every 60 cycles weight loss was calculated in an SSD condition. A standard flexure strength test (ASTM C78-10) was carried out followed by 300 cycles of freezing and thawing in order to compare samples with the specimens not having undergone freezing and thawing cycles.

Figure 3.17: Freeze-thaw test setup

3.5.2.3 Corrosion Test

A conventional corrosion test usually requires a long testing time and is quite expensive. There are three major types of corrosion tests: laboratory tests, field tests and service tests. A service test is the most reliable, followed by the field test. However, they are expensive and time consuming. Laboratory testing with the rapid accelerate corrosion test, however, offers qualitative data in a short period of time. Many researchers have successfully used an accelerated corrosion test in the laboratory. The typical experimental setup for an accelerated corrosion test is illustrated in Figure 3.18.

The accelerated corrosion test setup consisted of a plastic tank, an electrolyte solution (5% sodium chloride (NaCl) by the weight of the water), a steel mesh and an insulated square bracket. A cylindrical specimen with a 16mm diameter steel bar was placed on top of the steel mesh with an insulated square bracket underneath. A DC power supply with a constant 12V was connected to the top of the steel bars and the bottom of the steel mesh. The path of the current was arranged in such a way that the steel mesh was connected to the negative terminal of the DC power supply and the steel bars of the concrete specimen were connected to the positive terminal. Two

specimens of each mix were used in the experiment. The current was measured manually on a daily basis. The first four sets of specimens with steel fiber percentages of 2.4%, 2.0%, 1.6% and 1.2% by volume of concrete were taken from the corrosion tank after 39 days, when specimens were showing slight corrosion stains and hair line cracks. In order to get a relative comparison of different mixtures by fiber volume fraction, the remaining set of specimens (0.8%, 0.4% and 0%) was placed in the corrosion tank as per the first set of specimens.

After the corrosion test, each specimen was tested for bond strength using the standard pullout test. An end grinder with a wire brush was used to remove the rust from the corroded bars and the final mass of the bars were determined.

The theoretical mass loss of the reinforcing bars was calculated based on Faraday's equation (3.5) (Ijsseling, 1986).

$$\Delta M_{theoritical} = (t \times I \times M) / (z \times F) \qquad 3.5$$

where,

t = time (sec)

I = current (average current induced)

M = atomic weight of iron (55.847 gm/mole)

Z = ion charge (assumed 2 for $Fe \rightarrow Fe^{2+} + 2e^{-}$)

F = Faraday's constant (96487 Ampere.sec)

Experimental mass loss (ΔM_{actual}) was determined from Equation 3.6

$$\Delta M_{actual} = (W_i - W_f)/W_i \times 100 \qquad 3.6$$

where,

W_i = Initial mass of steel bar before corrosion

W_f = Final mass of steel bar after corrosion

Figure 3.18: Rapid corrosion test setup

3.5.2.4 Water Absorption and Porosity test

There is a wide range of simple experimental techniques that can be used to determine the water absorption and porosity of concrete. One of the methods to measure water absorption and apparent porosity is ASTM C948-81 (2009). The apparatus required for the experiment is balance sensitive to 0.025% of the mass of the specimen; a container suitable for immersing the specimen with a wire is used for suspending the specimen in water.

Two specimens of each mixture were cut into cylindrical shapes 100mm in diameter and 50±3mm high. The specimens were immersed in water for 24 hours, showing both faces of each specimen in order to expose a maximum surface area. The temperature of the water was approximately 21^{o}C. The mass of the SSD of the specimen was observed and designated as B. The mass of each specimen suspended in water was also measured and designated as A. Specimens were then placed in an oven at a temperature of 100 to 110^{o}C (212 to 230^{o}F) for at least 24 hours. After removal from the oven, they were allowed to cool down at room temperature, and the oven dried mass of the specimen was observed and designated as C.

The water absorption and apparent porosity were calculated using Equations 3.7 and 3.8: (ASTM C948-81, 2009)

$$\text{Water absorption (\%)} = (B-C)/C \times 100 \qquad 3.7$$

$$\text{Apparent porosity (\%)} = (B-C)/(B-A) \times 100 \qquad 3.8$$

where,

A = Immersed mass, gm

B = Saturated surface dry mass (SSD), gm

C = Oven-dry mass, gm

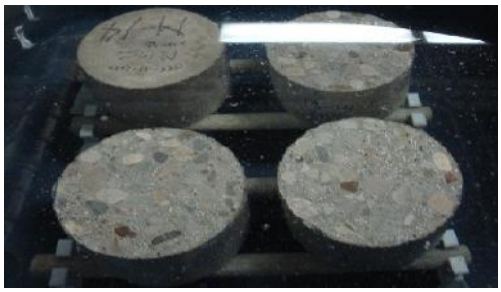

Figure 3.19: Test setup for water absorption and porosity tests

3.5.2.5 Water Sorptivity Test

In general, there are two mechanisms involved in concrete's ability to transport water: permeability and sorptivity. By definition, water sorptivity is the rate of absorption of water into the concrete by capillary suction, and permeability is the measure of water movement under hydraulic pressure in a saturated porous medium. Although water sorptivity is similar to permeability, they cannot be correlated with each other. The testing of uni-directional water absorption rate is described in ASTM C1585-04.

Two specimens of each mixture were prepared as per ASTM C1585. The test specimens were kept at constant temperature prior to testing. Special care was taken by sealing all sides of the specimens with adhesive aluminum foil in order to avoid any moisture absorption from the surrounding environment. Before testing, the mass of the specimens were measured to the nearest 0.01 gm and recorded as an initial mass for water absorption calculation. In addition, the specimen diameters were also measured to the nearest 0.1mm. Supporting devices were placed at the bottom of a pan, and water was added up to 1 to 3mm above the supporting device. The test setup is illustrated in Figures 3.20 and 3.21 (ASTM C1585-04, 2004).

A stop watch was started as soon as the specimen rested on top of the supporting device. As per the time specified by the ASTM standard, the specimen was removed from the water and the exposed surface was immediately wiped off with a paper towel and the mass were recorded. This process was continued for several time intervals over six hours on the first day and was recorded as an initial absorption rate. After initial absorption, the mass of each specimen was recorded every 24 hours prior to the start of the test for six days and used as a secondary absorption rate.

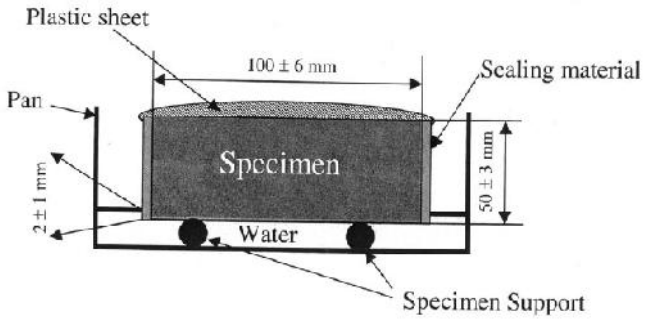

Figure 3.20: Schematic of the sorptivity procedure

Absorption I [mm] is calculated by a change in the mass of a specimen divided by the product of the cross-sectional area of the specimen and the density of water. The formula is as follows (ASTM C1585-04, 2004):

$$I = m_t / (a*d) \qquad 3.9$$

where,

I = absorption, mm

m_t = the change in mass of specimen in grams, at different time t.

a = the exposed area of the specimen, in mm^2, and

d = the density of the water in g/mm^3

Figure 3.21: Test setup for water sorptivity test

Chapter 4

Results and Discussions

4.1 Introduction

This chapter covers results and discussion of fresh properties (slump flow, slump flow time, and passing ability), mechanical properties (compression, flexure and bond strength) and durability (RCPT, water absorption rate, water absorption and porosity, corrosion and freeze-thaw cycles). A total of 13 concrete mixtures were developed with two different geometric shapes and fiber lengths. Table 4.1 describes the concrete mixture ID with two different types of fibers and percentages by volume.

Table 4.1: Concrete mixture ID representing different types of fiber and volume percentage

Mix No	**Mix ID**	**Fiber Type and Volume %**		**Comments**
		Length (L1):13mm Aspect Ratio (AR1): 65	**Length (L2): 25mm Aspect Ratio (AR2): 50**	
M08/01	0 Fiber	**0.00**	**0.00**	**Control SCC**
M02	4L1	**0.40**	0.00	Short steel fiber
M03	8L1	**0.80**	0.00	
M04	12L1	**1.20**	0.00	
M05	16L1	**1.60**	0.00	
M06	20L1	**2.00**	0.00	
M07	24L1	**2.40**	0.00	
M09	4L2	0.00	**0.40**	Long steel fiber
M10	8L2	0.00	**0.80**	
M11	12L2	0.00	**1.20**	
M12	16L2	0.00	**1.60**	
M13	20L2	0.00	**2.00**	
M14	24L2	0.00	**2.40**	

In the mixture ID of SFRSCC, the first number represents the percentage of fiber by volume, and the letter followed by the second number represents length. As shown in Table 4.1, the fiber volume fraction ranges from 0% to 2.4% by volume.

4.2 Fresh Properties

Fresh properties are also referred to as workability of the SFRSCC. The results of the slump flow, J-ring test, L-Box test and V-funnel test are summarized in Table 4.2.

Table 4.2: Workability properties of all concrete mixtures:

Mix No	Mix ID	Slump Flow		J-Ring			L-Box	V-Funnel
		Flow dia SF (mm)	T50 (Sec)	Flow dia SFj (mm)	T50j (Sec)	Blocking step (BJ) (mm)	PR (H2/H1) %	TVF (Sec)
M08/01	**0 Fiber**	690	3.50	655	4.40	20	94	13.00
M02	**4L1**	730	3.68	620	8.20	28	97	12.46
M03	**8L1**	700	5.10	685	6.20	15	97	16.62
M04	**12L1**	705	3.56	555	5.19	28	87	38.13
M05	**16L1**	690	5.90	540	11.90	61	63	33.88
M06	**20L1**	N/A	N/A	N/A	N/A	N/A	N/A	N/A
M07	**24L1**	N/A	N/A	N/A	N/A	N/A	N/A	N/A
M09	**4L2**	730	5.30	655	7.30	27	N/A	17.70
M10	**8L2**	690	6.10	585	16.60	48	N/A	17.70
M11	**12L2**	715	6.90	600	17.80	43	N/A	43.20
M12	**16L2**	710	7.70	585	19.20	53	N/A	45.50
M13	**20L2**	680	7.40	555	18.40	50	N/A	46.50
M14	**24L2**	650	13.50	N/A	N/A	N/A	N/A	N/A

Note: N/A (unable to perform the test)

4.2.1: Slump Flow test results

- **Slump Flow Diameter (SF)**

There are three categories of results (as shown in Table 2.1 of Chapter 2), namely: SF1 (550-650mm), SF2 (660-750mm) and SF3 (760-850mm). Table 2.1 clearly shows that the minimum SF diameter needed to create satisfactory SCC is 550mm (European SCC Guidelines, 2005). Typical slump flow spread is illustrated in Figure 4.1.

Figure 4.1: Flow diameter (Mix ID: 20L2AR2)

All mixtures show a slump flow diameter between 660-750mm and fall into the SF2 category. This shows that all mixtures have enough deformability under their own weight and hence, can be suitable for normal applications such as in walls and columns.

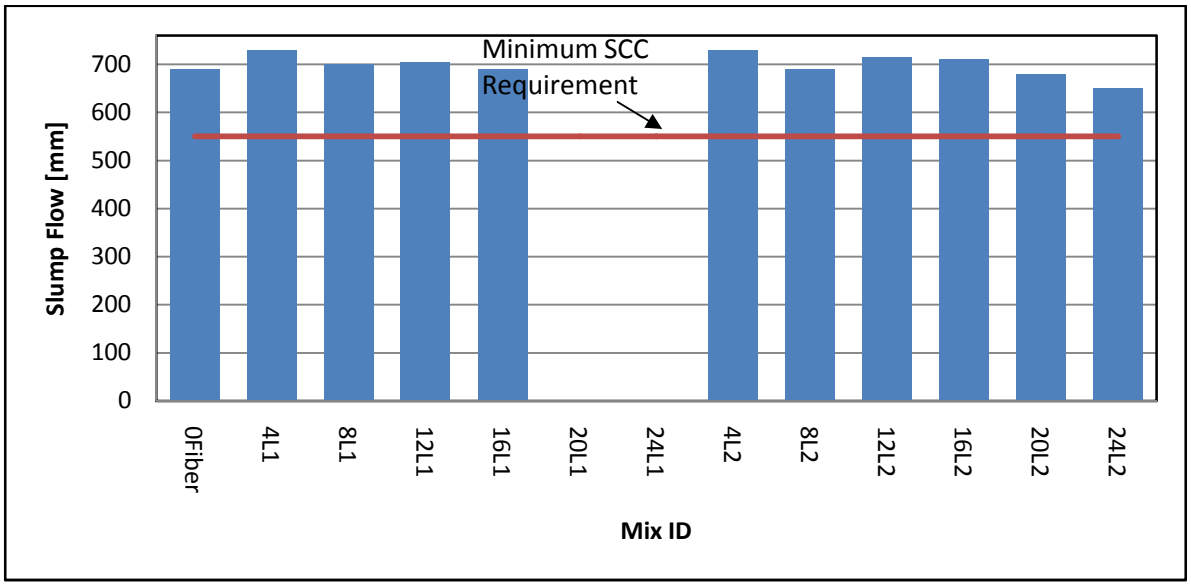

Figure 4.2: Slump flow diameter for all mixtures

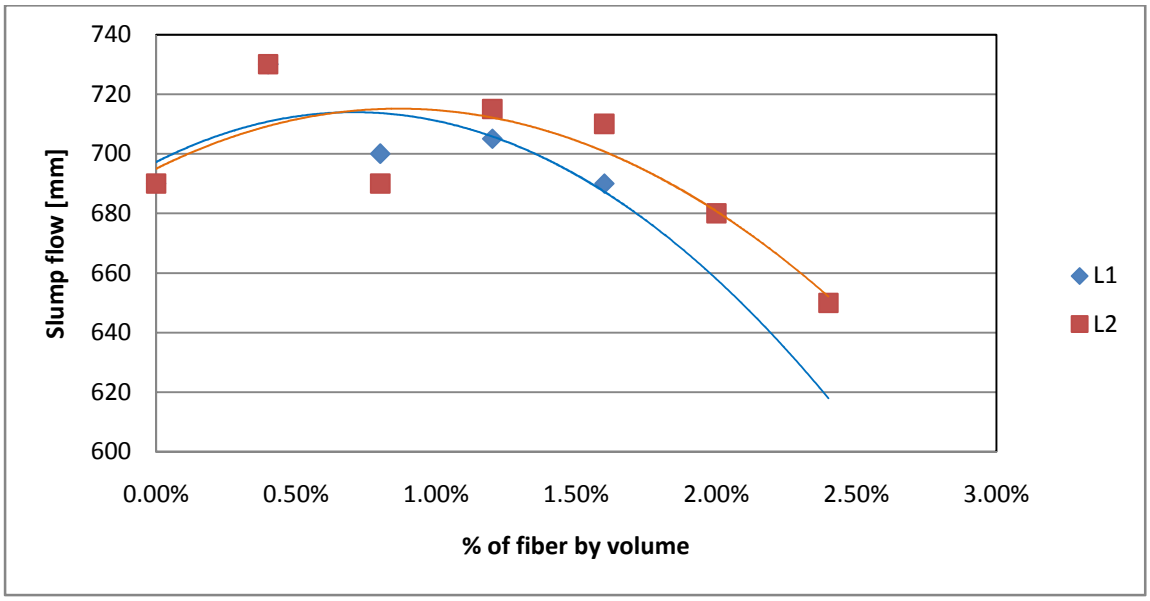

Figure 4.3: Effect of steel fiber volume fraction on slump flow diameter

Figures 4.2 and 4.3 show a decrease in slump flow diameter as steel fiber volume fraction increases for both long and short steel fibers. The studies done by Grunewald and Walraven (2001) and Sahmaran et al. (2005) also show a similar trend. However, incrementing the fiber volume fraction up to 1.2% does not result in significant change in slump flow. In fact, a significant decrease in slump flow diameter has been observed beyond 1.2% fiber volume fraction. This might be due to the effect of the higher number of steel fibers as well as higher internal resistance of the steel fibers in fresh concrete mixtures. No slump flows for concrete mixtures with shorter steel fibers with 2.0% and 2.4% (Mix ID: 20L1 and 24L1) fiber volume fraction have been observed. This might be due to the detrimental effect of the higher amount of short steel fibers in fresh concrete mixture compared to concrete mixtures with long steel fiber for the same fiber volume fraction.

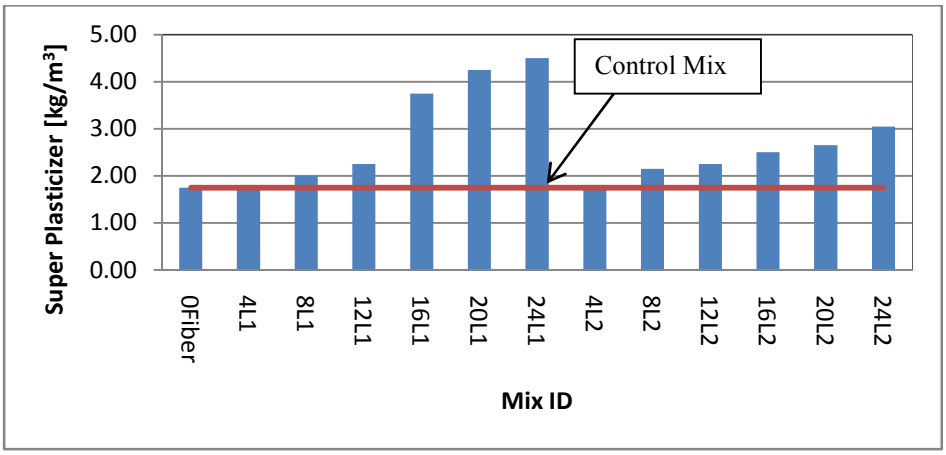

Figure 4.4: Use of super plasticizer for concrete mixtures

Figure 4.4 shows that the demand of super plasticizer (SP) increases with steel fiber volume fraction. This is also confirmed in the study done by Khayat and Roussel (2000). Significant SP increases in concrete mixtures with short steel fiber beyond 1.2% of fiber volume fraction have been observed, which indicates the effect of higher amounts of short steel fiber in concrete mixtures beyond 1.2% of fiber volume fraction. Higher SP content is needed when fiber volume fraction increases in order to maintain self-consolidated behavior of fibrous concrete mixtures. However, higher amounts of SP also lead to segregation of concrete mixtures. Thus, in this study, SP was added little by little until the desired self-consolidated character of concrete mixture was achieved.

- **Slump Flow Time (T50)**

During the slump flow test, the time required to reach the 500mm diameter was also measured and recorded as T50 (sec) (Slump Flow Time), which indicates the viscosity of the concrete. According to the European Guidelines (2005), SCC can be classified as VS1 for T50≤ 2 sec or VS2 for T50> 2 sec.

Figure 4.5 shows the effect of fiber inclusion on T50 time compared to the control mixture. Increase in fiber volume fraction increases the T50 measurement. All the mixtures, including the control, are in the VS2 class which is characterized by the viscosity of the concrete with high segregation resistance. Figure 4.6 shows the increment of T50 measurement with the increase of fiber dosages for both the long and short steel fiber. However, the short steel fiber shows lower

T50 measurement than the longer steel fiber for the same fiber volume fraction. This trend has also been reported by Sammour (2008), and may be due to higher internal resistance to flow for longer steel fibers compared to short ones. Figure 4.7 illustrates the general trend of T50 and flow diameter. As slump flow diameter increases, T50 measurement decreases as expected and reflects a linear relationship.

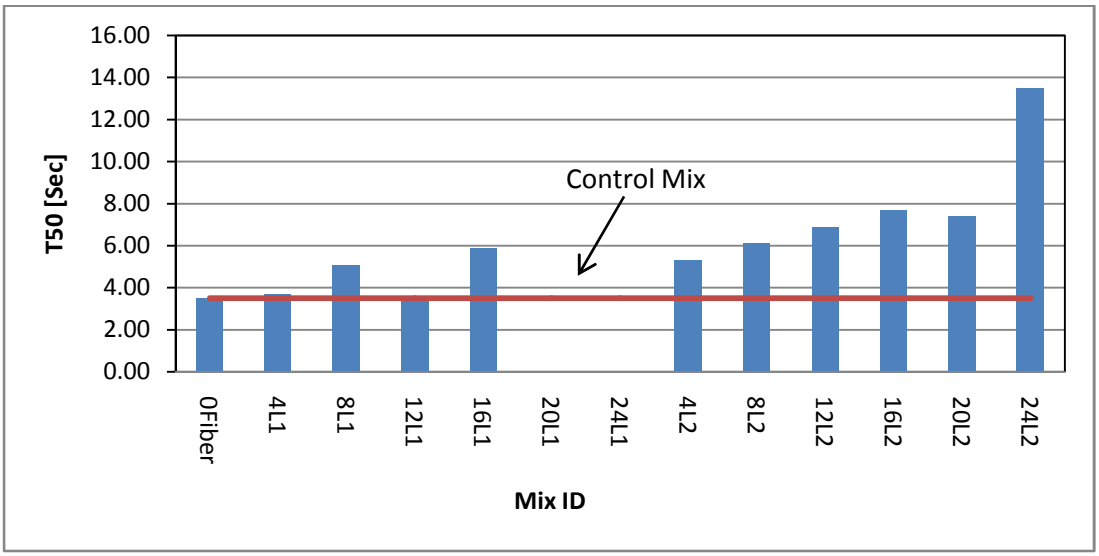

Figure 4.5: Slump flow time (T50) of all concrete mixtures

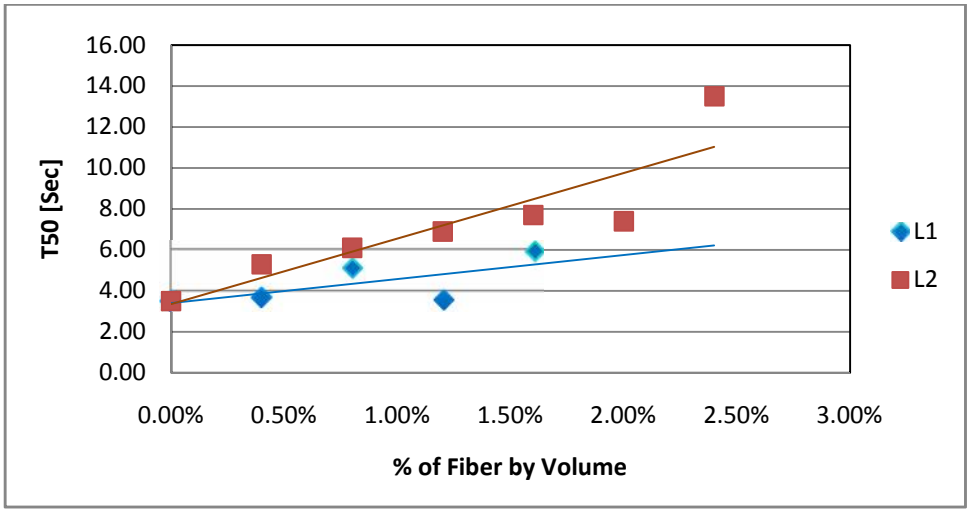

Figure 4.6: Effect of steel fiber volume fraction on T50 measurement of slump flow

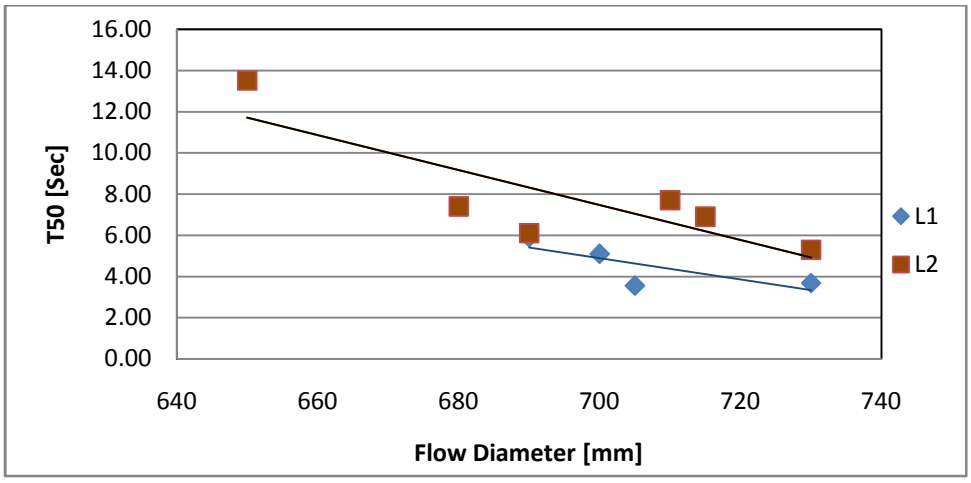

Figure 4.7: Relationship between T50 and slump flow diameter

4.2.2 J-ring Test Results

- **Slump Flow Diameter of J-ring (SFj)**

This test investigates both the filling ability and the passing ability of SCC. Filling ability is similar to slump flow diameter; classes are shown in Table 2.3. Based on the slump flow diameter of the J-ring test, SCC is classified into three categories: SFJ1 (550-650mm), SFJ2 (660-750mm), and SFJ3 (760-850mm) (Shutter, 2005). The J-ring flow diameter provides information on restricted flowability of SCC due to the blocking effect of reinforcing bars.

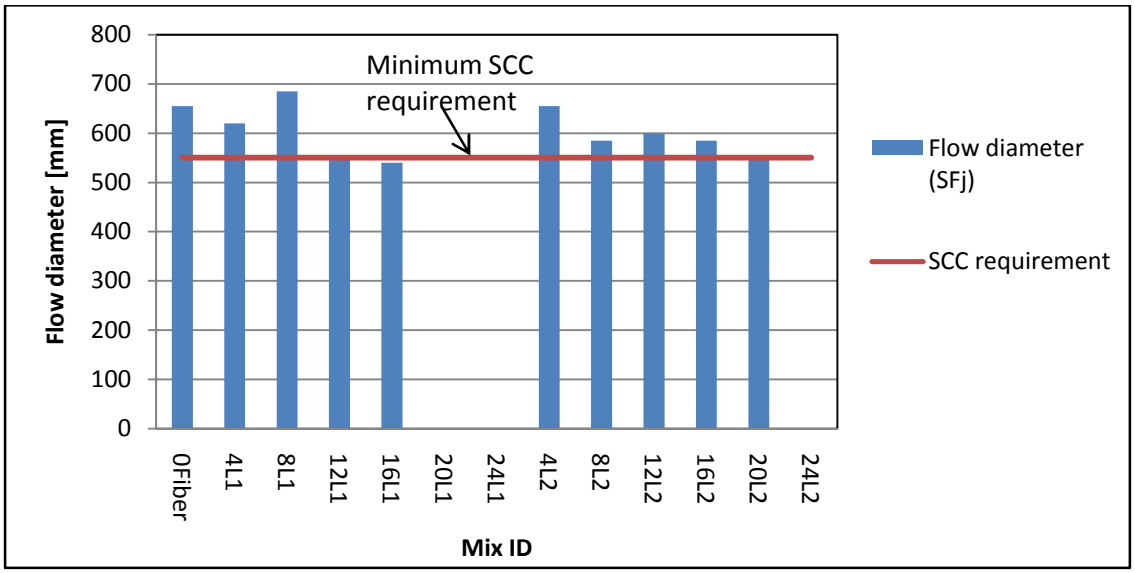

Figure 4.8: J-Ring slump flow diameter for all concrete mixtures

Figure 4.8 shows that the control mixture is in the class SFJ2 and has good filling ability. In addition, the percentage of fiber volume fraction beyond 1.2% shows low filling ability, which might be due to an increase in the internal resistance to flow.

Figure 4.9 shows that an increase in fiber volume fraction decreases the slump flow diameter of the J-ring test, which is similar to the regular slump flow test.

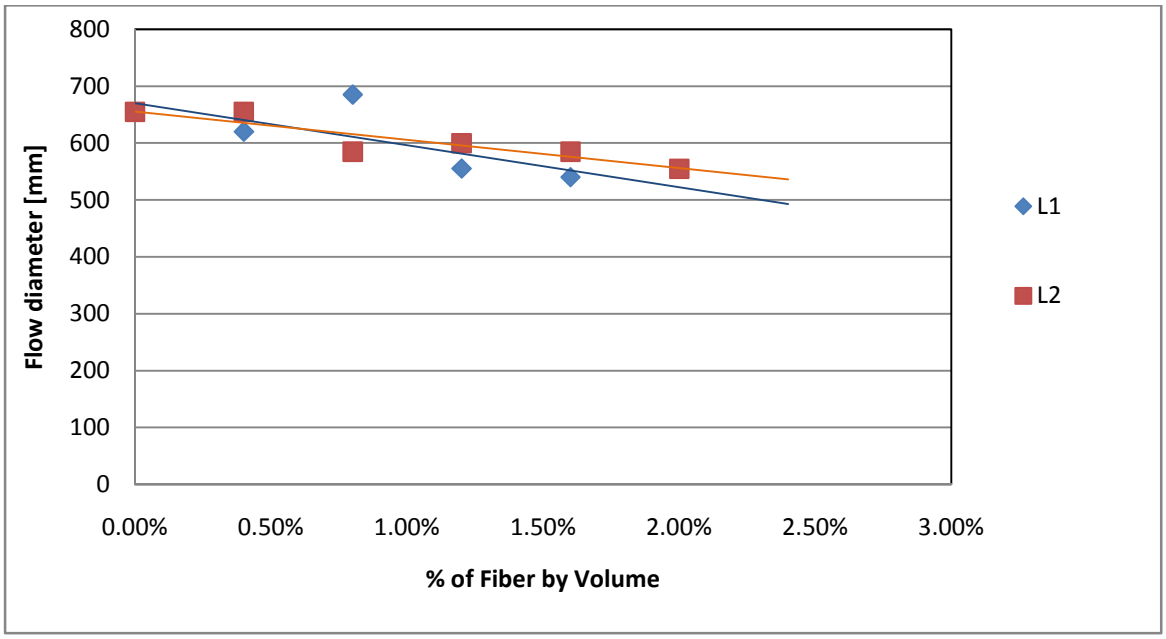

Figure 4.9: Effect of steel fiber volume fraction on the slump flow diameter of J-ring test

Slump Flow time for J-ring (T50j)

The slump flow time for the J-ring test (also called T50j) indicates the rate of deformation with specified flow distance. In general, T50j is higher than the normal slump flow time T50, as flow is restricted by the reinforcing bars.

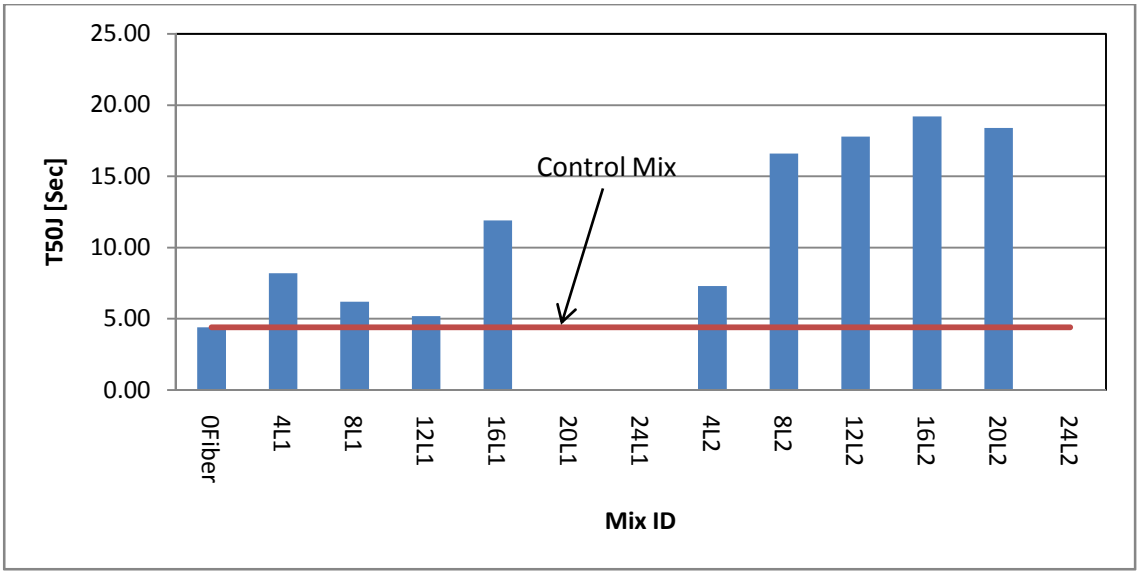

Figure 4.10: Slump flow time (T50J) of all concrete mixtures

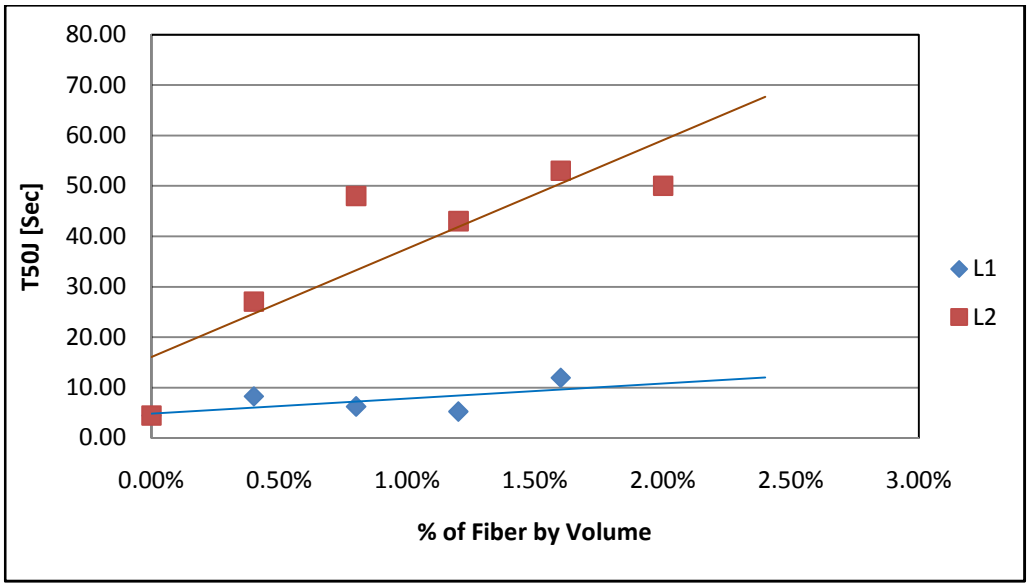

Figure 4.11: Effect of steel fiber volume fraction on T50j

Like the T50 time for slump flow test, the T50j time measurement for J-ring test gets longer with increased fiber volume fraction for all concrete mixtures. In addition, the short steel fibers show lower T50j time than the long steel fibers for the same percentage of fiber volume fraction, as expected. This may be due to the higher internal resistance to flow for the longer steel fibers in comparison to the short ones, and also due to the clustering effect of longer steel fibers in the narrow opening of the J-rings.

- **Blocking Step BJ: Passing ability**

The blocking step (BJ) from the J-ring test provides information on the passing ability of SCC when fresh concrete passes through the reinforcing bars. The range of BJ varies from 3-20mm (Schutter et al., 2008); classes are shown in Table 2.4.

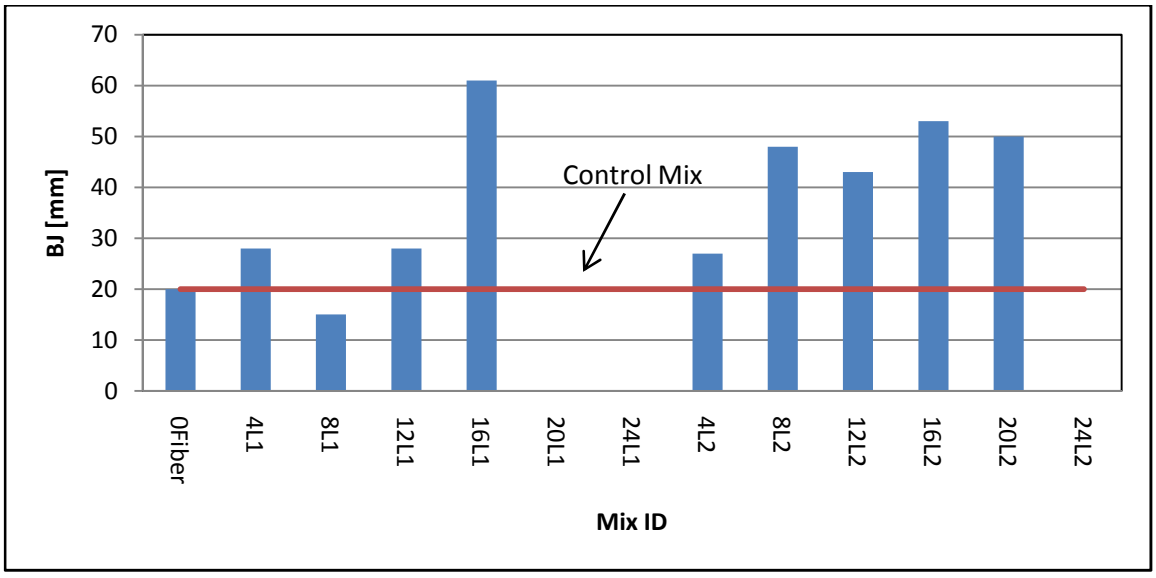

Figure 4.12: Blocking step BJ of all concrete mixtures

Figure 4.12 shows that BJ increases with increasing fiber volume fraction in both long and short steel fibers. Moreover, the concrete mixtures with the longer steel fibers have higher BJ in comparison to the shorter steel fibers for the same fiber volume fraction. This proves that the longer steel fibers have higher internal resistance to flow than the shorter ones and also shows the clustering effect of longer steel fibers in the narrow opening of the J-rings.

4.2.3 L-box: Passing Ability

The L-box test indicates the passing ability of SCC through the reinforcing bar. According to European Guidelines for SCC (2005), a passing ratio (H2/H1) of more than 80% represents good passing ability. The classes of passing ability for the L-Box test are shown in Table 2.5.

Generally, the passing ratio (PR) of L-box decreases with the increase in fiber volume fraction, as shown in Figures 4.13 and 4.14. Figure 4.13 shows no result for the longer steel fibers, as the passing ability of the concrete is severely blocked due to the clustering effect of the longer steel fibers in the narrow gaps of reinforcing bars. However, J-ring tests shows passing ability with higher blocking steps (BJ) for the concrete mixture with long steel fibers up to 2.0% fiber volume fraction. This may be because of less clustering effect around the J-rings as concrete flows horizontally in all directions, compared to more clustering tendency of the concrete mixture around the narrow reinforcing bar of the L-Box. Even concrete mixtures with small steel fibers with a fiber volume fraction higher than 1.2% show no passing ability. This implies that a

higher volume fraction beyond 1.2% for short steel fibers did not satisfy the passing ability of fibrous concrete. Therefore, only concrete mixtures with short steel fibers up to 1.2% volume fraction can be considered as SFRSCC.

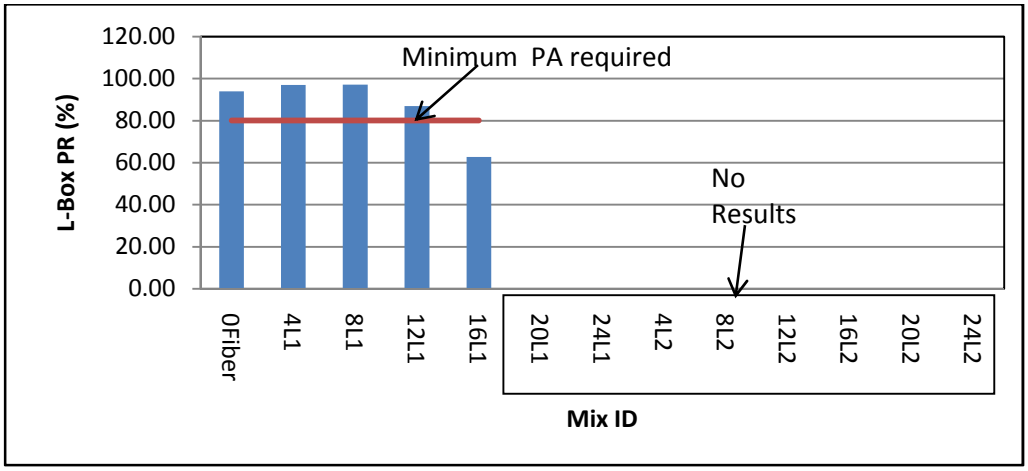

Figure 4.13: L-Box passing ratio (PR) of all concrete mixtures

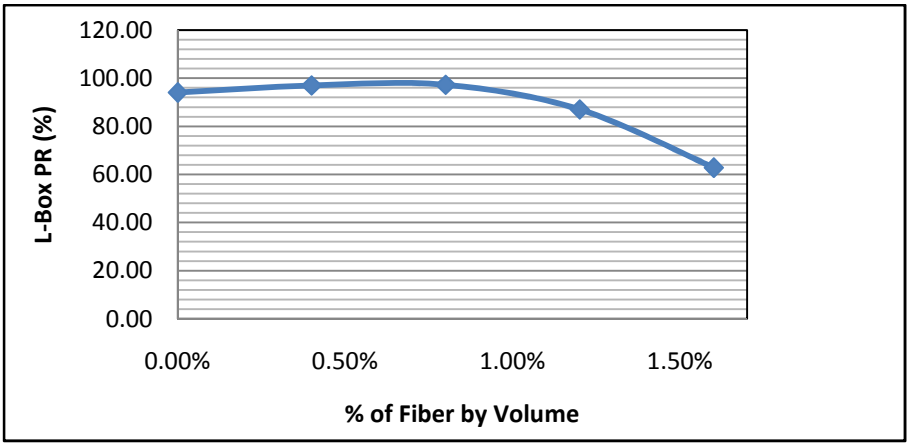

Figure 4.14: Effect of fiber volume fraction on L-Box passing ratio (PR) for concrete mixtures with short steel fibers

Figure 4.15 shows the relationship between the L-Box PR (%) and the slump flow diameter (SF) for concrete mixtures with short steel fibers. The PR increases as slump flow diameter increases, as expected. This is also confirmed in the study conducted by Sammour (2008).

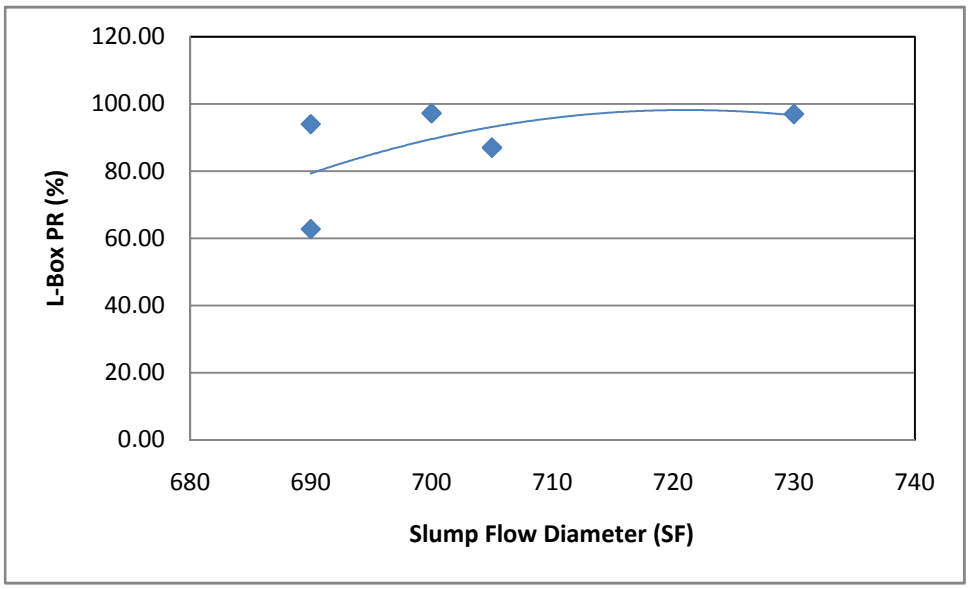

Figure 4.15: Relationship between L-Box passing ability and slump flow diameter for L1 (Concrete mixtures with short steel fibers).

4.2.4: V-Funnel Time (TVF)

The V-Funnel Time [TVF (Sec)] represents the filling ability of the concrete mixtures and measures their viscosity. Table 2.3 shows the classes of filling ability as per European Guidelines for SCC (2005). Based on the flow time, SCC is classified into two categories: VF1 (≤ 8 sec) and VF2 (9-25 sec) (European SCC Guidelines, 2005).

Figures 4.16 and 4.17 show that an increase in the fiber volume fraction increases TVF time. A significant increase in TVF time beyond 0.8% of fiber volume has been observed in concrete mixtures with both long and short steel fibers. This shows the effect of the higher amounts of steel fibers and also illustrates the clustering effect of steel fibers in the narrow opening of the V-Funnel at the bottom beyond 0.8% of the fiber volume fraction (for both long and short steel fibers). Moreover, the trend lines in Figure 4.18 show that TVF time for the longer steel fibers is higher than that of the shorter steel fibers for the same fiber volume fraction. This may be because of the high possibility of the clustering effect for the longer steel fibers over the shorter ones in the narrow opening at the bottom of the V-funnel.

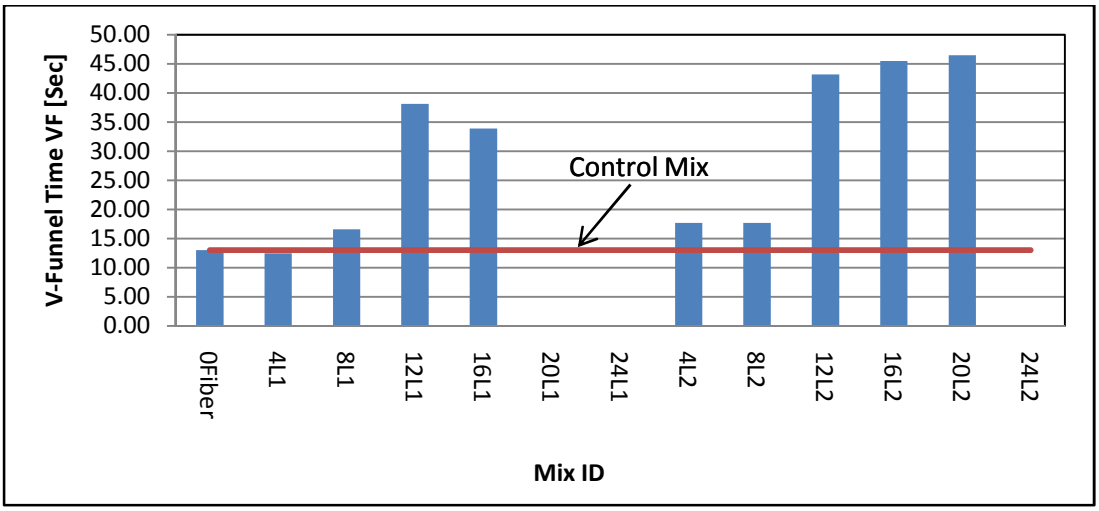

Figure 4.16: V-Funnel flow time (TVF) for all concrete mixtures

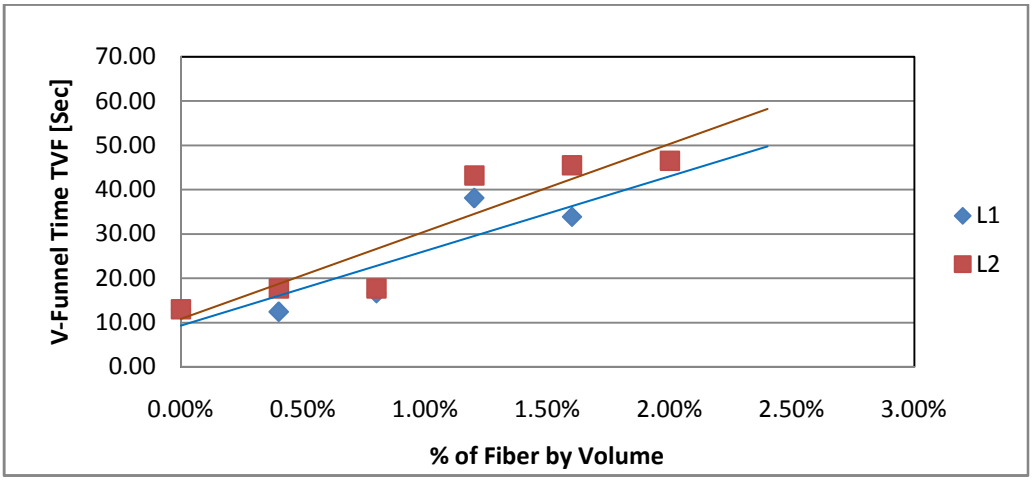

Figure 4.17: Effect of fiber volume fraction on V-Funnel time (TVF)

Summary of Fresh Properties Test

The workability of concrete mixtures with short steel fibers is higher than for the longer ones for same percentage of fiber volume fraction. Moreover, concrete mixtures with short steel fibers up to 1.2% fiber volume fraction can be considered SFRSCC as they have passed all fresh properties tests. Besides that, all concrete mixtures with long steel fibers and those with short steel fiber beyond 1.2% fiber volume fraction can be considered fibrous concrete.

4.3 Mechanical Properties

To determine mechanical properties, compressive strength, flexural strength and bond strength tests were performed. Summaries of the mechanical properties tests are illustrated in Table 4.3 below. The density of concrete with short steel fibers varies from 2319 to 2544 Kg/m^3. With long steel fibers, it varies from 2319 to 2525 Kg/m^3. The density of the concrete mixture gradually increases within the fiber volume fraction, as expected.

Table 4.3: Mechanical properties of all concrete mixtures

Mix No.	Mix ID	Comp. Strength [MPa]	MOR [MPa]	Bond Strength [MPa]	JSCE FT at δ=2.4mm [MPa]	Post crack strength (PCS) at L/m=2.4mm [MPa]	Density [Kg/m^3]
M08/01	**0 Fiber**	52.3	4.68	4.95	N/A	N/A	2319
M02	**4L1**	53.5	4.12	11.46	2.99	3.44	2428
M03	**8L1**	65.2	5.95	16.91	4.22	4.81	2436
M04	**12L1**	66.6	6.20	14.57	5.01	5.80	2469
M05	**16L1**	64.5	8.91	15.00	5.90	7.45	2480
M06	**20L1**	68.6	7.95	16.69	7.42	9.38	2490
M07	**24L1**	75.7	9.18	16.41	6.08	8.55	2544
M09	**4L2**	53.9	5.77	11.18	3.23	3.66	2340
M10	**8L2**	53.8	5.69	12.66	3.81	4.67	2384
M11	**12L2**	56.6	7.66	15.63	4.28	5.50	2386
M12	**16L2**	54.4	9.71	16.27	6.15	9.06	2416
M13	**20L2**	52.1	8.46	14.85	6.47	8.07	2493
M14	**24L2**	58.5	10.63	17.05	8.04	10.95	2525

Note: FT: Flexural toughness

4.3.1 Compressive Strength

After investigating the compressive strength of all mixtures, the results showed that the concrete mixtures without steel fibers exhibited sudden brittle failure, while the concrete mixtures with steel fibers exhibited a ductile failure because of the energy absorbing capacity of the fibrous concrete. Figure 4.18 represents the 28-day compressive strength of all concrete mixtures. The 28-day compressive strength of mixtures with short steel fibers varies from 53 MPa to 76 MPa while those with longer steel fibers are between 54 MPa to 59 MPa.

Figures 4.19 and 4.20 show the effect of fiber volume fraction on the compressive strength of concrete mixtures. An increase in the compressive strength with the inclusion of steel fibers is supported by a previous study conducted by Dhonde et al. (2007) and Yildirim et al. (2010). There was only a marginal increase in the compressive strength up to 12% (compared with the control mixture) for concrete mixtures with longer steel fibers. With the concrete mixtures with short steel fibers, increments of 45% (compared with the control mixture) had been observed. Figure 4.20 also shows higher compressive strength for the concrete mixtures with shorter steel fibers than for the longer ones for the same fiber volume fraction. This observation is also confirmed by the study conducted by Yildirim et al. (2010). Yildirim et al. (2010), which reported a 32.5% increment in compressive strength in the specimens made with short steel fiber (13mm in length) compared to the control mixture. In addition, a decrease in compressive strength values beyond 1.2% fiber volume fraction has been observed in both concrete mixtures with long and short steel fibers. This may be because of the non-uniform distribution of steel fibers in some of the specimens after 1.2% of fiber volume fraction, especially no mechanical vibration was used to ensure uniform distribution of the steel fibers.

Yildirim et al. (2010) also mentioned the limitation of the opening of micro-cracks at the higher short steel fiber content, which has a positive effect on compressive strength. The concrete mixtures with short steel fibers have higher amounts of steel fibers in comparison with the long steel fibers for the same percentage of the fiber volume fraction. Hence, the higher amount of short steel fiber plays an important role in increasing compressive strength. It may be noted that increasing the percentage of short steel fibers results in a steady improvement in the compressive strength up to 1.2% fiber volume fraction in both concrete mixtures.

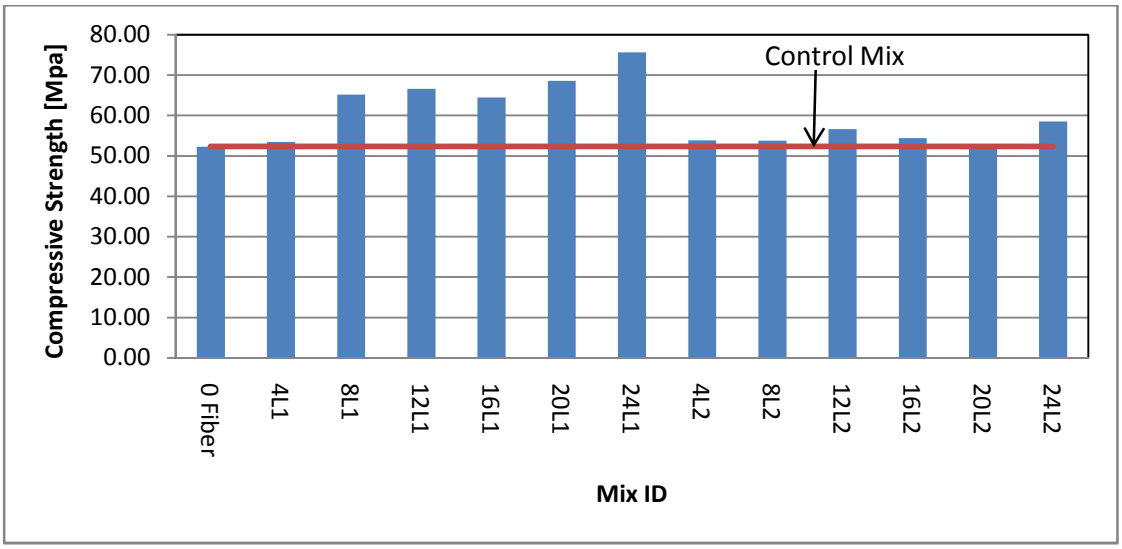

Figure 4.18: 28-day compressive strength of all concrete mixtures

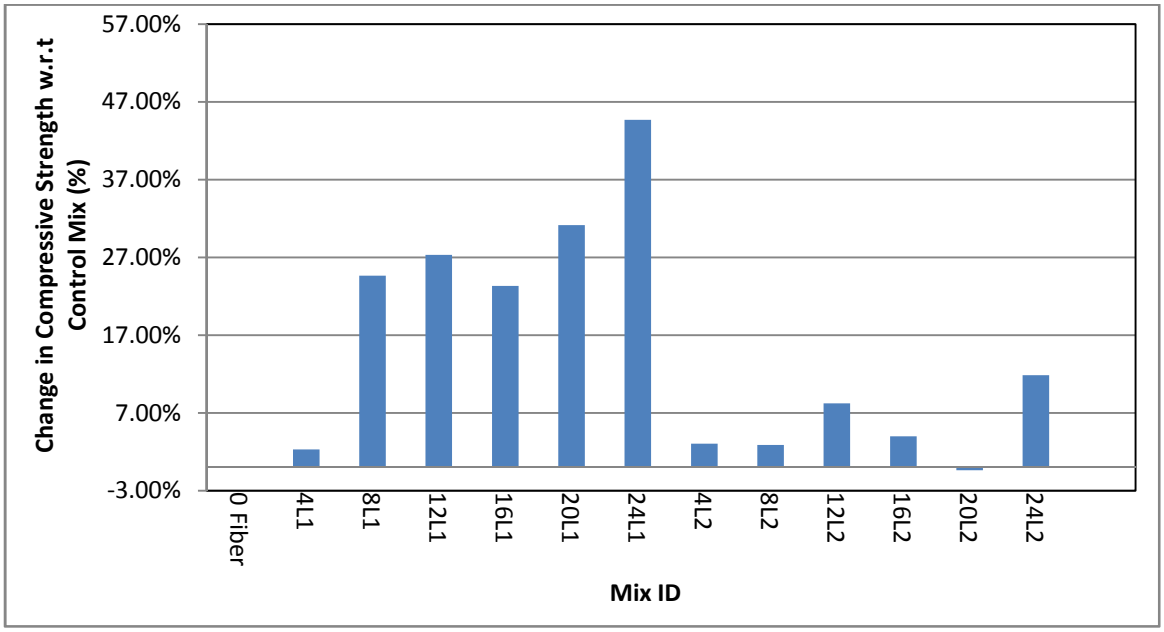

Figure 4.19: Change in compressive strength with respect to control mixture

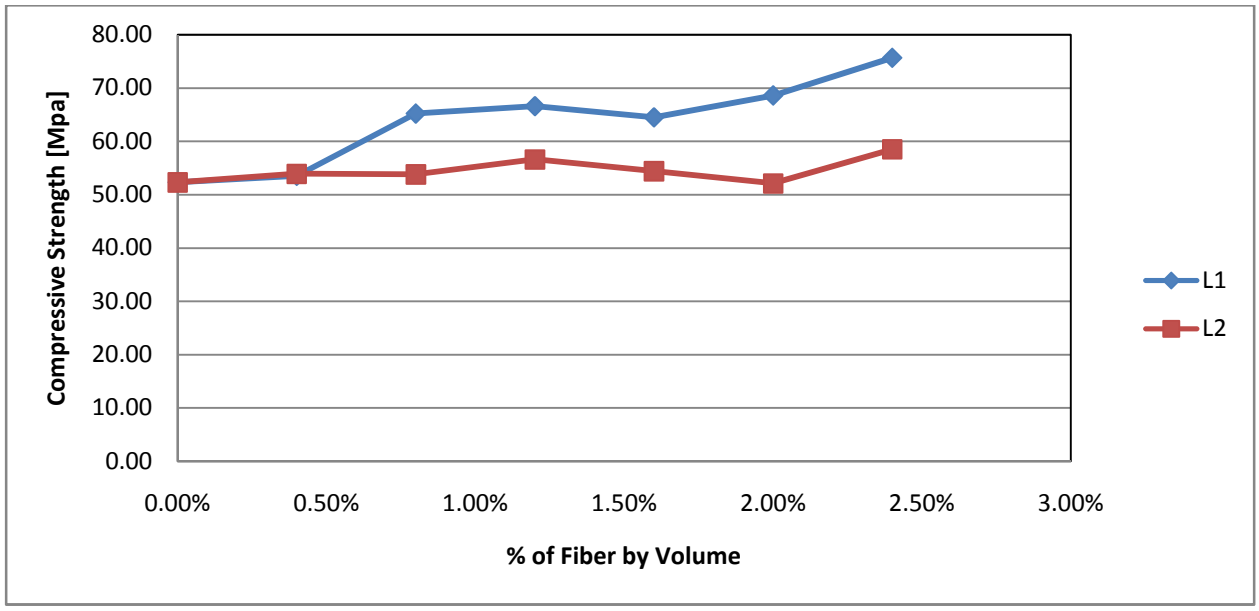

Figure 4.20: Effect of fiber volume fraction on compressive strength

4.3.2 Bond Strength

The 28-day pullout tests were performed in order to calculate the bond strength of the concrete mixture. The inclusion of steel fibers improved the pullout resistance of the concrete mixture. The pullout of the reinforcing steel rebar caused cracks in the concrete perpendicular to the ribs of the rebar. However, steel fibers present in the SFRSCC matrix helped bridge the cracks and provided a sufficient clamping effect after cracking (Chao et al., 2006). Therefore, the clamping effect of the steel fibers allows more bar ribs to contribute to higher bond strength. Figures 4.22 and 4.23 show that the peak bond stress is much higher in the concrete mixture with steel fiber than in the control mixture without steel fiber. A previous study also showed a higher increase in bond strength after the inclusion of steel fibers (Krstulovic-Opara et al., 1994). Figure 4.23 shows the exponential increase in bond strength as fiber volume fraction increases. The concrete mixtures with short steel fibers up to 1.2% volume fraction have a higher value of bond strength than those with long steel fibers for the same percentage of fiber volume fraction. This may be due to the higher number of short steel fibers in comparison to the long steel fibers for the same percentage of fiber dosage. Moreover, better distribution of the short steel fibers around reinforcing bar also has a positive impact on the bond strength. An increase in bond strength up to 244% and 231% was observed in concrete mixtures with 2.4% volume fraction of long and short fibers, respectively (Figure 4.21).

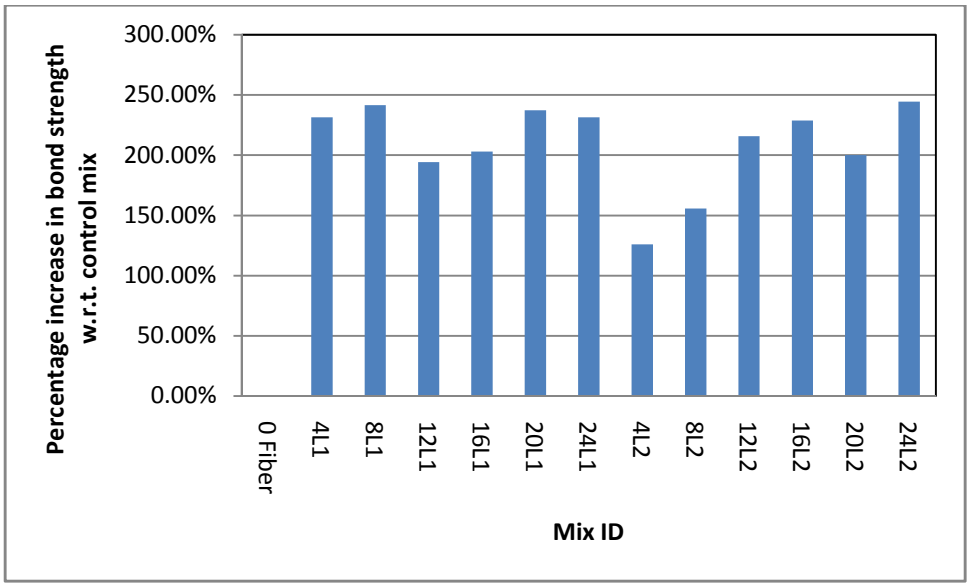

Figure 4.21: Change in bond strength with respect to the control mix

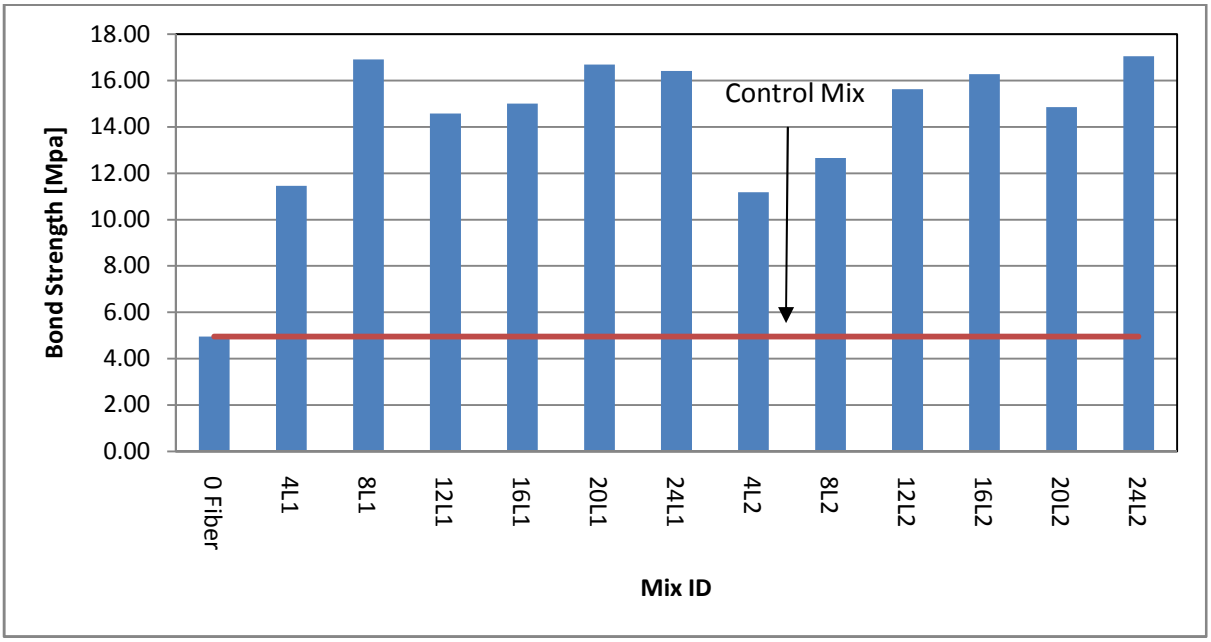

Figure 4.22: Bond strength test of all concrete mixtures

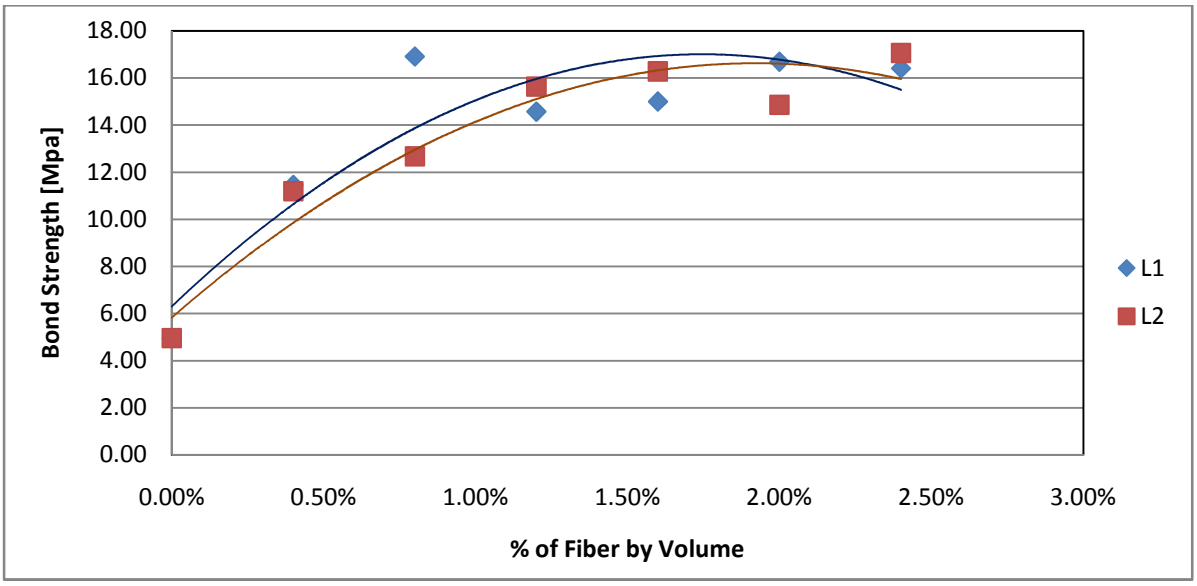

Figure 4.23: Effect of fiber volume fraction on bond strength

4.3.3 Flexural Strength

- **Modulus of Rupture (MOR)**

Figure 4.24 represents the 28-day flexural strength of all concrete mixtures. The modulus of rupture (MOR) or flexural strength for concrete mixtures with short steel fibers falls between 4.12MPa and 9.18MPa, whereas for long steel fibers, it is between 5.77 and 10.63MPa. Figures 4.24 and 4.25 show that the addition of steel fibers (both short and long) notably improves the flexural strength compared to the control mixture.

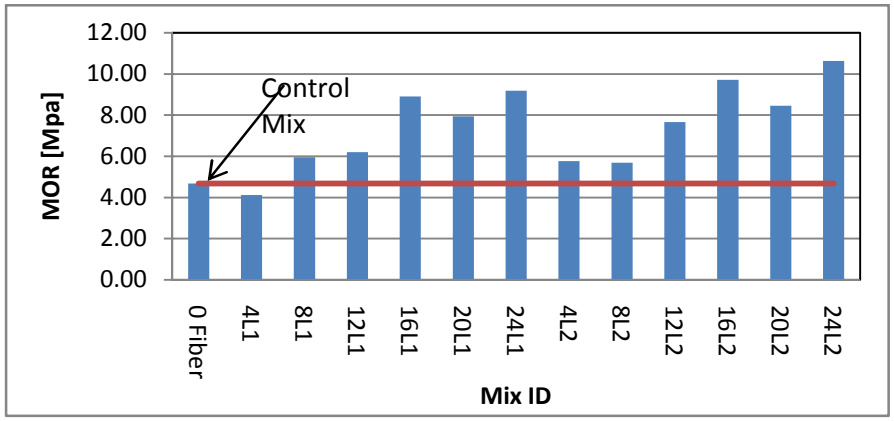

Figure 4.24: MOR value for all concrete mixtures

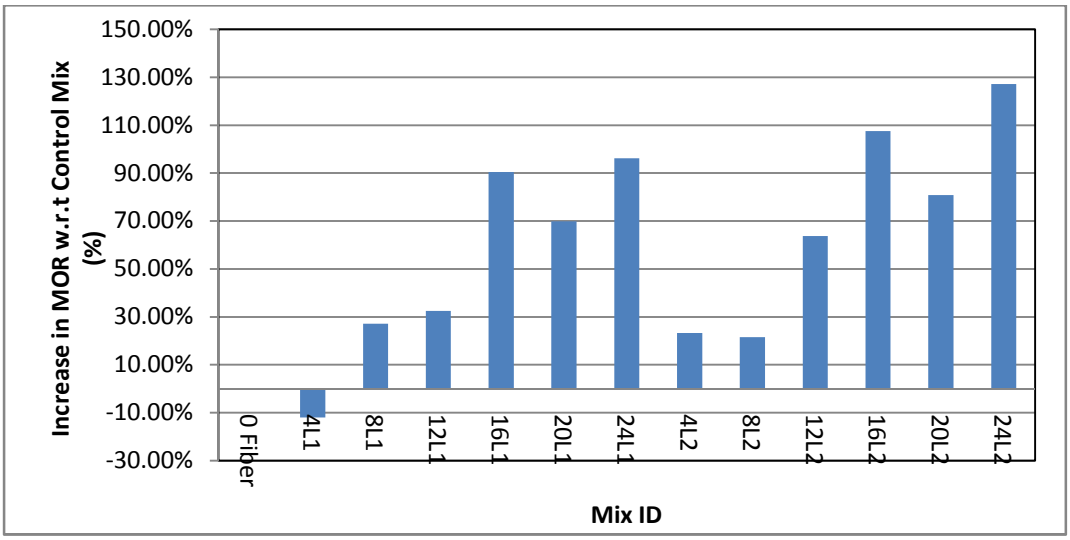

Figure 4.25: Change in MOR with respect to the control mixture

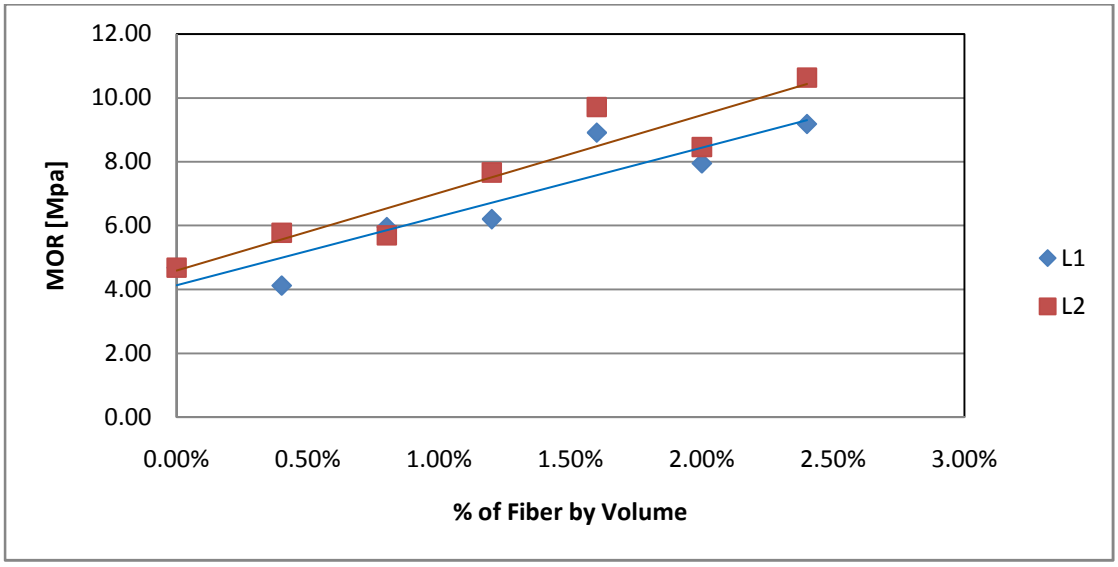

Figure 4.26: Effect of fiber volume fraction on MOR

A maximum increase in MOR of about 127% for concrete mixtures with longer steel fibers has been observed. An increase of about 124% in the SFRSCC was reported in a study by Sammour (2008). The increase in MOR with the addition of steel fibers has been studied by other researchers as well (Dhonde et al., 2007; Yildirim et al., 2010). Figure 4.25 shows that the small increments of fiber dosages have some effect on MOR value. Figure 4.26 shows the increase in MOR with the increase in fiber volume fraction. The MOR value of concrete mixtures with long steel fibers is greater than the mixture with short steel fibers for the same percentage of fiber

volume fraction. Studies done by Dhonde et al. (2007) and Yildirim et al. (2010) also show a higher MOR value for longer steel fibers.

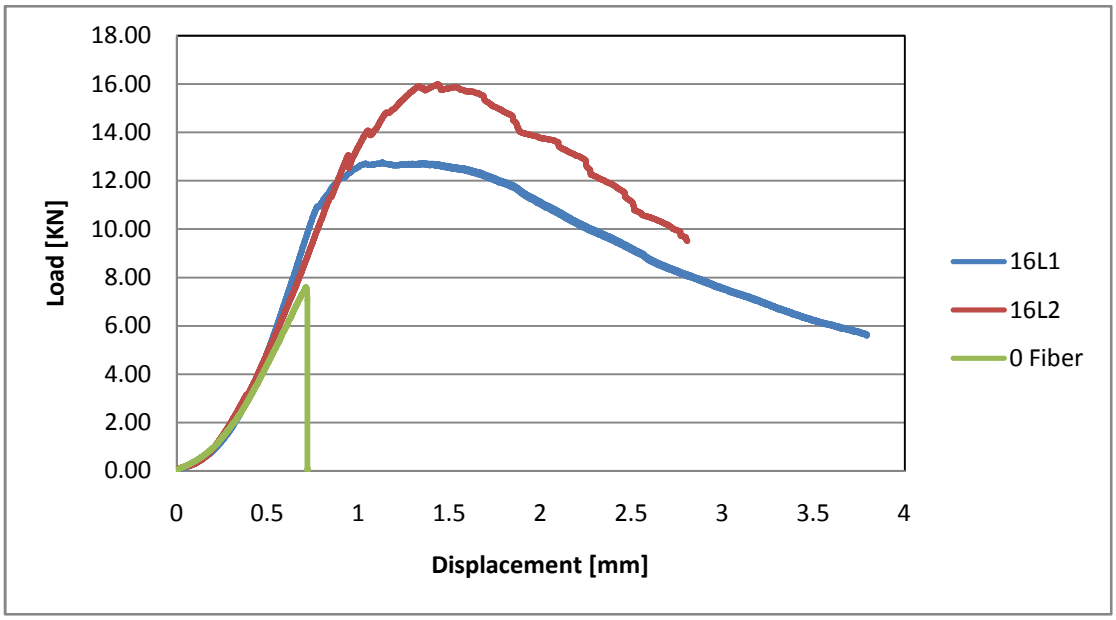

Figure 4.27: Load deflection graph showing control mix and 1.6% volume fraction of short and long steel fiber concrete mixtures

Figure 4.27 shows the load deflection curve for the control mixture and the 1.6% volume fraction of the mixtures with short and long steel fibers (Mixes 16L1 and 16L2). The figure also shows the deflection hardening behaviour of the steel fiber-reinforced concrete mixtures compared to the control mixture. The area beneath the load deflection curve is a measure of the energy required to gain specific deflection, which leads to the concept of "toughness" for fiber-reinforced concrete (Papworth, 1997). Flexural toughness is described in the next section. Load deflection curves for all 13 concrete mixtures are shown in Appendix A.

Flexural Toughness

Flexural toughness is an important parameter when dealing with fibrous concrete. Increased in strength of the concrete results in higher brittleness and reduced ductility. Hence, incorporating steel fibers in concrete helps improve ductility by carrying the extra load after cracking. This is considered post-cracking behaviour or toughness. Flexural toughness is defined as the area under the load deflection curve in flexure, which includes an area away from elastic behaviour on the

load deflection curve. Flexural toughness is calculated according to the JSCE-SF4 (JSCE SF-4, 1984), ASTM C1018-97 and PCS methods, which are based on third point loading in the flexural test.

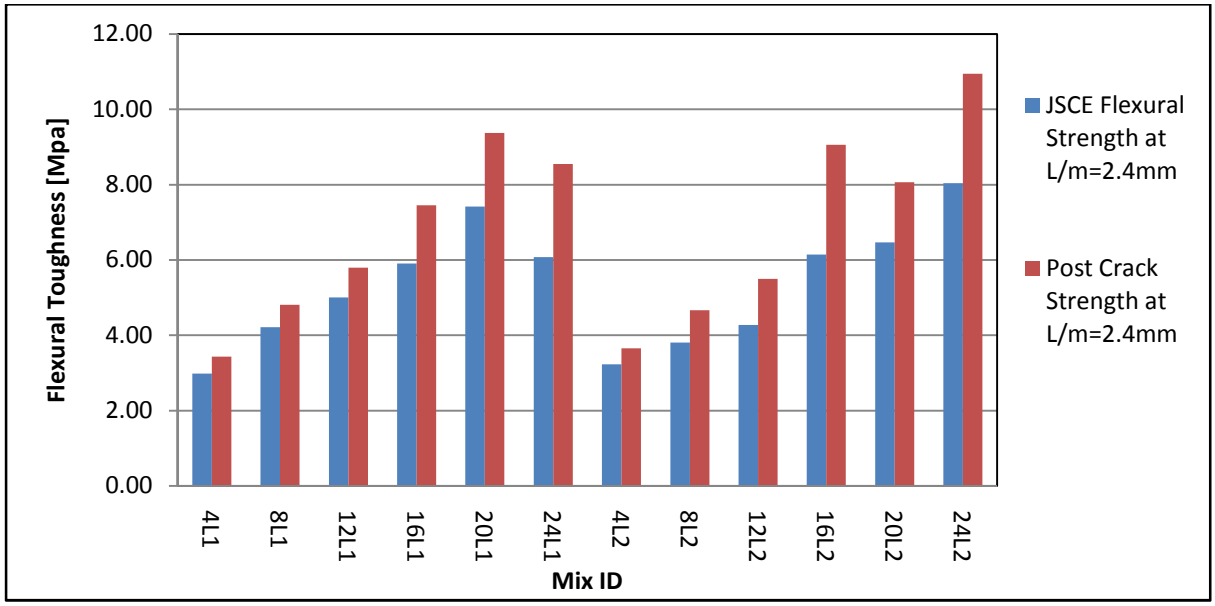

Figure 4.28: Flexural toughness as per JSCE-SF4 and PCS method at L/m = 2.4mm

Figure 4.28 shows the JSCE flexural strength and the PCS flexural strength for all concrete mixtures. An increase in flexural toughness has been observed in both JSCE flexural strength and PCS strength at L/m = 2.4 mm as fiber volume increases. The study done by Nataraj et al. (2000) observed a similar trend with the increase of fiber dosage. Here, PCS flexural strength values are a little higher than in the JSCE flexural strength value. The study conducted by Banthia and Sappakittipakorn (2007) also found higher PCS flexural strength value than the JSCE.

Table 4.4: Flexural toughness values as per JSCE-SF4 and PCS methods

Mix No.	Mix ID	Peak load [KN]	Deflection at peak load [mm]	Post crack strength at L/m=2.4mm [MPa]	JSCE flexural toughness at δ=2.4mm [MPa]
M02	4L1	7.71	0.649	3.44	2.99
M03	8L1	7.90	0.645	4.81	4.22
M04	12L1	9.75	0.714	5.80	5.01
M05	16L1	12.75	1.128	7.45	5.90
M06	20L1	15.00	1.111	9.38	7.42
M07	24L1	15.61	1.560	8.55	6.08
M09	4L2	8.64	0.699	3.66	3.23
M10	8L2	8.31	0.994	4.67	3.81
M11	12L2	10.91	1.119	5.50	4.28
M12	16L2	15.98	1.434	9.06	6.15
M13	20L2	13.03	1.848	8.07	6.47
M14	24L2	19.32	1.294	10.95	8.04

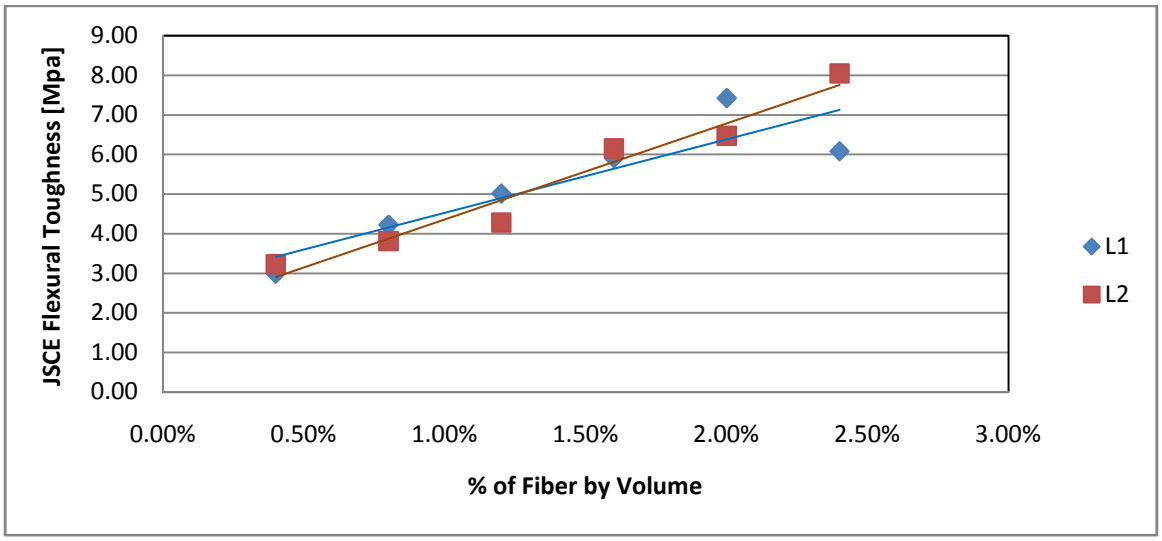

Figure 4.29: Effect on JSCE flexural strength value with increased percentage of fiber volume

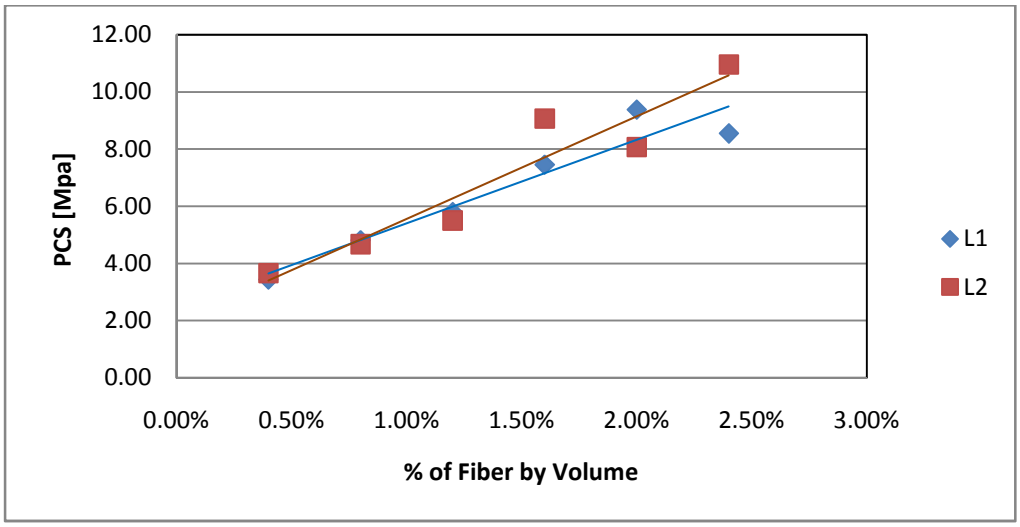

Figure 4.30: Effect on PCS flexural strength value with increased percentage of fiber volume

Figures 4.29 and 4.30 show the effect on JSCE flexural strength and PCS flexural strength values with the increased percentage of fiber volume. The increase in fiber volume fraction up to 1% does not have a significant effect on either short or long steel fibers. As the fiber volume fraction increases above 1%, the mixtures with longer steel fibers with hooked ends have a higher value of flexural toughness (in terms of both JSCE flexural strength and PCS flexural strength) than those with shorter steel fibers for the same fiber volume fraction. This has also been observed in a study done by Nataraj et al. (2000). One reason behind this may be a more progressive debonding behavior for the longer steel fibers during the post-cracking period than for the shorter fibers. Also, the hooked ends of the long steel fibers also play an important role in the progressive debonding.

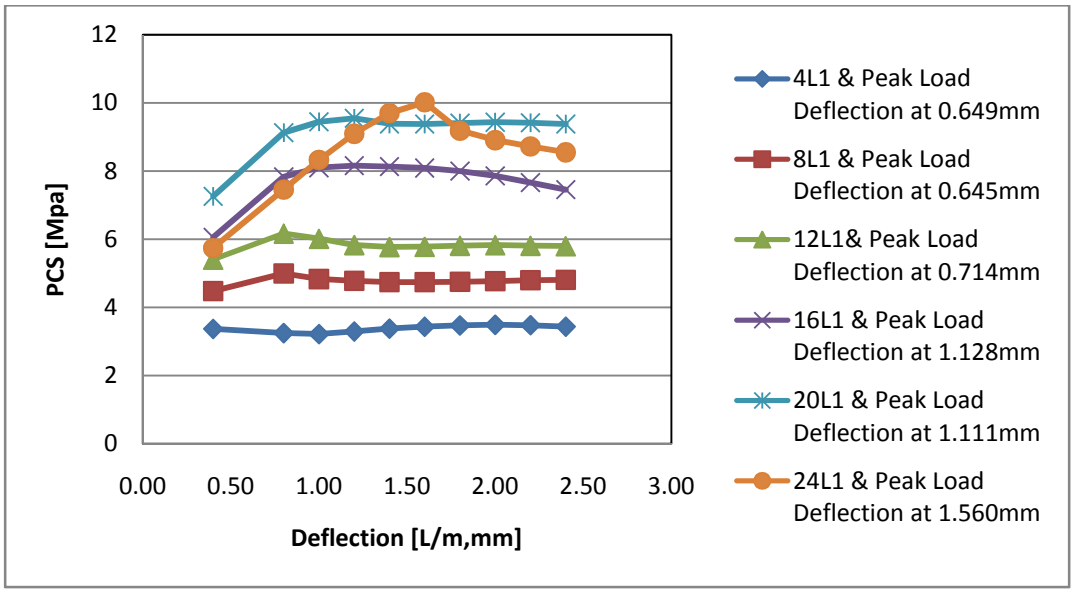

Figure 4.31: PCS flexural strength value at different L/m for short steel fibers

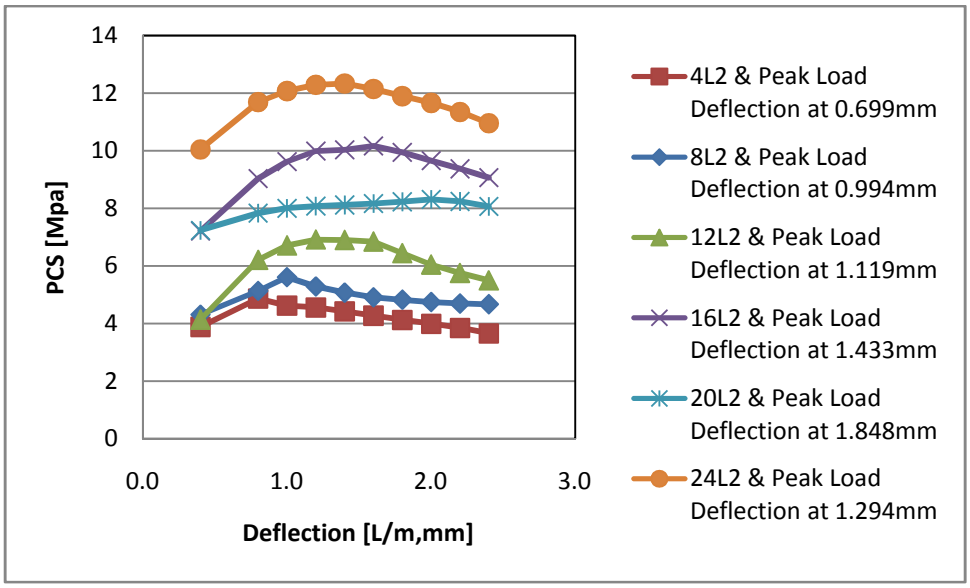

Figure 4.32: PCS flexural strength value at different L/m for long steel fibers

In the PCS calculation, 10 different deflection points (0.4, 0.8, 1.0, 1.2, 1.4, 1.6, 1.8, 2.0, 2.2 and 2.4 mm) have been used and the graphs are shown in Figures 4.31 and 4.32. Overall, the PCS flexural strength values increased as the percentage of fiber volume fraction increased. Moreover, the PCS method demonstrates the post-crack deflection hardening behaviour as the percentage of fiber volume increases.

Table 4.5: Toughness index and residual strength as per ASTM C1018

Mix No.	Mix ID	Flexural Index I_5	Flexural Index I_{10}	I_5/I_{10}	$R_{5,10}$
M02	4L1	4.75	7.55	1.59	56.03
M03	8L1	4.37	8.36	1.92	79.90
M04	12L1	4.74	7.91	1.67	63.32
M05	16L1	8.21	13.67	1.66	109.08
M06	20L1	6.95	13.12	1.89	123.27
M07	24L1	9.02	18.97	2.10	199.10
M09	4L2	4.47	4.87	1.09	8.01
M10	8L2	5.56	9.08	1.63	70.50
M11	12L2	12.74	14.34	1.12	31.77
M12	16L2	9.65	12.93	1.34	65.52
M13	20L2	6.07	10.56	1.74	89.84
M14	24L2	6.21	7.79	1.25	31.63

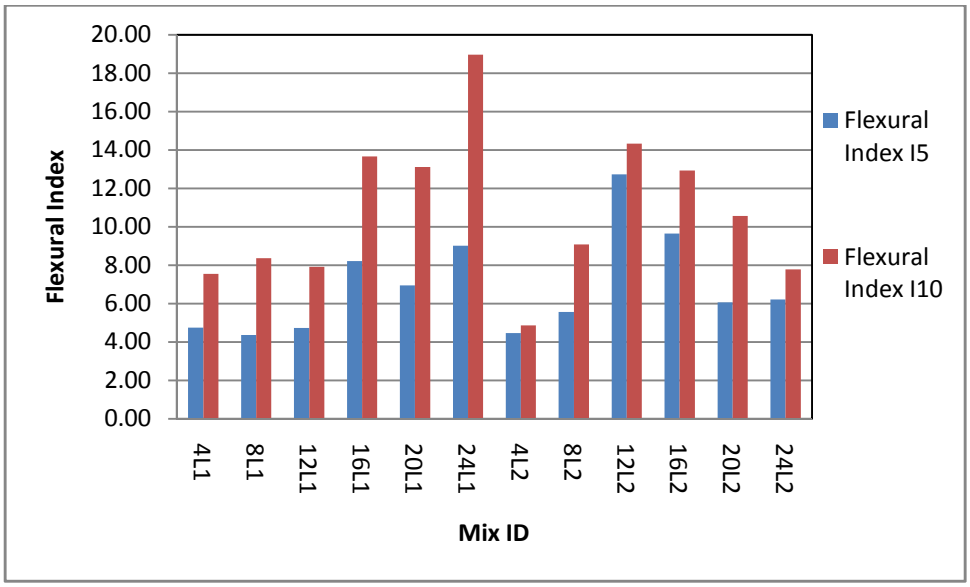

Figure 4.33: Flexural indices I_5 and I_{10} as per ASTM C1018

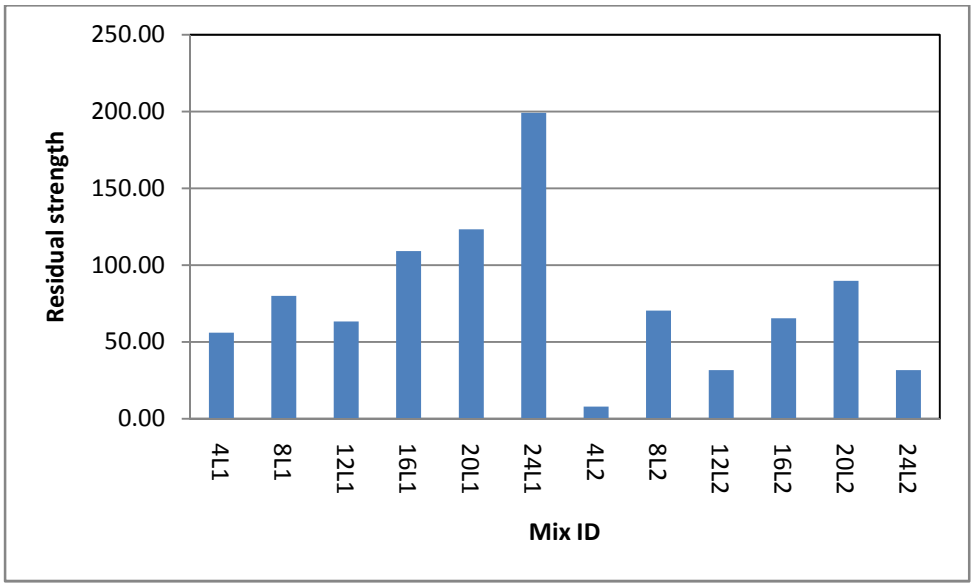

Figure 4.34: Residual strength $R_{5,10}$ as per ASTM C1018

ASTM C1018 flexural indices I_5 and I_{10} and residual strength $R_{5,10}$ are calculated and shown in Figures 4.33 and 4.34, respectively. Both ASTM flexural indices and the residual strength of concrete mixtures incorporating short steel fibers show a continuous trend, whereas the concrete mixtures with long steel fibers do not, as indicated in Figures 4.33 and 4.34. This be because of the difficulty of finding the exact location of the "first crack" on the load-deflection curve. As fiber volume increases, the peak load deflection also increases, as shown in Table 4.4. Therefore, the first crack might change as peak load deflection increases. The difficulty of finding the first crack deflection affects the toughness indices as well as residual strength. A study done by Banthia and Sappakittipakorn (2007) also mentions the drawback of ASTM C1018 when dealing with the first crack.

Overall, the JSCE flexural strength value and the PCS flexural strength value can be directly used for design purposes because they provide numerical values regarding allowable stresses at a given deflection based on the load deflection curve.

Summary of the Mechanical Properties Test

Overall, inclusion of steel fiber in concrete mixtures improved the mechanical properties of concrete. Incorporation of short steel fibers in concrete mixtures up to 1.2% fiber volume fractions (considered SFRSCC) improved the bond strength as well as the compressive strength of the concrete in comparison with concrete mixtures with long steel fibers at the same percentage of fiber volume fraction. This may be because of the effect of higher amount of short steel fibers in the concrete mixtures as well as uniform distribution of short steel fibers compared to longer ones for same percentage of fiber volume fractions. MOR values and flexural toughness values are higher for concrete mixtures with long steel fibers that they are for shorter ones with the same percentage of fiber volume fractions.

4.4 Durability Properties

For durability properties, water sorptivity, water absorption and porosity, rapid chloride permeability, corrosion and freeze-thaw cycle tests were performed. Summaries of the test results are shown in Tables 4.6 and 4.7.

4.4.1 Water sorptivity test

The water absorption rate or sorptivity is the rate of penetration of water through one side into the pores of the concrete by capillary suction. This test estimates the quality of the concrete based on the surface pores of the concrete sample. The effects of initial and secondary absorption rates in all concrete mixtures with short and long steel fibers of different fiber volume fractions were observed.

Table 4.6: Durability properties of concrete mixture: sorptivity, absorption, porosity and RCPT

Mix No	Mix ID	Sorptivity Test		Absorption (%)	Porosity (%)	RCPT
		Initial Absorption [mm/√min]	Secondary Absorption [mm/√min]			Avg. Charged passed [coulomb]
M08/01	0 Fiber	0.1539	0.0368	5.31%	1.19%	1095
M02	4L1	0.1423	0.0562	5.55%	1.24%	1616
M03	8L1	0.1263	0.0583	5.23%	1.21%	1710
M04	12L1	0.1281	0.0538	4.83%	1.15%	2311
M05	16L1	0.0999	0.0329	5.44%	1.27%	2982
M06	20L1	0.0994	0.0319	5.41%	1.28%	OVF*
M07	24L1	0.0972	0.0292	5.74%	1.37%	OVF
M09	4L2	0.1579	0.0560	5.00%	1.15%	1685
M10	8L2	0.1379	0.0598	5.04%	1.14%	2818
M11	12L2	0.1394	0.0634	5.10%	1.16%	2810
M12	16L2	0.1350	0.0626	5.05%	1.18%	5314
M13	20L2	0.1234	0.0508	5.11%	1.22%	OVF
M14	24L2	0.1390	0.0512	4.75%	1.22%	OVF

* OVF: indicates overflowed current [No result]

Table 4.7: Durability properties of concrete mixtures cont'd: corrosion and freeze-thaw cycles

Mix No.	Mix ID	% Change in bond strength after corrosion test	% of mass loss of reinforcing bar	Avg. % of wt. drop on concrete prism	% drop after freeze-thaw cycles	
					FT	MOR
M08/01	0 Fiber	14.34%	0.49%	0.29%	-20.89%	-23.93%
M02	4L1	-5.58%	0.10%	0.05%	-90.06%	-8.25%
M03	8L1	-33.89%	0.67%	0.08%	-26.98%	-2.18%
M04	12L1	-34.93%	0.90%	0.09%	-4.65%	-1.29%
M05	16L1	-19.83%	1.24%	0.08%	-9.91%	-13.92%
M06	20L1	-33.91%	4.25%	0.05%	5.39%	14.84%
M07	24L1	-32.78%	1.07%	0.04%	-6.06%	-0.11%
M09	4L2	-4.47%	1.55%	0.06%	-61.93%	-6.41%
M10	8L2	-26.22%	3.24%	0.08%	-39.35%	7.38%
M11	12L2	-83.69%	4.36%	0.05%	11.74%	-4.18%
M12	16L2	-73.94%	5.71%	0.04%	-13.51%	-1.65%
M13	20L2	-38.59%	3.42%	0.05%	-22.37%	7.80%
M14	24L2	-34.43%	1.15%	0.04%	-15.98%	-16.65%

Note: Wt: Weight, FT: Flexural Toughness and MOR: Modulus of Rupture

Figure 4.36 shows all the results of water sorptivity tests for all concrete mixtures. The initial and secondary absorption rates for all mixtures (including short steel fiber and long steel fiber) range from 0.0972-0.1579 mm/√min and 0.0290-0.0634 mm/√min respectively, which is lower than 0.77 mm/√min (Nawy, 1997), indicating that the durability performance of concrete with steel fibers is excellent (Ramadoss & Nagamani, 2008). Figure 4.37 shows that the initial absorption rates for mixtures with both types of steel fibers decrease as the percentage of fiber volume fraction increases. Figure 4.38 shows the increases in secondary absorption rate up to 1.2% of fiber volume fraction and decreases beyond 1.2% of fiber volume fraction. Studies conducted by Ramodas and Nagamani (2008) also show a similar trend. In addition, the secondary absorption rates for mixtures with short steel fibers are lower than for long steel fibers. A possible explanation is that a higher number of short steel fibers per unit volume of concrete (compared to long steel fibers for the same percentage of fiber dosage) might improve bonding of the concrete matrix.

The initial and secondary absorption rates (I [mm]), are plotted against the square root of the time, as shown in Figure 4.35. The initial absorption rate is defined as the slope of the trend line from regression analysis. The points are from one minute to six hours. The secondary absorption rate is calculated in the same way from day one to day six.

The initial absorption rate is : Si= 0.1260 mm/√min

The secondary absorption rate is: Ss= 0.0542 mm/√min

Table 4.8: Sample calculation of initial and secondary absorption for mix ID:12L1

Minute	Days	Mass (gm)	Mass difference	Absorp. I (mm)	Sqr.Time √min
0	0	1403.80			0.00
1	1 min	1405.78	1.98	0.25	1.00
5	5 min	1407.32	3.52	0.45	2.24
10	10 min	1408.57	4.77	0.61	3.16
20	20 min	1410.40	6.60	0.84	4.47
30	30 min	1411.34	7.54	0.96	5.48
60	1 hour	1414.07	10.27	1.31	7.75
120	2 hour	1417.41	13.61	1.73	10.95
180	3 hour	1419.37	15.57	1.98	13.42
240	4 hour	1420.75	16.95	2.16	15.49
300	5 hour	1422.43	18.63	2.37	17.32
360	6 hour	1423.63	19.83	2.53	18.97
1440	1 day	1436.24	32.44	4.13	37.95
2880	2 day	1444.61	40.81	5.20	53.67
4320	3 day	1450.04	46.24	5.89	65.73
5760	4 day	1453.99	50.19	6.39	75.89
7200	5 day	1457.09	53.29	6.79	84.85
8640	6 day	1459.79	55.99	7.13	92.95

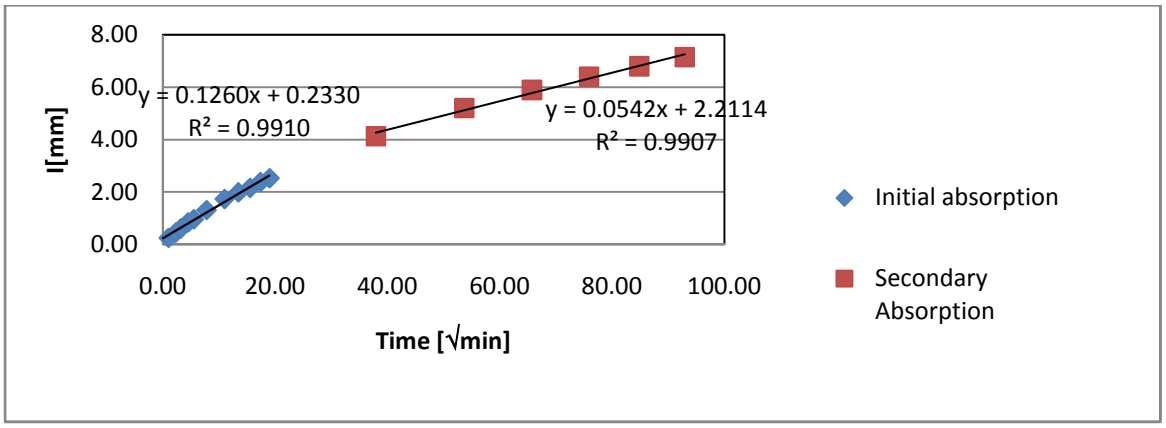

Figure 4.35: Absorption (I) against the square of time [√min] with linear regression analysis

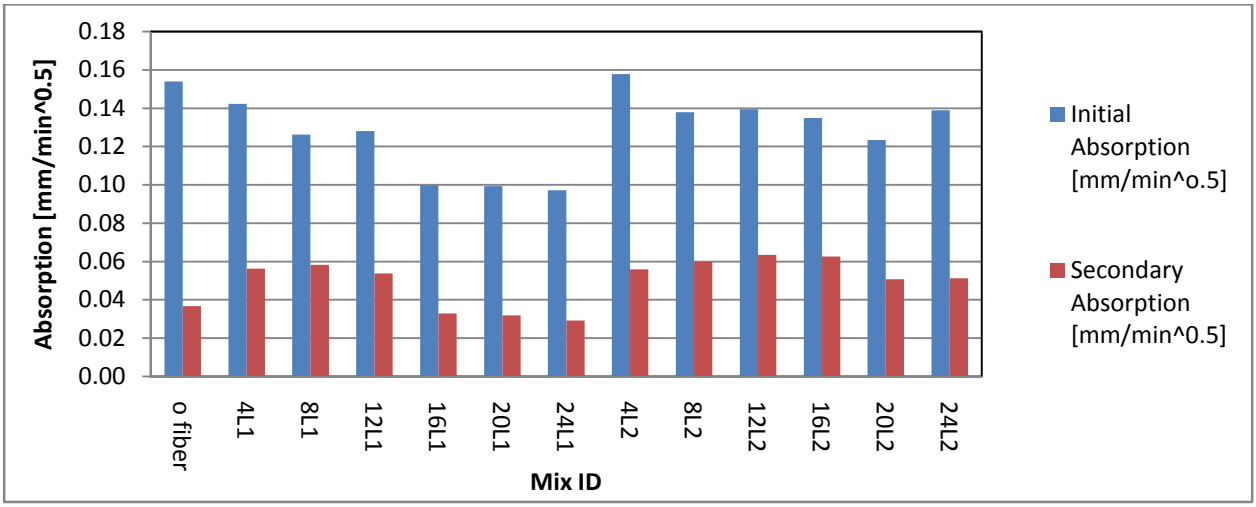

Figure 4.36: Water sorptivity test results for all concrete mixtures

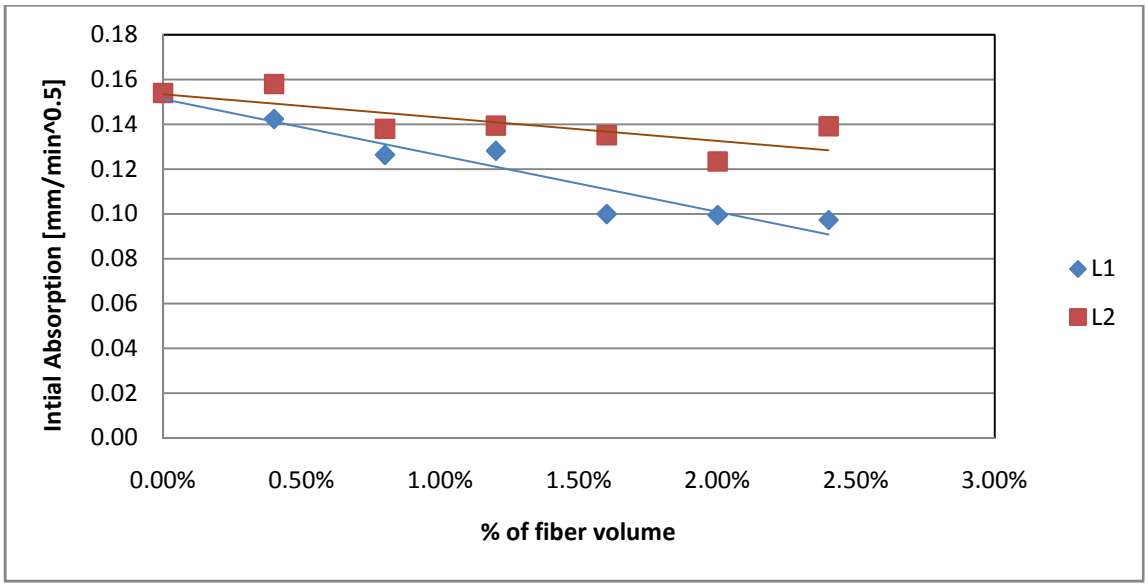

Figure 4.37: Effect of fiber volume fraction on initial absorption rates

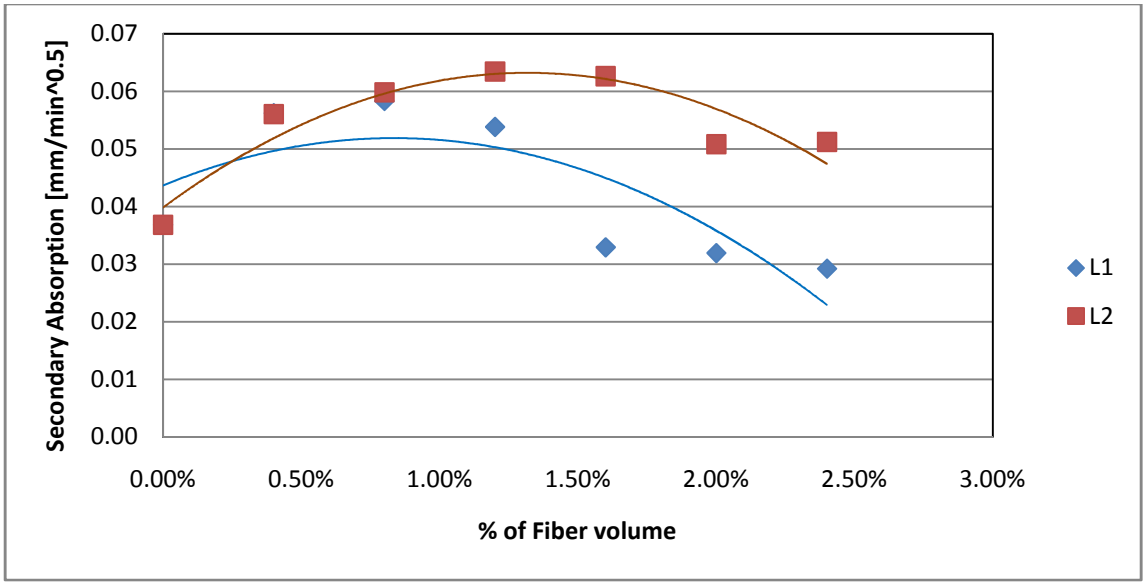

Figure 4.38: Effect of fiber volume fraction on secondary absorption rates

4.4.2 Water Absorption and Porosity Test

Water absorption and porosity are also important parameters when considering the durability of concrete.

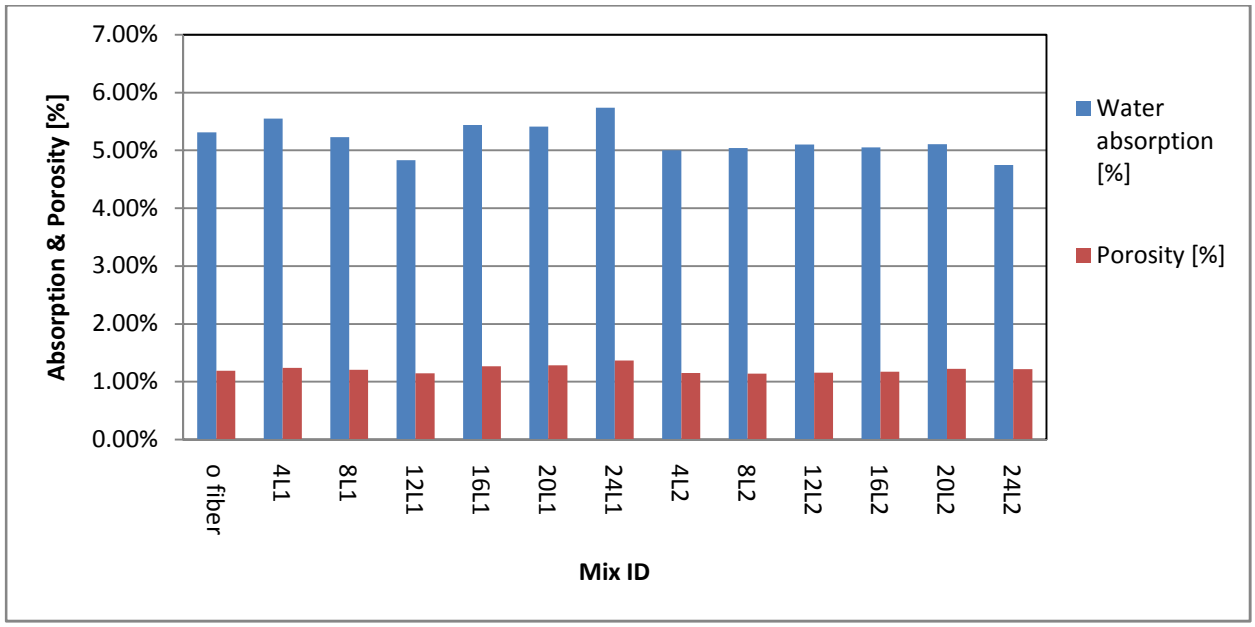

Figure 4.39: Water absorption and porosity test results for all concrete mixtures

Figure 4.39 represents the percentage of water absorption and porosity for all concrete mixtures. The water absorption (%) and porosity (%) investigated after 28 days of curing for both long and short steel fibers range from 4.75% to 5.74% and 1.14% to 1.37%, respectively. Experimental water absorption by immersion ranges from 3 to 6.5%, which indicates that the durability consideration with respect to water absorption is satisfactory for the concrete mixtures with steel fibers. Figures 4.40 and 4.41 show that neither water absorption and porosity is affected by the percentages of fiber volume fractions used in the mix. A study done by Ramadoss and Nagamani (2008) also showed similar behaviour. Figures 4.40 and 4.41 also indicate that the inclusion of steel fibers in concrete mixtures does not cause a significant change in water absorption or porosity. Other studies have also proven that the fiber addition does not significantly increase the number of pores as compared to normal concrete (Miloud, 2005). However, Figures 4.42 and 4.43 show that the concrete mix 24L1 (short steel fibers with 2.4% volume fraction) has a higher value of water absorption and porosity with respect to the control mix. This might be because of the lower compaction of the concrete mixture with short steel fibers at a fiber volume fraction of 2.4%. Fresh properties described in the previous section also show that the mix 24L1 has no SCC properties and requires mechanical vibration for proper compaction.

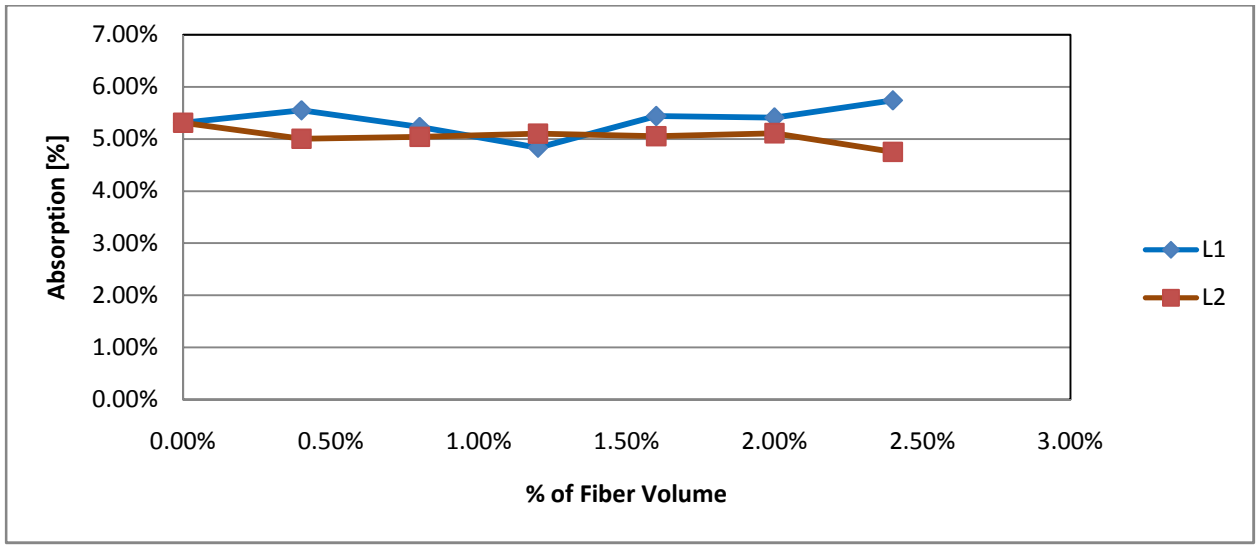

Figure 4.40: Effect of fiber volume fraction on water absorption of concrete

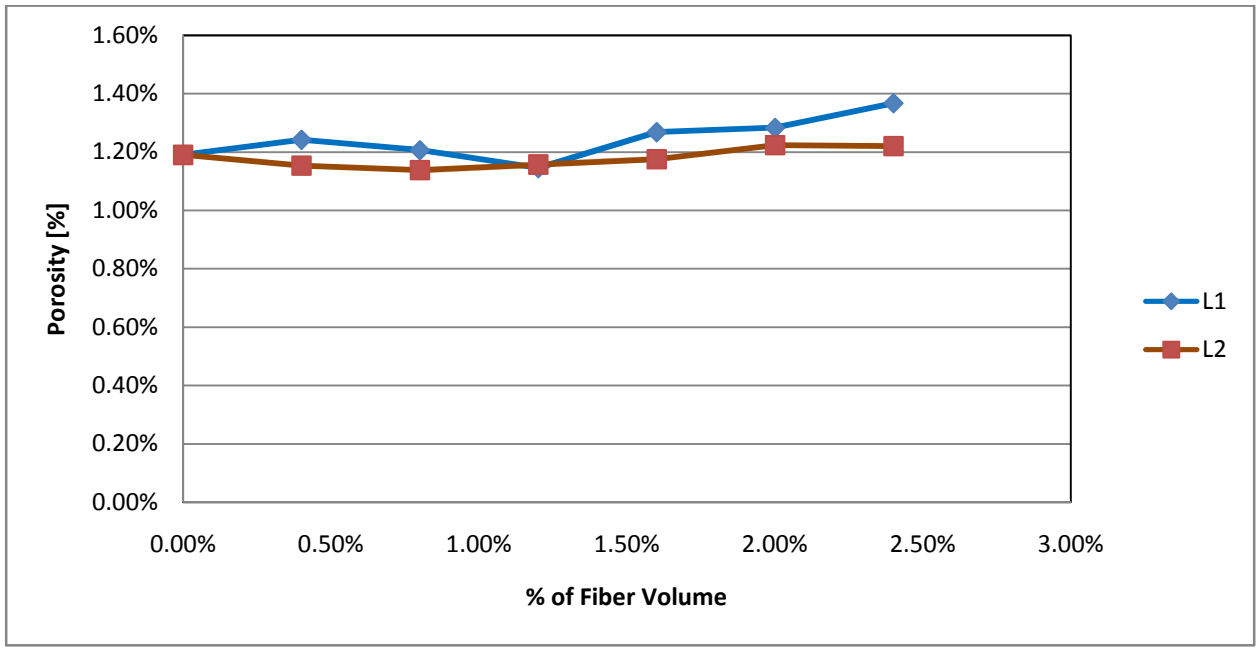

Figure 4.41: Effect of fiber volume fraction on porosity of concrete

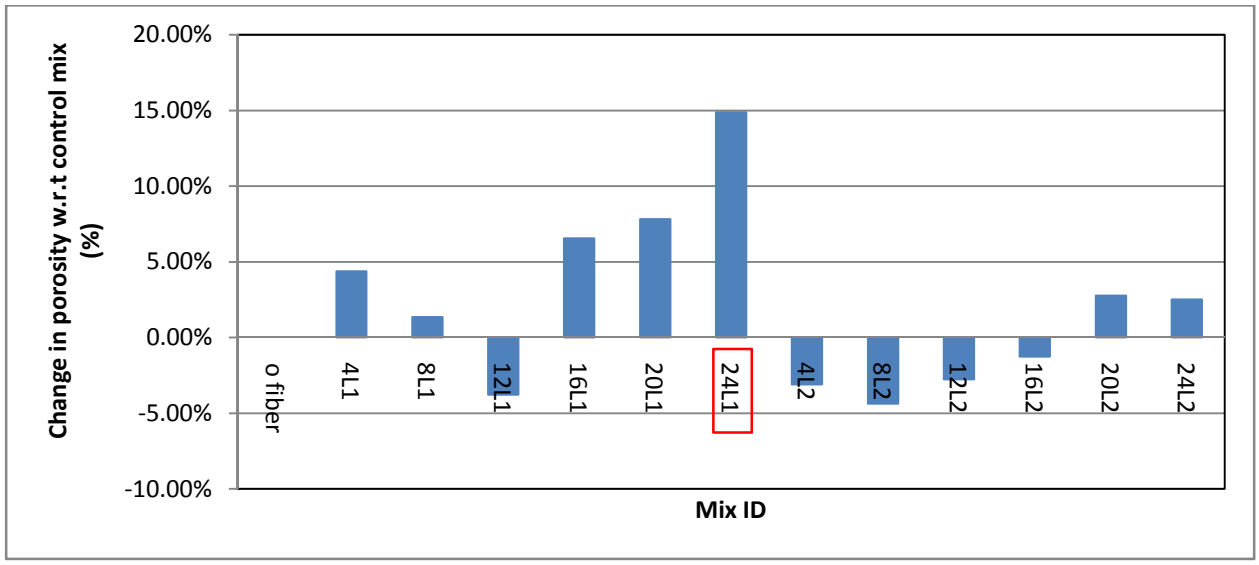

Figure 4.42: Change in water porosity with respect to control mixture

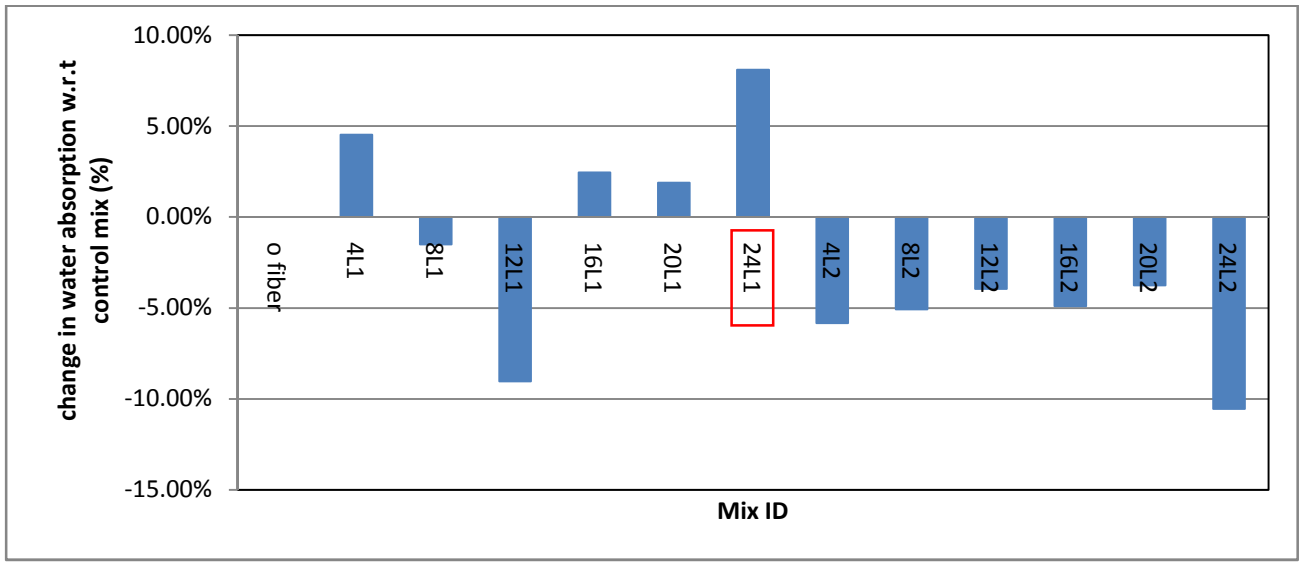

Figure 4.43: Change in water absorption with respect to control mix

4.4.3: Rapid Chloride Permeability Test (RCPT)

The ASTM C1202 method was adopted in this study to measure the electrical indication of a concrete's ability to resist chloride ion penetration. This test is one of the easiest and quickest methods for evaluating chloride ion ingression and the protection of reinforcement against corrosion.

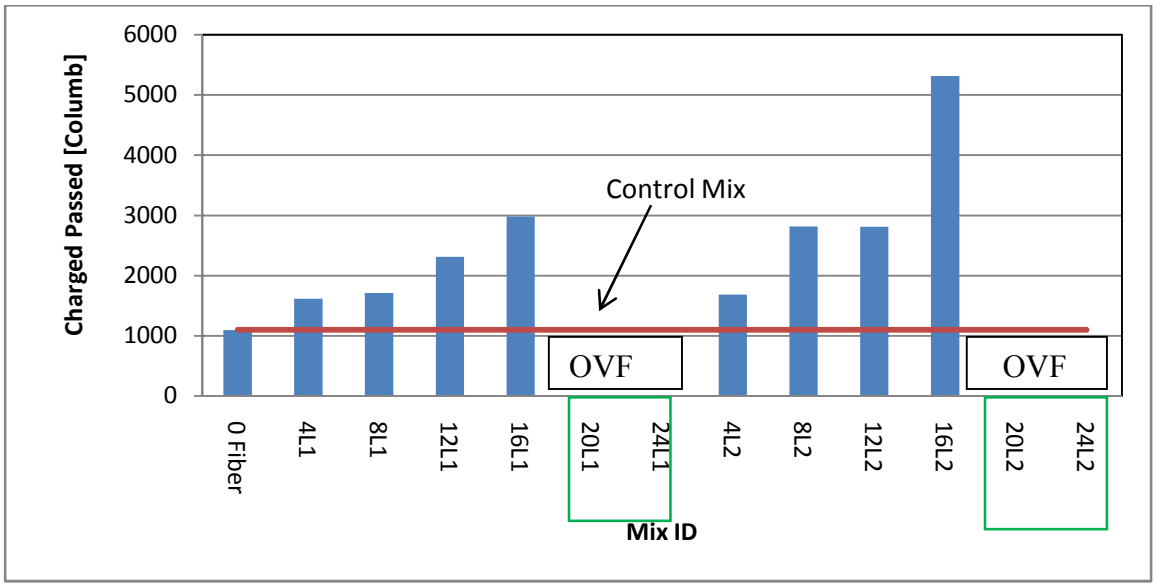

Figure 4.44: Chloride penetration resistance of all concrete mixtures

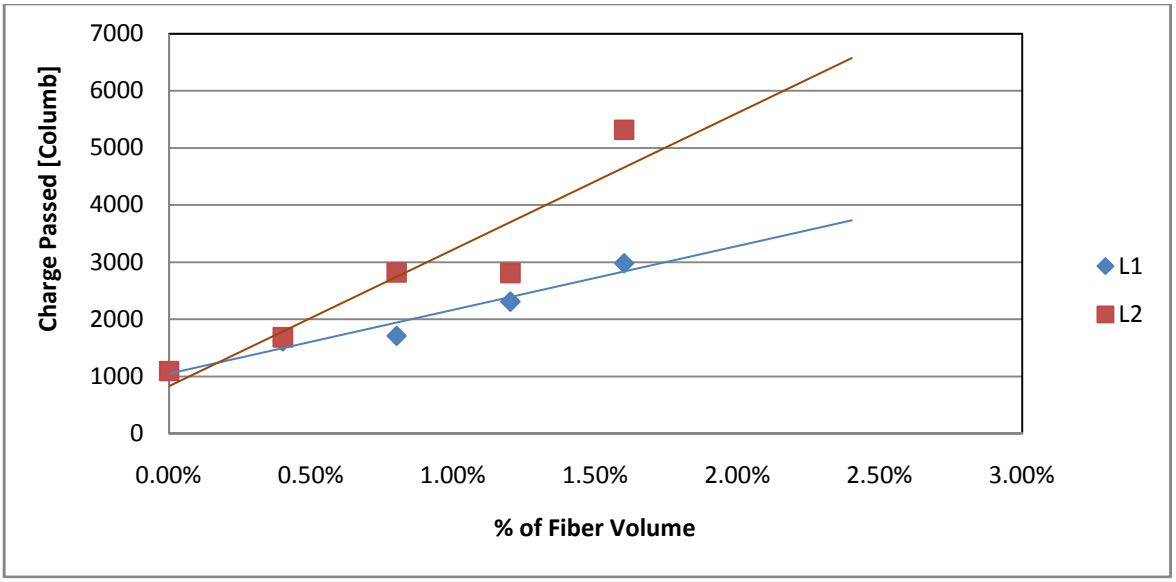

Figure 4.45: Effect of fiber volume fraction on chloride penetration resistance of all concrete mixtures

Figure 4.44 shows the total charge passing through all concrete mixtures obtained from the RCPT. Figures 4.44 and 4.45 both show that the charge passed increases as steel fiber volume fraction increases. This could be due to the electrical conductivity of the fibers in concrete mixtures. Studies conducted by Tsai et al. (2009) and El-Dieb (2009) also found increase in the charge passed (Coulomb) and in electrical conductivity as steel fiber content increased. The level

of chloride ion penetration for concrete mixtures with steel fiber volume fraction below 1.6% [including short steel fiber (13mm) and long steel fiber (25mm)] remains in a low to moderate range of the charge spectrum as per ASTM C1202, indicating that the concrete mixture with steel fiber has a good ability to resist chloride ion penetration. Figure 4.45 also shows that the charge passed in the concrete mixture with long steel fibers is higher than that in the mixture with short steel fibers for the same percentage of fiber volume fraction. Beyond 1.6% of fiber volume fraction, mixtures with both long and short steel fibers show an overflow of current. Therefore, with the presence of a higher percentage of long steel fibers (beyond 1.6%), electrical conductivity of the specimen is higher and has a significant effect on chlorine ion penetration through concrete. The higher value of the charge passed in the concrete mixture with long steel fibers and a higher percentage of fiber volume may be due to the alignment of fibers in a longitudinal direction, which provides a continuous electrical path between two ends of the specimen (ASTM C1202-10, 2010).

4.4.4 Corrosion test

Accelerated corrosion tests have been successfully performed by many researchers in order to determine the degree of corrosion in a short period of time (Hassan et al., 2009). In Hassan's study, the current was supplied by a constant 12-volt DC power source and was monitored on daily basis. The theoretical mass loss of reinforcing steel bar was calculated according to Faraday's equation [Eq. 3.3], which is related to the electrical energy consumed as a function of time and current (Ampere) (Hassan et al., 2009). After testing, the experimental mass loss was observed and calculated using equation 3.5, which is also called percentage of mass loss or degree of corrosion, as previously discussed in Chapter 3.

Generally, corrosion of the reinforcing bar occurs when iron (Fe) in the anodic region (steel reinforcing bar) breaks and releases electrons (e^-). which combine with oxygen and moisture in the cathodic region and transform into hydroxyl ions (OH^-). These OH- later react with free irons (Fe^{++}) in anodic regions and form corrosion products such as ferrous hydroxide [$Fe(OH)^2$], ferric oxide (Fe_3O_4), etc. This phenomenon increases the diameter of the reinforcing bar, creating radial stress across the concrete and initiating longitudinal cracks in the concrete cover. These cracks provide easy access for harmful substances such as chlorine ion and hydroxyl ions, and further accelerate the corrosion process.

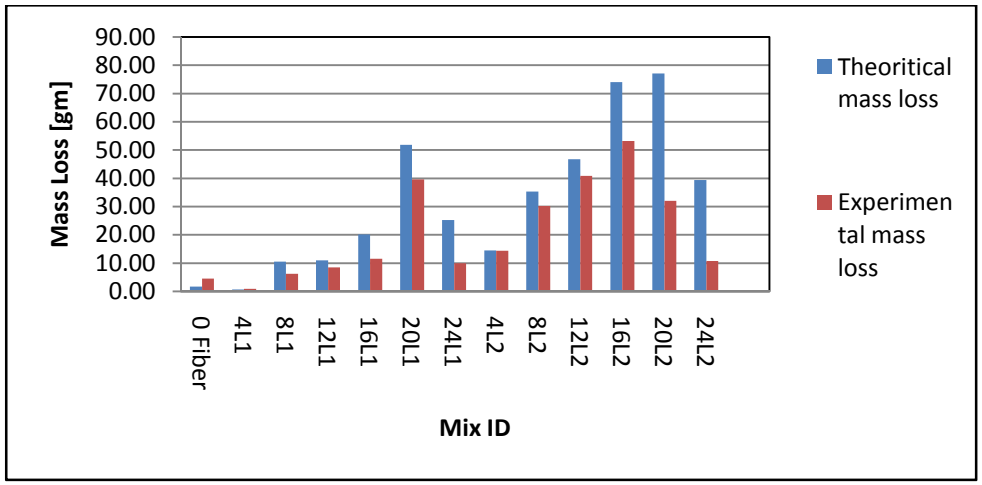

Figure 4.46: Comparison of theoretical and experimental mass loss of reinforcing bar in all concrete mixtures

Figure 4.46 shows the comparison between the theoretical and the experimental mass loss of the reinforcing bar in all concrete mixtures. It has been observed that the theoretical mass loss is usually higher than the experimental mass loss.

In the accelerated corrosion test shown in the Figure 4.**47**, wire mesh was connected with a negative terminal (cathode) of DC (direct current) supply, and reinforcement is connected to a positive terminal (anode). Therefore, electrons (e^-) are forced to travel towards the wire mesh and combine with the water and oxygen available in the vicinity of the concrete specimen. These electrons convert to hydroxyl ions (OH^-) and chloride ions (Cl^-) which are then attracted to the Fe^{++} ions in the reinforcing bar (anode) and cause corrosion. Figure 4.**47** also shows that some of the steel fibers connected to the reinforcing bar act as an anodic region (also called sacrificial anodic region) (Mihashi et al., 2011). These steel fibers are in close proximity to the cathodic region and corrode first. This explains the higher theoritical mass loss of the reinforcing bar by Faraday's law in comparison with the experimental mass loss.

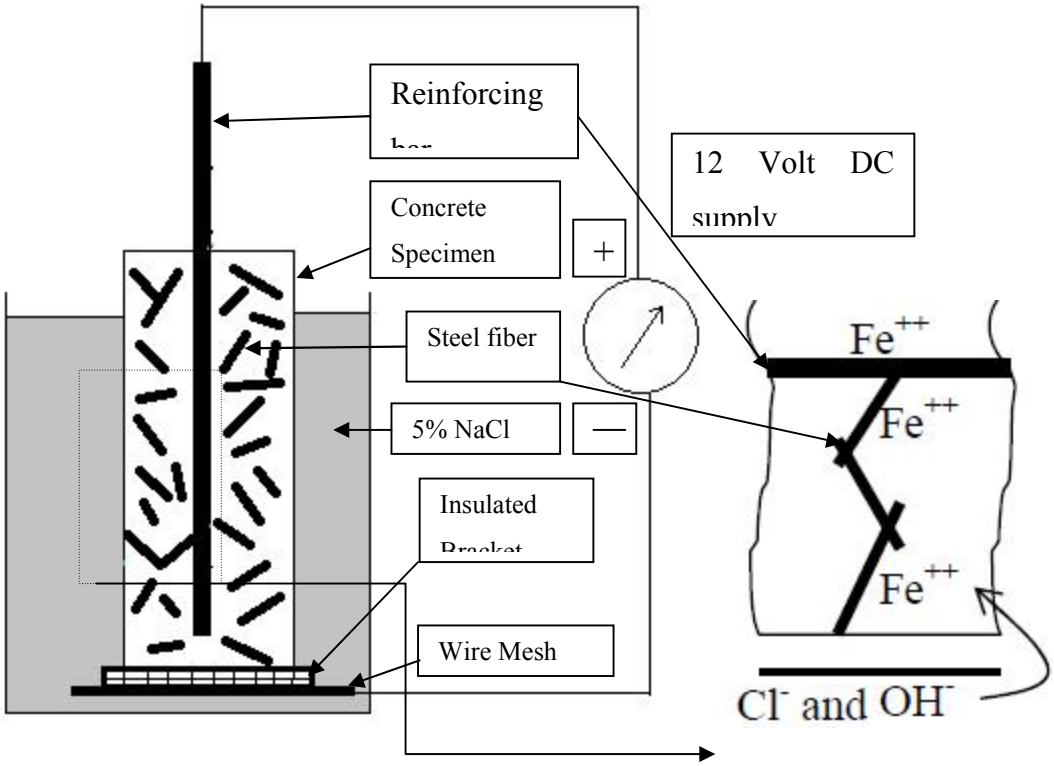

Figure 4.47: Specimen showing accelerated corrosion test

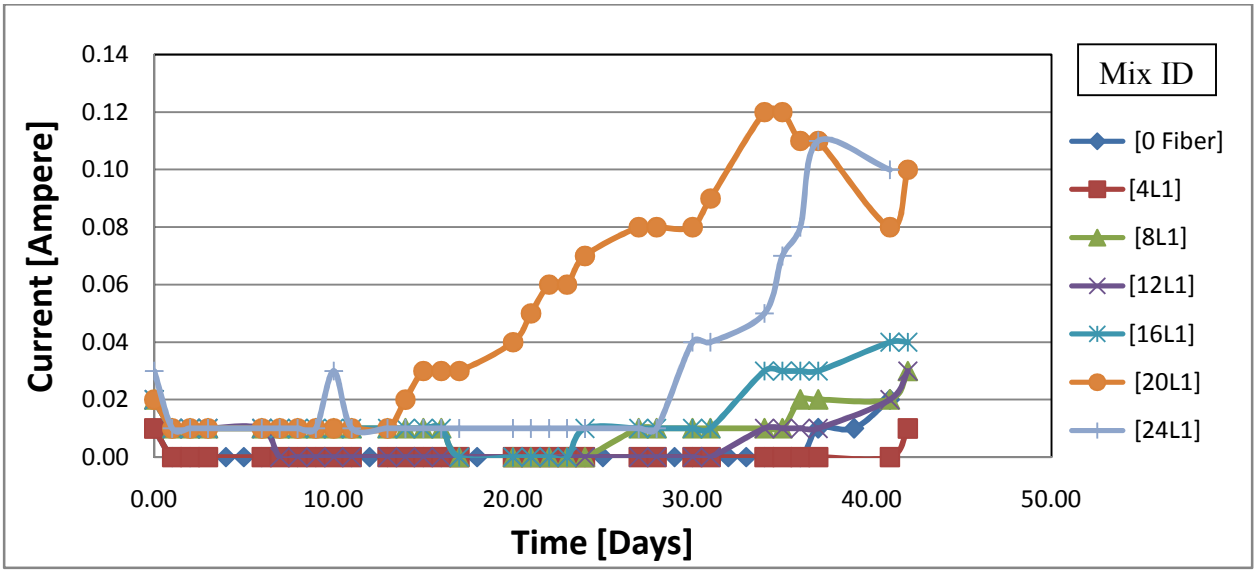

Figure 4.48: Current versus time result for all concrete mixtures with short steel fibers

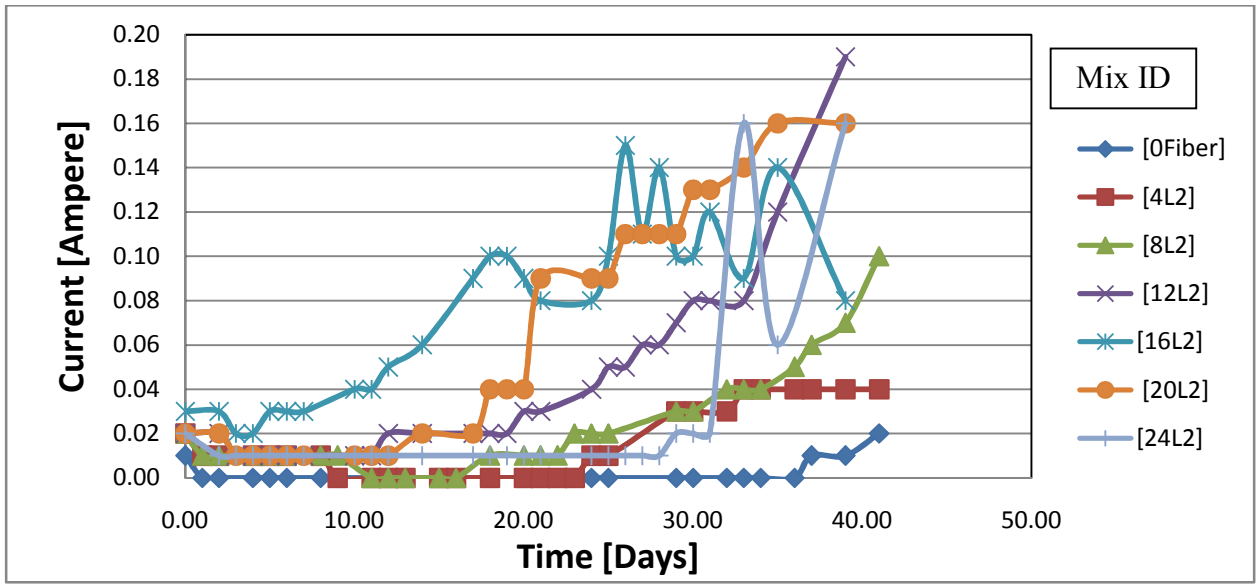

Figure 4.49: Current versus time result for all concrete mixtures with long steel fibers

Figures 4.48 and 4.49 show a decrease in the current after a few days of the experiment, indicating the formation of a passive film around the reinforcing bar which protects it from corrosion. As soon as de-passivation of the protective film starts, the corrosion in a reinforcing bar begins and the rate of corrosion increases significantly along with the increase in the electric current (Hassan et al., 2009).

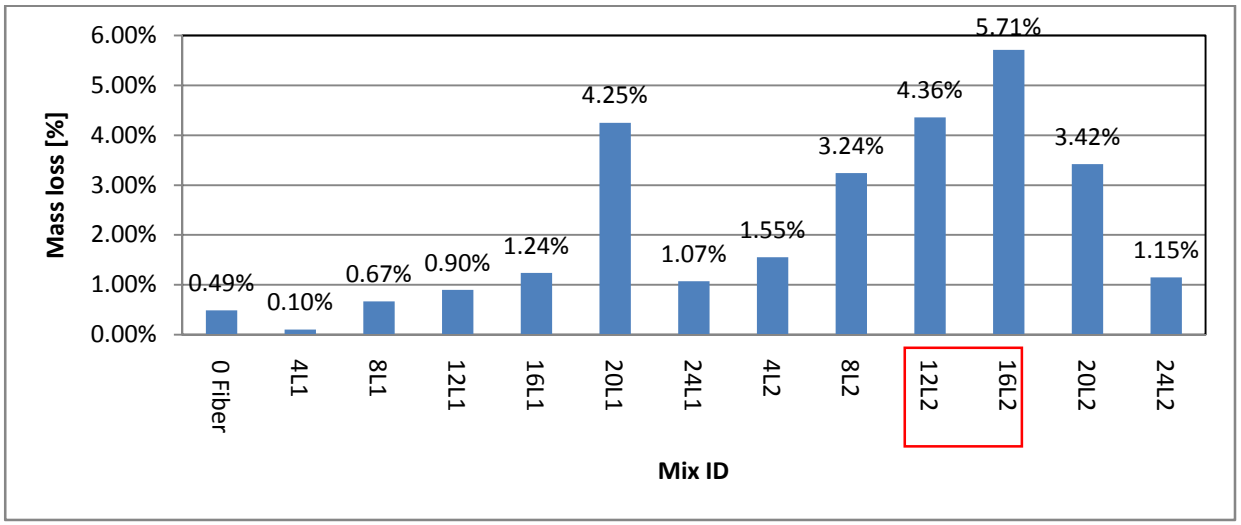

Figure 4.50: Average percentage of experimental mass loss of the reinforcing bar in all concrete mixtures

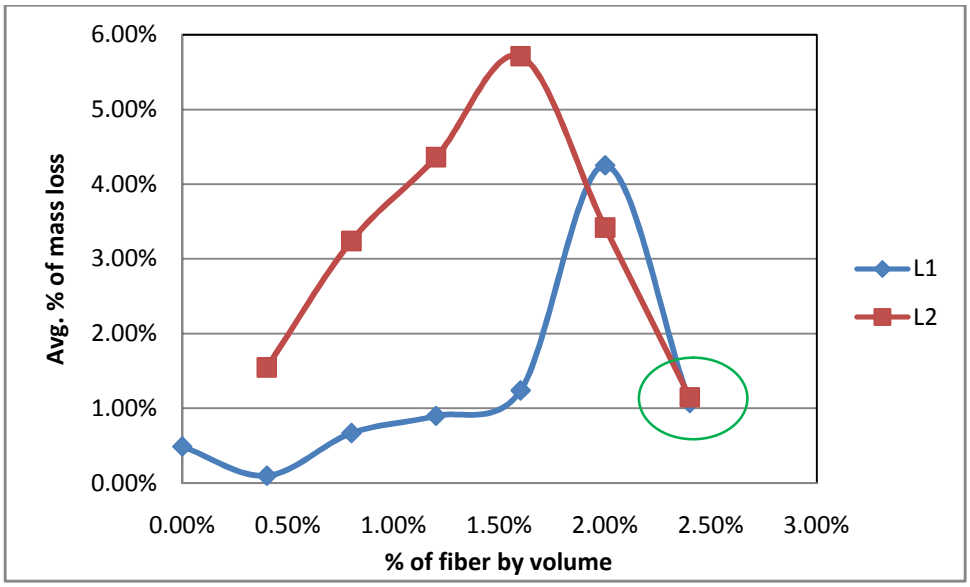

Figure 4.51: Effect of fiber volume fraction on percentage of experimental mass loss of the reinforcing bar in all concrete mixtures

Figures 4.50 and 4.51 show that the experimental percentages of mass loss of the reinforcing steel bar (also called degree of corrosion) for the concrete mixtures with long steel fibers is higher than for the mixtures with short steel fibers. This can also be seen from Figures 4.48 and 4.49, which show that the de-passivation of protective film around the steel bar in the concrete mixture with longer steel fibers occur earlier than in those with a shorter steel fibers at the same percentage of fiber volume fraction. This leads to more corrosion and ultimately a higher mass loss.

Bond strength decrease in concrete mixtures with short steel fibers ranged from 5.58% to 34.93%, whereas for long steel fibers, it ranged from 4.47% to 83.69% (from Figure 4.52 and 4.53). The control sample showed little increase in bond strength; after initial decrease in current, no current was shown during the entire experiment and the de-passivation started only at the end of the experiment. Therefore, an early stage of corrosion occurred in the control sample, which caused some roughness around the reinforcing bar. Also, a frictional component of bond between the reinforcing bar and the concrete was increased, which might increase bond strength. A previous study also showed an increase in the bond strength at an early stage of corrosion (Almusallam et al., 1996).

Another study of corrosion behaviour in concrete showns that the degrees of corrosion and bond strength were governed by many factors such as (Bhargava et al., 2007):

- Electrical properties of mineral in concrete
- Composition of the rebar (bar is assumed to be pure iron)
- Deviation in material properties of concrete
- Corrosion rate
- Cover depth
- Tensile strength and modulus of elasticity of concrete
- Creep coefficient
- Modulus of elasticity of reinforcement plus expansive corrosion product combined

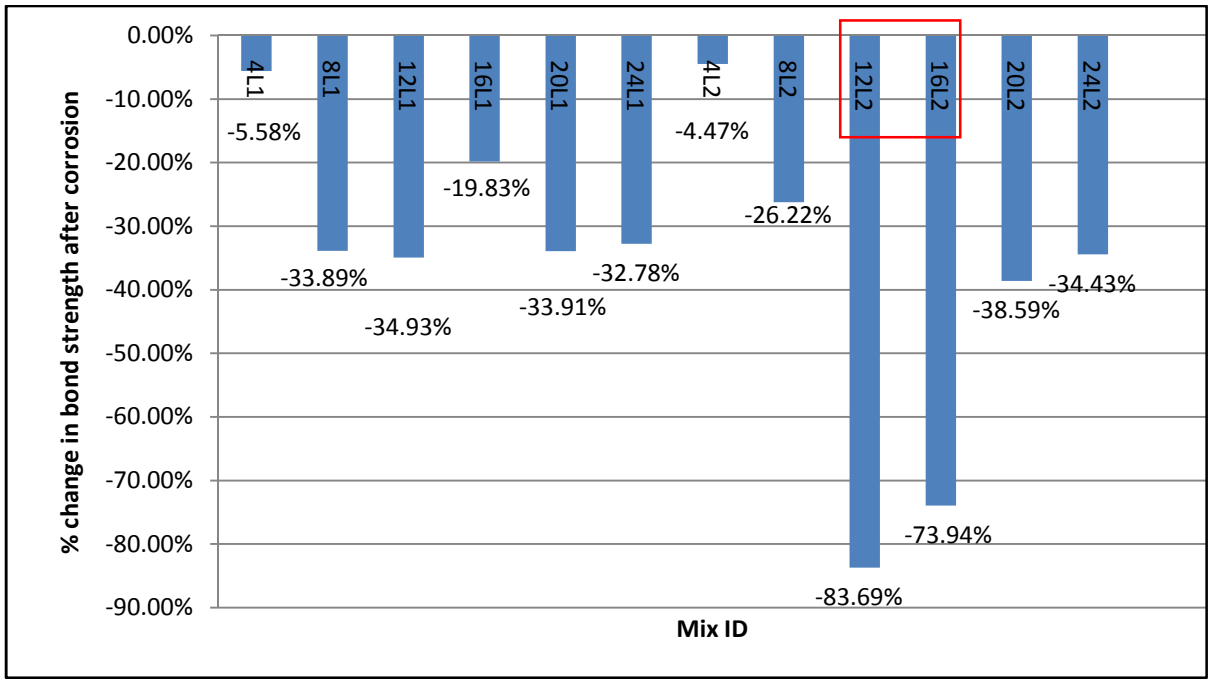

Figure 4.52: Percentage change of bond strength in all concrete mixtures

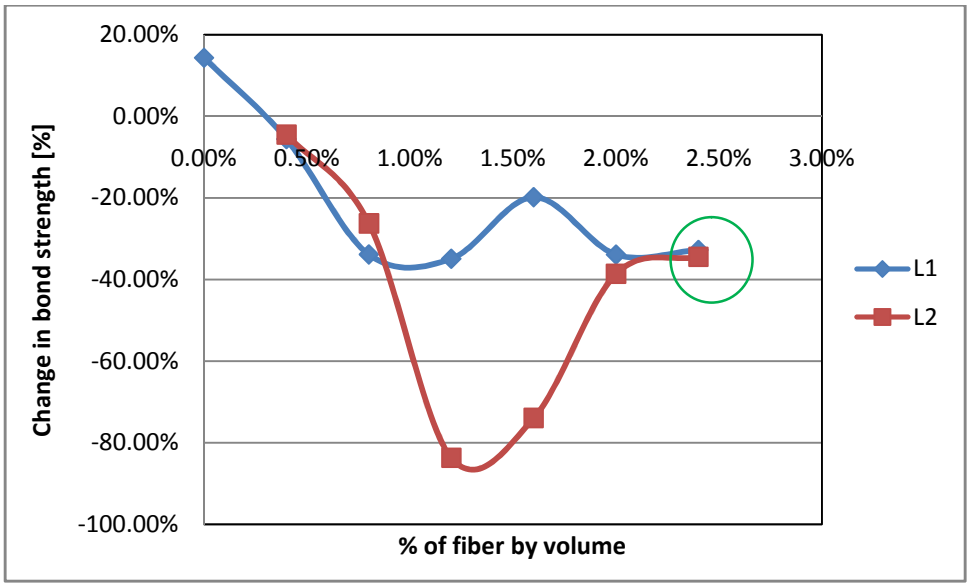

Figure 4.53: Effect of fiber volume fraction on change in bond strength of all concrete mixtures after accelerated corrosion test

Figures 4.50 and 4.52 show that the concrete mixtures with long steel fibers with 1.2% (12L2) and 1.6% (16L2) fiber volume fraction have higher mass loss of reinforcing bar as well as a greater decrease in bond strength. This may be because of insufficient concrete cover depth as well as higher electrical conductivity of the long steel fiber. According to ACI 318-08, for a corrosive environment, the concrete cover for walls and slabs should be higher than 50mm. Previous studies also show that the optimum concrete cover should be more than 50mm for marine exposure (Song & Saraswathy, 2007). As concrete specimen diameter is 100mm, slight inclination as well as misalignment of reinforcing bars in mixture IDs 12L2 and 16L2 decreases the concrete cover depth. Figure 4.54 shows pictures of specimens with insufficient concrete cover depth. Insufficient concrete cover depth initiates the ingression of chlorine ions (Cl-) faster than usual and corrodes the reinforcing bar. In addition, the RCPT test results discussed in the previous section also prove that the longer steel fiber plays an important role in the chlorine ion transfer as the electrical conductivity is high in long steel fiber. The decrease in the bond strength can be verified by the rib profile of the reinforcing bar after pullout test, as shown in Figure 4.55.

However, concrete mixtures with steel fibers (both long and short) in 2.4% fiber volume fraction have identical mass loss and decrease in bond strength as the other mixture IDs for both long and short steel fibers, as shown in Figures 4.51 and 4.53(marked with circle). This suggests that, even

with higher fiber volume fraction, corrosion of the reinforcing bar is limited. The reason behind this is improved alignment of the reinforcing bar. Also, some of the steel fibers, which are randomly distributed in the concrete specimen, might be interconnected with the reinforcing bar as shown in Figure 4.47. These interconnected fibers act as anodes and create a galvanic couple which initiates corrosion (Someh et al., 1997), which reduces the corrosion of the reinforcing bar. These steel fibers are also called sacrificial anodic steel fibers as they sacrifice to reduce the corrosion of the reinforcing bar (Mihashi et al., 2011). In addition, for steel fibers which are not interconnected with the reinforcing bar, the maximum cathodic regions available are limited and the subsquent rate of corrosion is also limited.

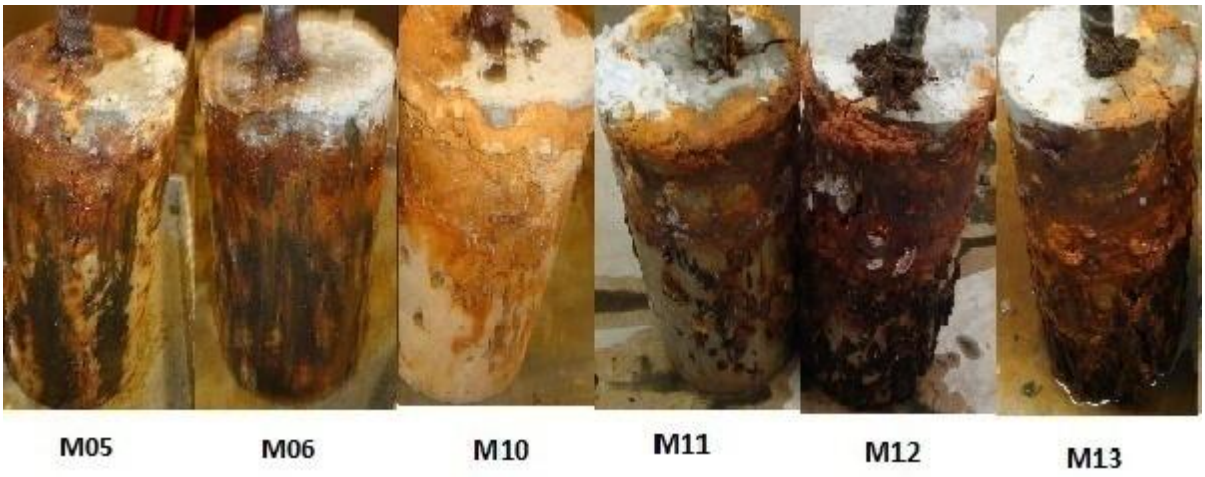

Figure 4.54: Effect on corrosion due to insufficient cover depth (start from left: 16L1, 20L1, 8L2, 12L2, 16L2, and 20L2)

Figure 4.55: Rib profile of rebar after brushing corrosion dust (Mix ID 16L2)

When the steel fiber volume fraction increases, the visual surface corrosion of the steel fiber can be observed, as shown in Figures 4.55 and 4.56.

Figure 4.56: Effect of corrosion on concrete mixtures with shorter steel fibers (start from left: 4L1, 8L1, 12L1, 16L1, 20L1 and 24L1)

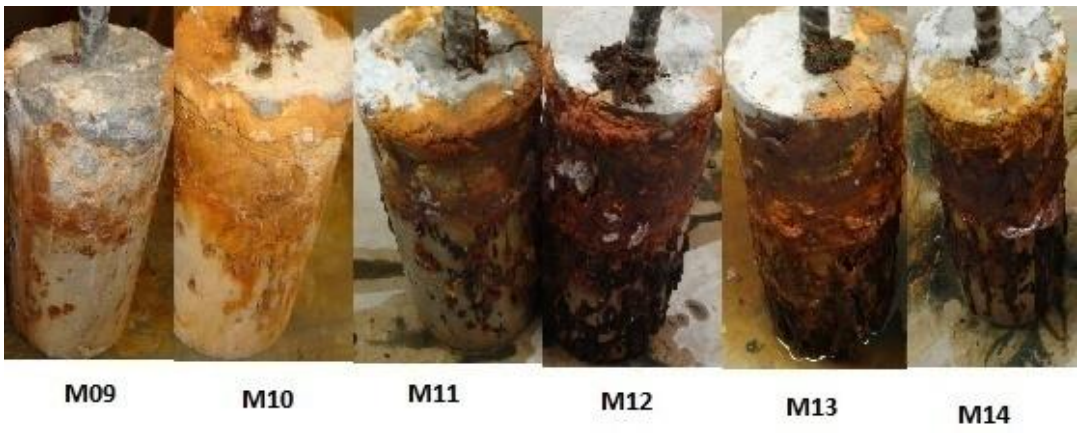

Figure 4.57: Effect of corrosion on concrete mixtures with longer steel fibers (start from left: 4L2, 8L2, 12L2, 16L2, 20L2, and 24L2)

Overall, the concrete mixtures with shorter steel fibers shows more resistance to corrosion than those with longer fibers. The formation of a sacrificial anodic zone by steel fibers helps lower the corrosion. However, concrete mixtures with long steel fibers are sensitive to concrete cover depth and their higher conductivity to electricity has a positive impact on higher corrosion.

Moreover, short steel fibers with a larger surface area to volume ratio are more effectively protected by the alkaline environment of the concrete (Mihashi et al., 2011). There is limited research available to support the experimental results; thorough research is needed in order to understand the phenomenon of corrosion of reinforcing bars in SFRSCC and SFRC.

4.4.5: Freeze-thaw resistance

It has been established that concrete is vulnerable to drastic change in temperature, especially in cold climates. There are several parameters that affect the freezing and thawing of concrete such as w/cm ratio, curing method, use of supplementary cementitious materials (fly ash, slag etc.), pore structure, temperature factors, and the use of air entraining agents.

As mentioned in Chapter 3 of this study, two samples from each concrete mixture were used for the rapid freezing and thawing resistance test. All the concrete prisms were subjected to 300 cycles of rapid freezing and thawing. The changes in weight of the concrete prisms were recorded every 60 cycles. Table 4.9 shows the average percentage of drop in weight, flexural toughness (MPa), and MOR (MPa) value after freeze-thaw cycles.

Figure 4.58 shows the average percentage of weight loss in all concrete mixtures after freeze-thaw cycles. The average percentages of weight loss with respect to number of cycles in concrete mixtures with long and short steel fibers are shown in Figures 4.59 and 4.60, respectively. Figure 4.61 shows the effect of fiber volume fraction on the average percentage of weight drop after freeze-thaw cycles. The concrete mixtures with higher volume fraction (in samples with long and short steel fibers) show the lowest drop in weight (from Figures 4.59 and 4.60). The weight drops in the concrete mixtures with short steel fibers are a little higher than for the mixtures with long steel fibers for the same percentage of volume fraction (from Figures 4.58 and 4.61). All of these graphs prove that there are no significant losses of weight after freeze-thaw cycles for concrete mixtures with steel fibers (both long and short). However, the control mixture without steel fibers shows relatively high loss of weight in comparison with the mixtures containing steel fibers. As volume increases due to freezing water, concrete begins to expand and cause tensile stress. Concrete is known to be weak in tension and these tensile stresses will disintegrate the concrete when they exceed the tensile stress of concrete. This is also confirmed by the study done by Atis and Karahan (2009) in which steel fiber-reinforced concrete incorporated fly ash as

a supplementary cementitious material. Hence, a control mixture without steel fibers shows a relatively higher loss of weight.

Table 4.9: Effect of freeze-thaw cycles on weigh drop, flexural toughness and modulus of rupture

Mix No.	**Mix ID**	**Avg. % of Wt. drop of Concrete Prism**	**% drop in Flexural Toughness**	**% drop in MOR values**
M08/01	0 Fiber	0.29%	N/A	-23.93%
M02	4L1	0.05%	-90.06%	-8.25%
M03	8L1	0.08%	-26.98%	-2.18%
M04	12L1	0.09%	-4.65%	-1.29%
M05	16L1	0.08%	-9.91%	-13.92%
M06	20L1	0.05%	5.39%	14.84%
M07	24L1	0.04%	-6.06%	-0.11%
M09	4L2	0.06%	-61.93%	-6.41%
M10	8L2	0.08%	-39.35%	7.38%
M11	12L2	0.05%	11.74%	-4.18%
M12	16L2	0.04%	-13.51%	-1.65%
M13	20L2	0.05%	-22.37%	7.80%
M14	24L2	0.04%	-15.98%	-16.65%

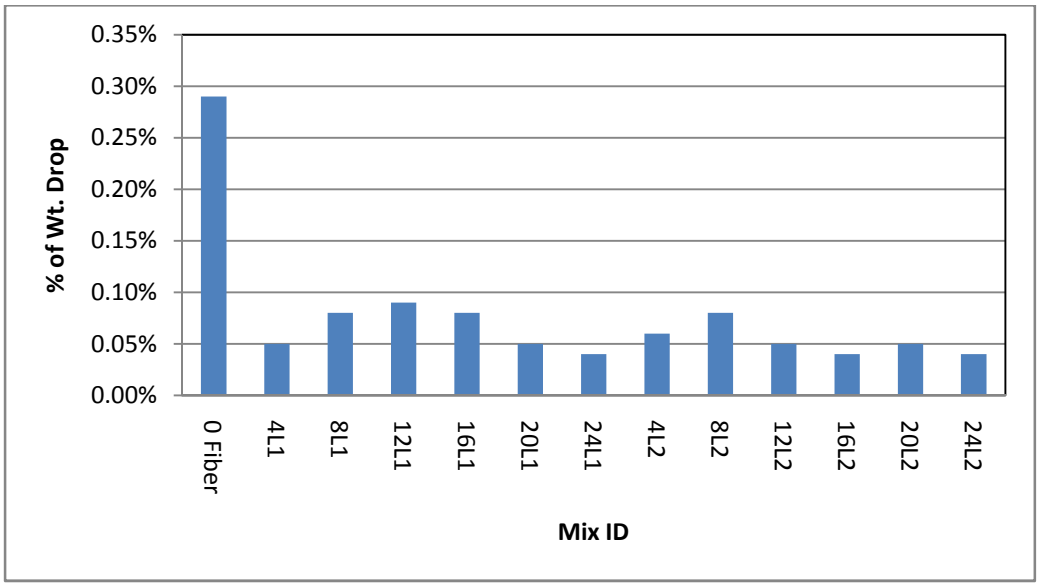

Figure 4.58: Effect of freeze-thaw cycles on weight of the concrete prism

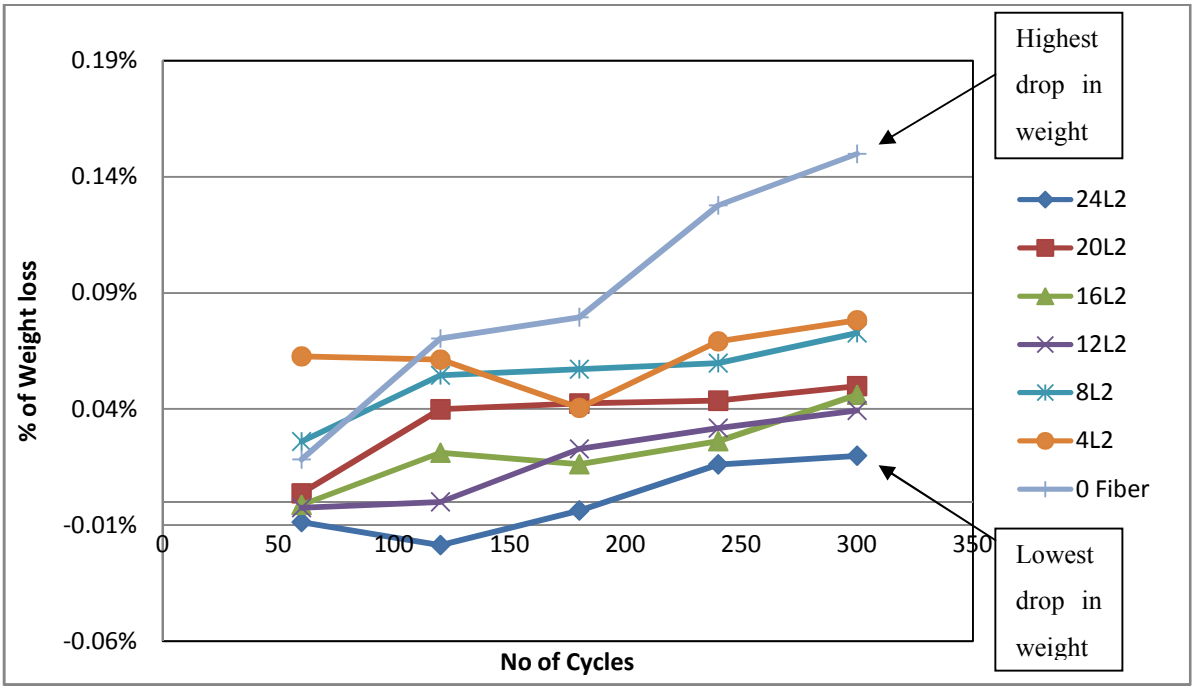

Figure 4.59: Effect of freeze-thaw cycles on percentage of weight loss of the concrete prism with respect to number of cycles on long steel fiber

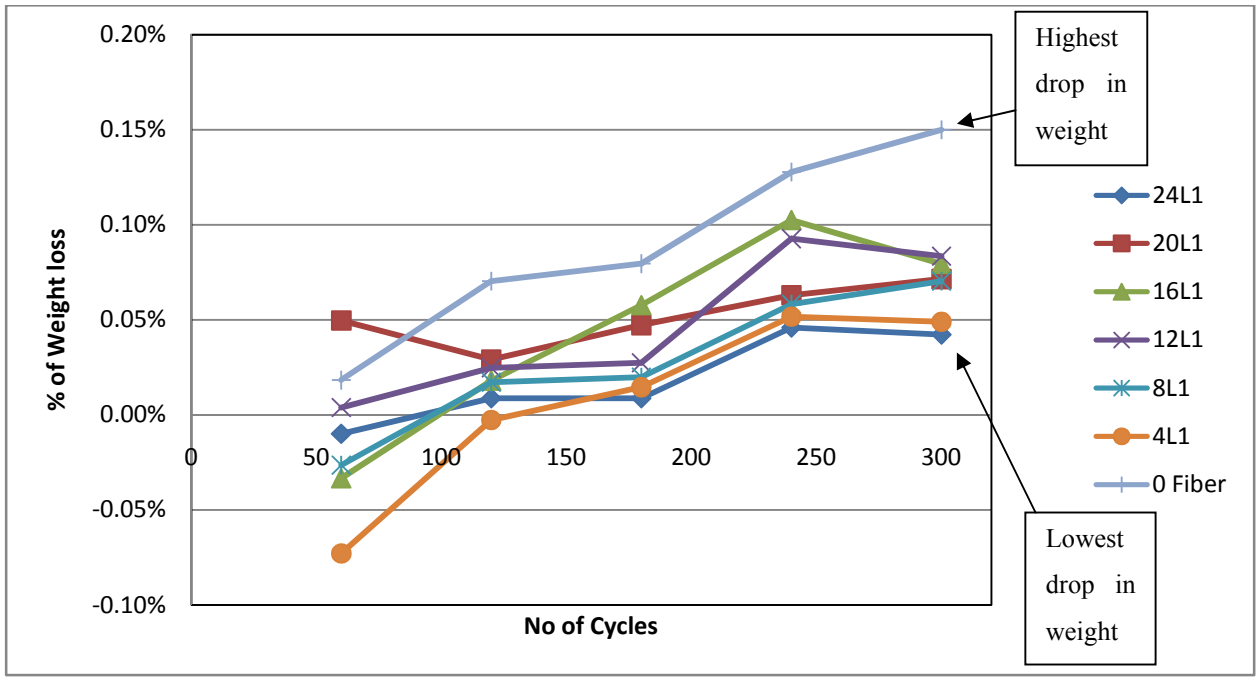

Figure 4.60: Effect of freeze-thaw cycles on percentage of weight loss of the concrete prism with respect to number of cycles on short steel fiber

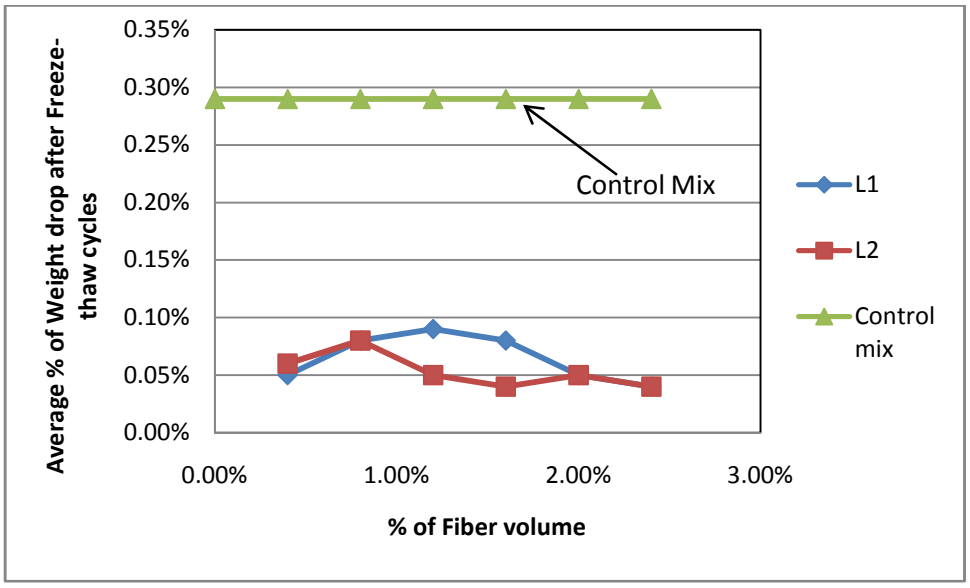

Figure 4.61: Effect of fiber volume fraction on average percentage of weight drop after freeze-thaw cycles

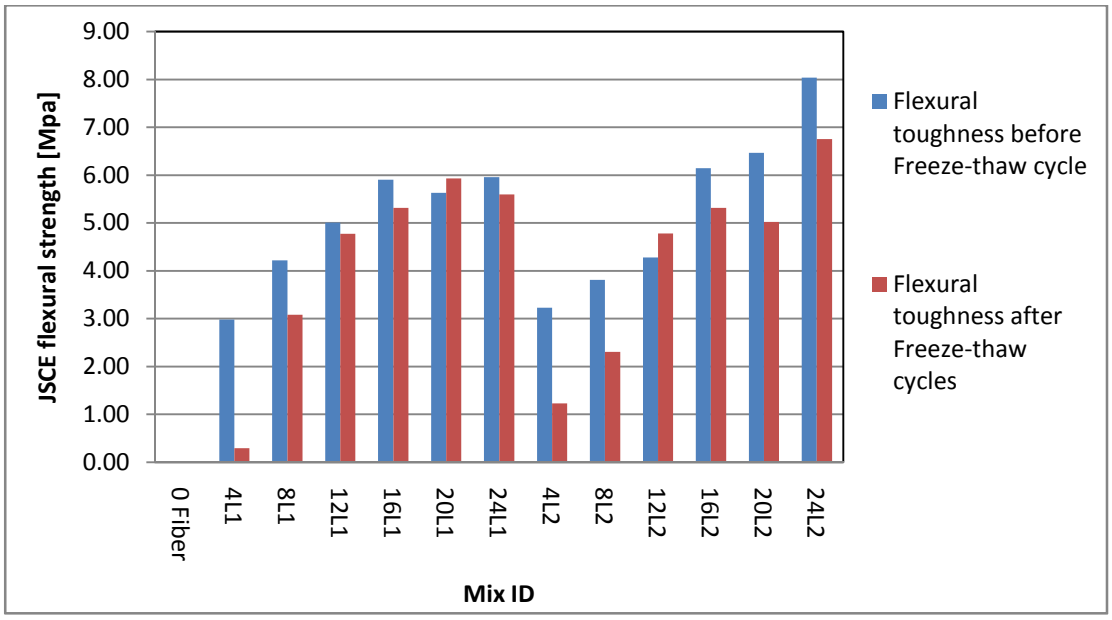

Figure 4.62: Effect of freeze-thaw cycles on JSCE flexural strength for all concrete mixtures

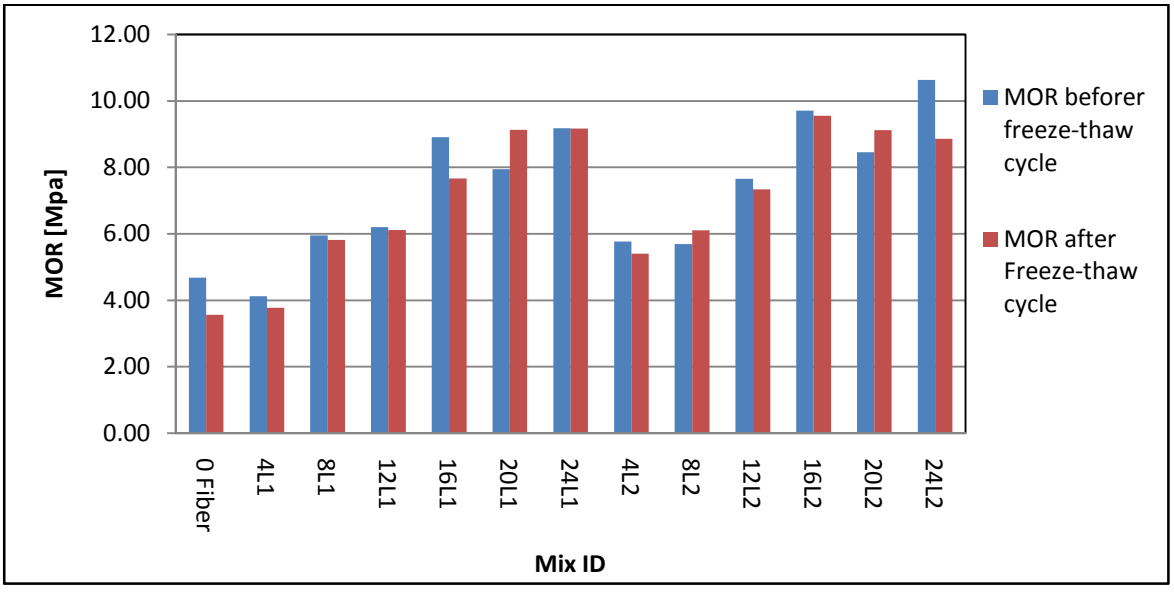

Figure 4.63: Effect of freeze-thaw cycles on MOR for all concrete mixtures

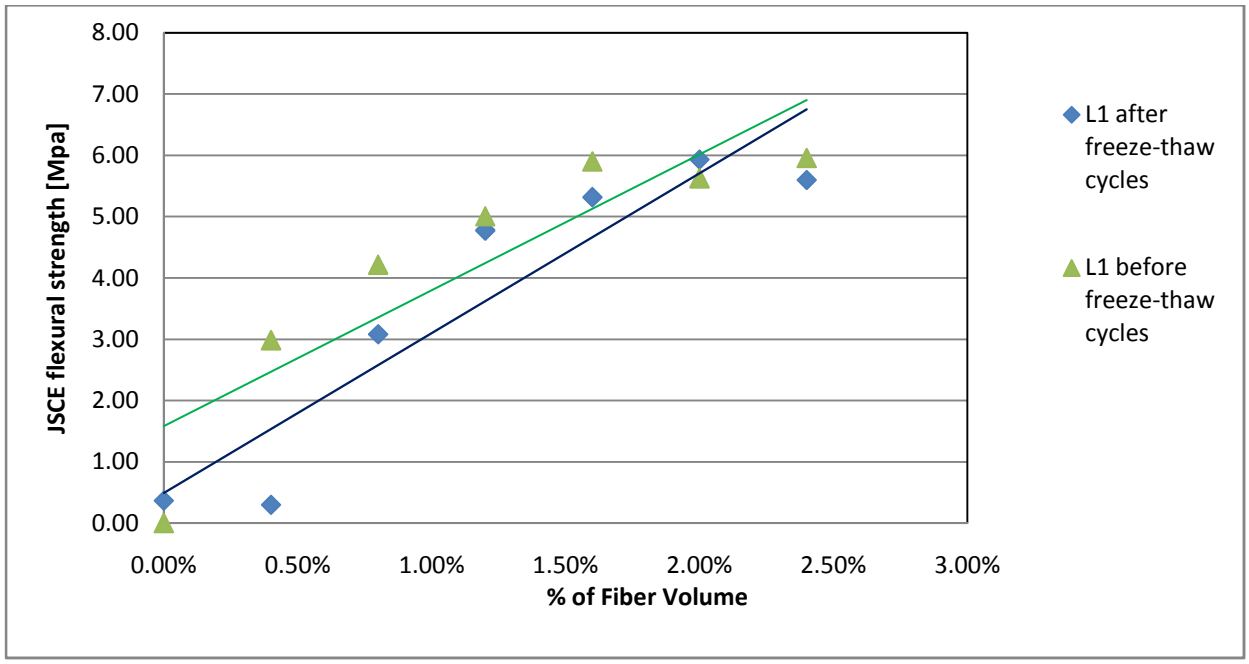

Figure 4.64: Effect of fiber volume fraction on JSCE flexural strength before and after freeze-thaw cycles on concrete mixtures with short fibers

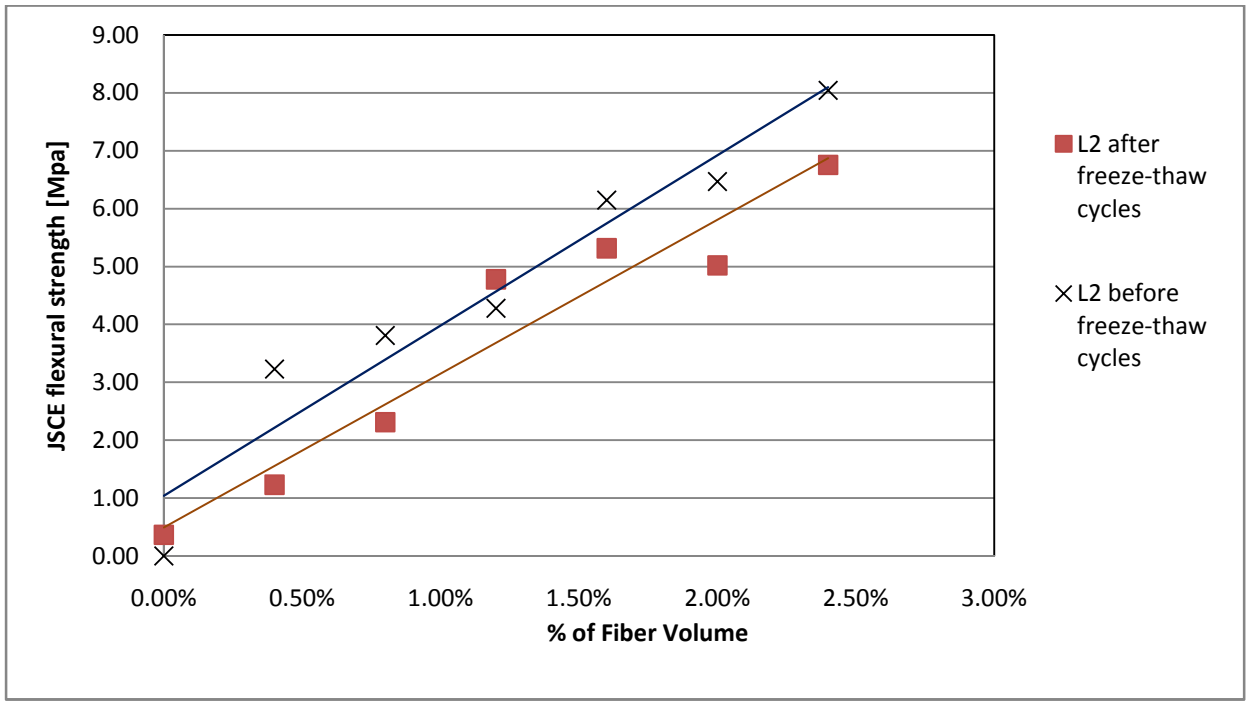

Figure 4.65: Effect of fiber volume fraction on JSCE flexural strength before and after freeze-thaw cycles on concrete mixtures with long fibers

Flexural toughness was calculated after the freeze-thaw cycles using the JSCE-SF4 (Japanese Standard Code). The graphs show a reduction in JSCE flexural strength (MPa) and MOR (MPa) after freeze-thaw cycles for all concrete mixtures (from Figures 4.62 and 4.63). Figures 4.64 and 4.65 show the effect of fiber volume fraction on JSCE flexural strength before and after freeze-thaw cycles. Trend lines in Figures 4.64 and 4.65 clearly indicate the reduction in flexural toughness before and after freeze-thaw cycles as the percentage of fiber volume increases (for both mixtures with long and short steel fibers).

It is well known that when water freezes, it turns into ice and induces a volume increase (about 9%). Due to the increment of volume, concrete begins to expand and causes tensile stress. A random distribution of steel fibers on concrete mixtures restrains this expansion and reduces the freeze-thaw damage to concrete (Atis and Karahan, 2010). Induced tensile stress due to freeze-thaw cycles will be carried by the steel fibers. However, Figures 4.62, 4.64 and 4.65 show drastic reduction of flexural toughness in mixes 4L1and 4L2 (4% of fiber volume fraction). Random distribution of steel fibers in concrete mixtures incorporating 0.4% of fiber volume fraction may not be enough to carry the induced tensile stresses throughout the concrete matrix. This might be the reason for the drastic drop in flexural toughness. Changes in the load-deflection curve for 0.4% fiber volume fraction also show the changes in toughness before and after freeze-thaw cycles (Figures 4.66and 4.67). Load-deflection graphs for all 13 concrete mixtures shown before and after freeze-thaw cycles are presented in Appendix B.

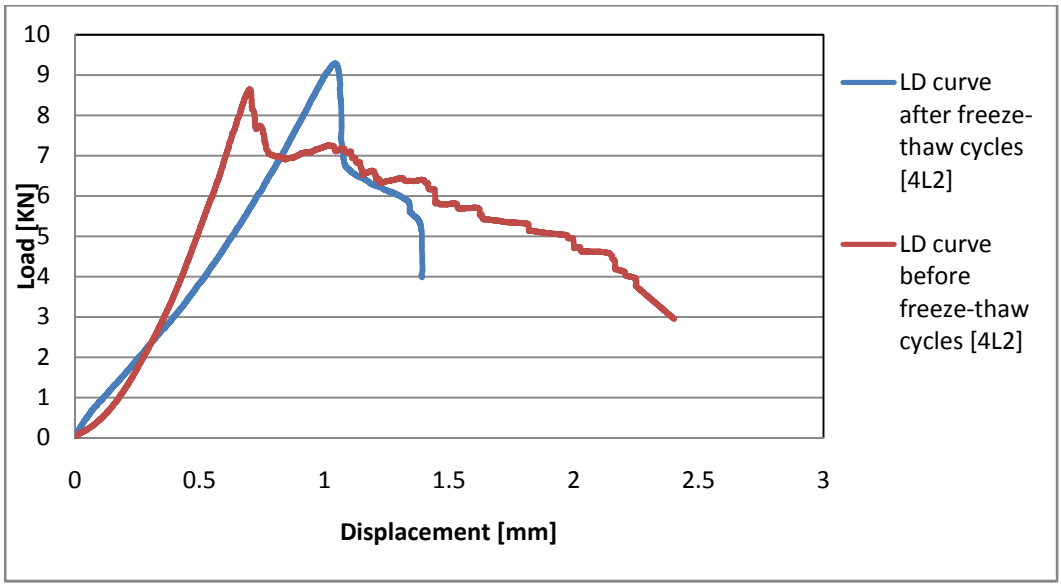

Figure 4.66: Effect of freeze-thaw cycles on flexural toughness of Mix ID 4L2

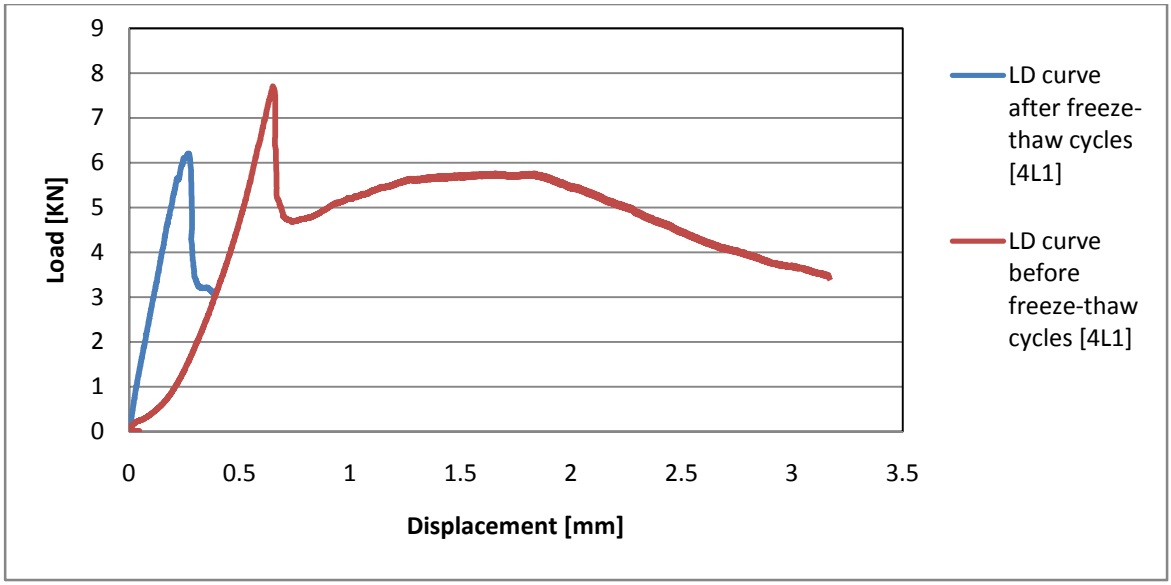

Figure 4.67: Effect of freeze-thaw cycles on flexural toughness of Mix ID 4L1

Summary of durability properties test

Overall, the inclusion of steel fibers in concrete mixtures improved the durability properties of the concrete. The sorptivity index for concrete mixtures with short steel fibers performed better than the ones with long steel fibers with the same percentage of fiber volume fraction. The inclusion of steel fibers in concrete mixtures did not have a significant effect on water absorption and porosity of the concrete mixture compared to control mixtures without steel fibers. A significant effect of chlorine ion permeability has been observed in higher fiber volume fraction (beyond 1.6% fiber volume fraction) in the RCPT test. Formation of a sacrificial anodic zone by steel fibers helped lower the corrosion of the steel reinforcing bar. However, concrete mixtures with long steel fibers have more influence on concrete cover depth as well as higher electrical conductivity.

Chapter 5

CONCLUSIONS AND RECOMMENDATIONS

5.1 Introduction

The application of SFRSCC is gaining momentum in the precast/prestressed concrete industry. Many thin-walled concrete components and sheet piles for water retaining structures, tunnels and sub-basement levels are made from SFRSCC. Incorporating steel fibers into SCC mixtures reduces the sectional dimension. In comparison to normal concrete, the use of SFRSCC provides the following advantages:

- Placement of SFRSCC is much easier in structural elements (such as precast thin-walled elements and prestressed precast sheet piles) with no reinforcing bars and no external vibration.
- The thickness of structural components using SFRSCC can be reduced because of its higher toughness value and improvement of post-cracking behaviour. Thus, SFRSCC provides an economically feasible solution for the construction industry.

Such advantages were the driving force for conducting this study, which was performed to contribute to a better understanding of the durability aspects of SFRSCC. This chapter draws the main conclusions of the current research and presents some recommendations for further research on the topic.

This research was performed to examine steel fiber-reinforced self-consolidating concrete (SFRSCC) by incorporating two different geometric shapes and lengths of steel fiber. A total of 13 concrete mixtures were developed including a control SCC mix without steel fibers. Concrete mixtures were produced with fiber volume fraction ranging from 0% to 2.4%. The workability of the fresh properties of SFRSCC was evaluated as per European Guidelines for self-compacting concrete. The fresh properties were evaluated using slump flow, J-ring, L-Box and V-funnel tests. In addition, mechanical and durability properties tests were performed to evaluate the hardened properties of concrete. To determine mechanical properties, compressive strength, flexural strength and bond strength tests were performed. For durability properties, water

sorptivity, water absorption and porosity, rapid chloride permeability test (RCPT), accelerated corrosion and freeze-thaw cycle tests were conducted.

5.2 Conclusion

The following conclusions can be drawn from this research:

1. Overall, slump flow test diameter, slump flow diameter of J-ring test and L-Box passing ability ratio decrease with an increase in the fiber volume fraction of the concrete mixture.
2. Similarly, slump flow time, slump flow time for J-ring, blocking step BJ, and V-funnel time increase with the increase in the fiber volume fraction of the concrete mixture.
3. The use of short steel fibers improved the workability of the concrete mixture compared to the use of longer ones, as indicated by results from the slump flow, J-ring, V-funnel and L-Box tests. This supports the fact that the longer steel fibers with a hooked end have more detrimental interference with aggregate and can hinder flow more than the short steel fibers.
4. There are no available results for the L-Box passing ratio in concrete mixture with the long steel fibers with a hooked ends. Moreover, the concrete mixtures with the short steel fibers having fiber volume fraction more than 1.2% shows no passing ability. The study results show that only the concrete mixtures with up to 1.2% of volume of the short steel fibers behave as SFRSCC. Therefore, it may be concluded that short fiber volume fraction should not exceed 1.2% for the development of SFRSCC. Also, concrete mixture with long steel fiber with low volume fraction (below 1% of fiber volume fraction) can be use as SFRSCC if use on structural member without reinforcing bar such as precast/prestressed sheet pile.
5. Increases in the compressive strength for all concrete mixtures (including both short and long steel fibers) have been observed as a percentage of fiber volume increase. The increment of the compressive strength up to 12% and 45% in the concrete mixtures with long steel fibers and short steel fibers, respectively. Concrete mixtures with short steel fibers show significant increase in compressive strength compared to those with long steel fibers for same percentage of fiber volume fraction.

6. The addition of steel fibers into concrete mixtures significantly improved their bond strength. Increase in bond strength for all concrete mixtures has been observed as the percentage of fiber volume fraction increased.
7. Steel fibers (both long and short) are more effective in increasing the modulus of rupture (MOR) than the compressive strength. A maximum of 127% increase in the MOR value compared to the control mix has been observed in the concrete mixtures with long steel fibers.
8. An incorporation of steel fibers (both long and short) successfully enhances the toughness of fibrous concrete mixtures. JSCE (Japanese standard code) and PCS (Post Crack Strength method) flexural strength values can be directly used for design purposes because they provide numerical values regarding the allowable stresses at given deflection based on the load-deflection curve.
9. The durability performance of concrete with steel fibers is excellent in terms of the sorptivity index. Overall, the sorptivity index of the short steel fiber concrete mixtures performs better than the long steel fiber mixtures with the same fiber dosages.
10. The addition of steel fibers does not significantly increase water absorption and porosity as compared to the control mixture.
11. Chloride ion penetration increases as fiber volume percentage increases (for both long and short steel fiber mixtures).
12. Steel fibers themselves do not initiate the corrosion as they are not interconnected. Formation of sacrificial anodic zones by steel fibers helps to lower the corrosion of steel reinforcing bars. The depth of the concrete cover is more influential on the corrosion aspect for concrete mixtures with long steel fibers. Therefore, there should be enough clear cover depth to protect the steel reinforcing bar from corrosion.
13. The corrosion of the steel reinforcing bar is more sensitive in the concrete mixtures with long steel fibers because of their higher electrical conductivity.
14. There is no significant loss in the weight of concrete specimens after freeze-thaw cycles for concrete mixtures with steel fibers compared with the control mixture without steel fibers.
15. Reductions in MOR values and JSCE flexural toughness have been observed after freeze-thaw cycles.

16. Overall, steel fibers in concrete mixtures performed well on both mechanical and durability aspects.
17. The short steel fibers in concrete mixtures up to 1.2% volume fraction behave as SFRSCC, whereas the other remaining concrete mixture acts as normal fiber-reinforced concrete.

5.3 Recommendation for further research

Further research is required to:

- Improve the behavior of SFRSCC in special cases accommodating higher volume of steel fibers (less than 1.2%) especially long fibers with hooked ends including wide range of mix proportion.
- Evaluate the rheological parameter using the BML-viscometer, which could quantify the properties of SFRSCC fresh mixture regarding yield stress and plastic viscosity.
- Enhance the fire durability and wear resistance of SFRSCC.
- Investigate means to obtain higher flowability and less segregation in the concrete mixture with a higher volume of steel fibers, and clarify the parameters affecting the flowability of fresh mix.
- Evaluate the effect of other types of steel fibers such as crimped round and flat steel fibers on properties of self-consolidated concrete mixtures.
- Develop performance-based standards and test specifications for SFRSCC regarding the wide range of construction applications as related to mix design, fresh mix properties, pumpability, production method and quality control.

Appendix A: Load deflection graphs for flexural strength test.

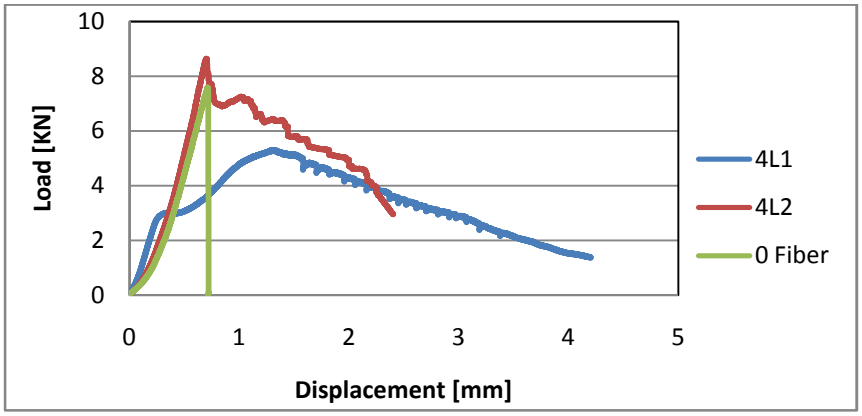

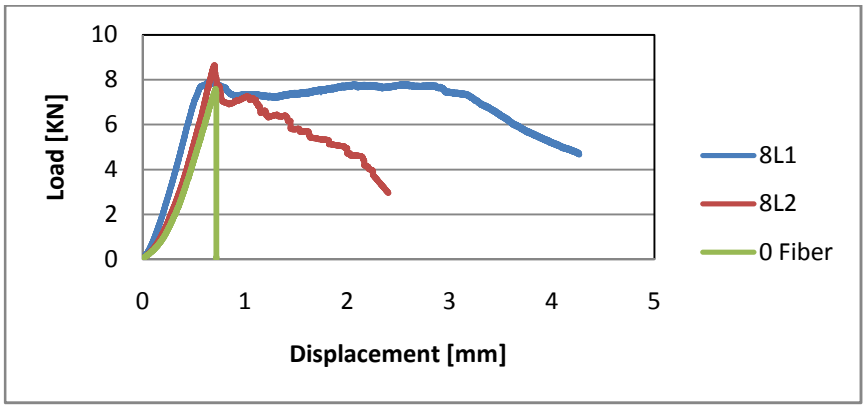

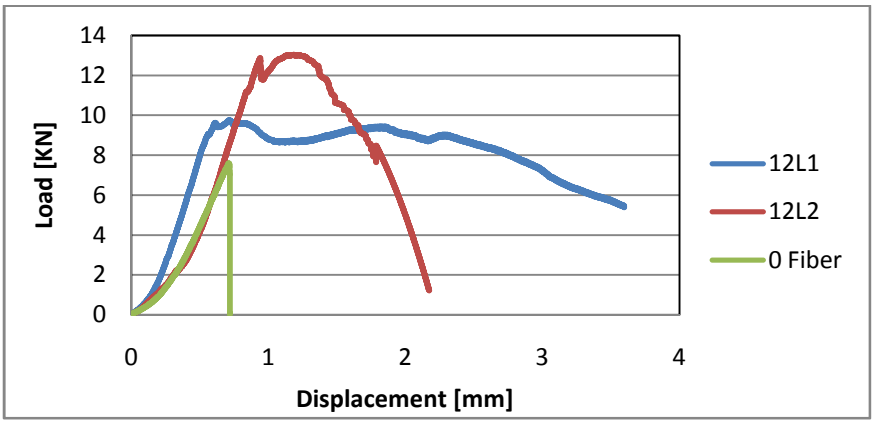

Figures A.1: Load deflection graphs showing comparison between long and short steel fibers containing same amount of fiber volume fraction including control mixture.

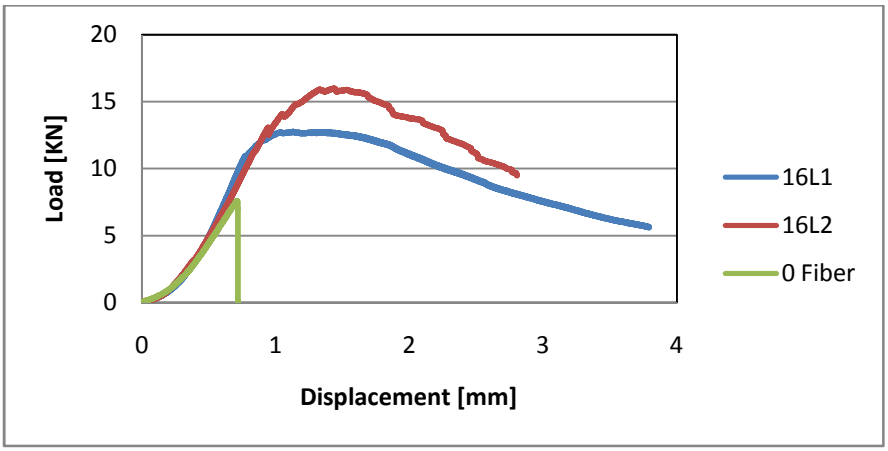

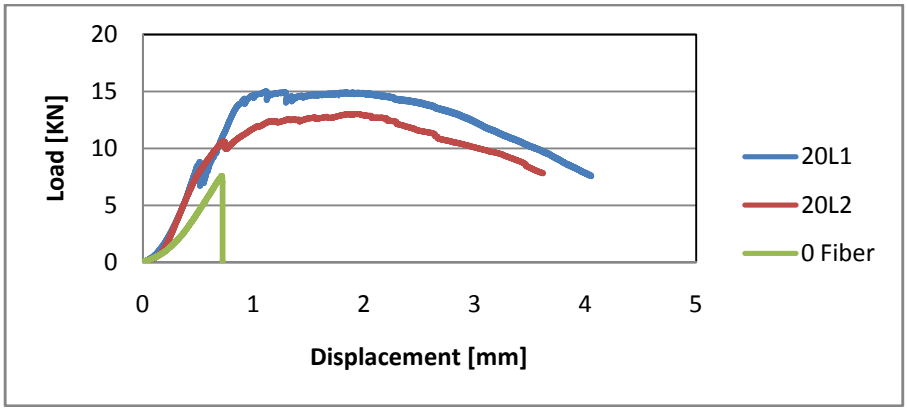

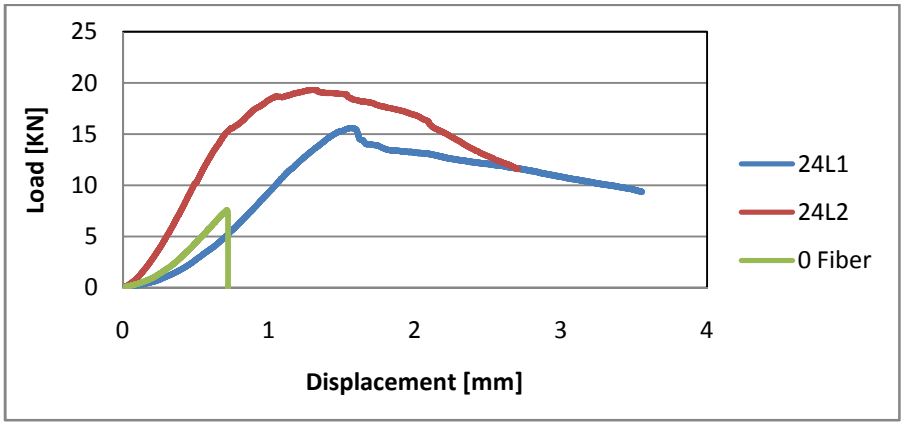

Figures A.2: Load deflection graphs showing comparison between long and short steel fibers containing same amount of fiber volume fraction including control mixture.

Appendix B: Load deflection graphs before and after Freeze-thaw cycles.

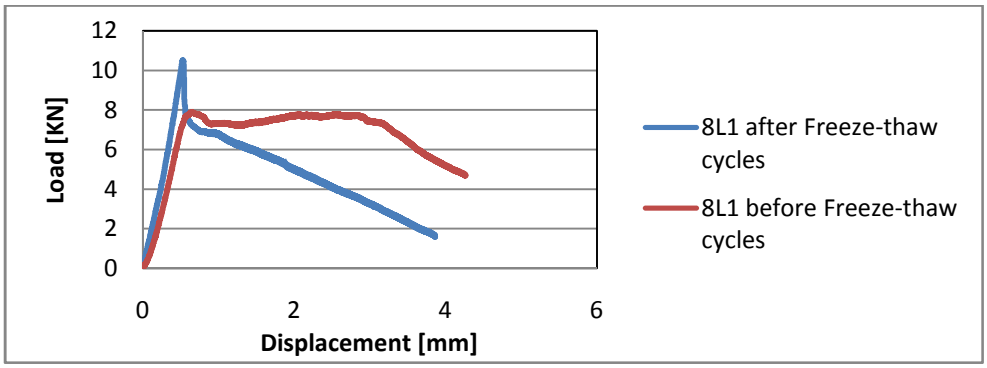

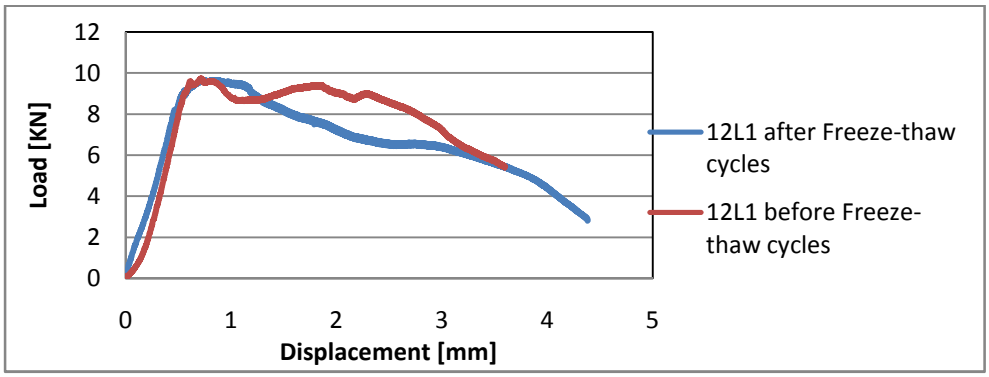

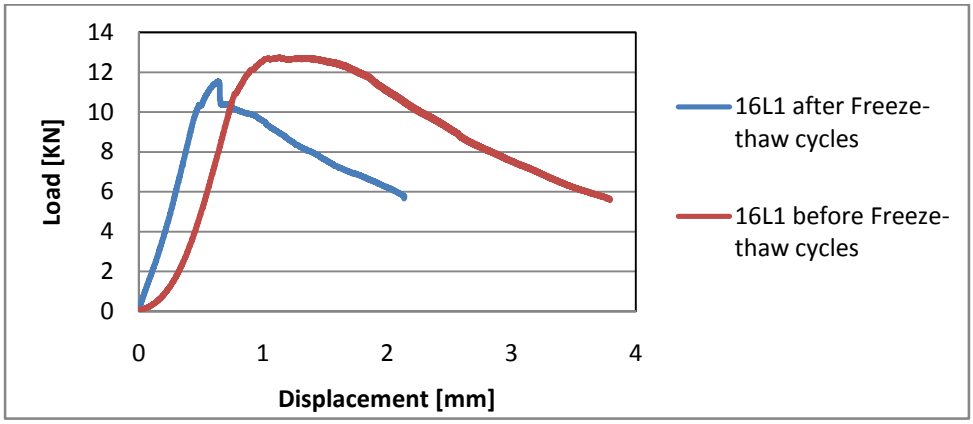

Figure B.1: Load deflection graphs before and after Freeze-thaw cycles showing comparison between same amounts of fiber volume fraction for concrete mixtures with short steel fibers.

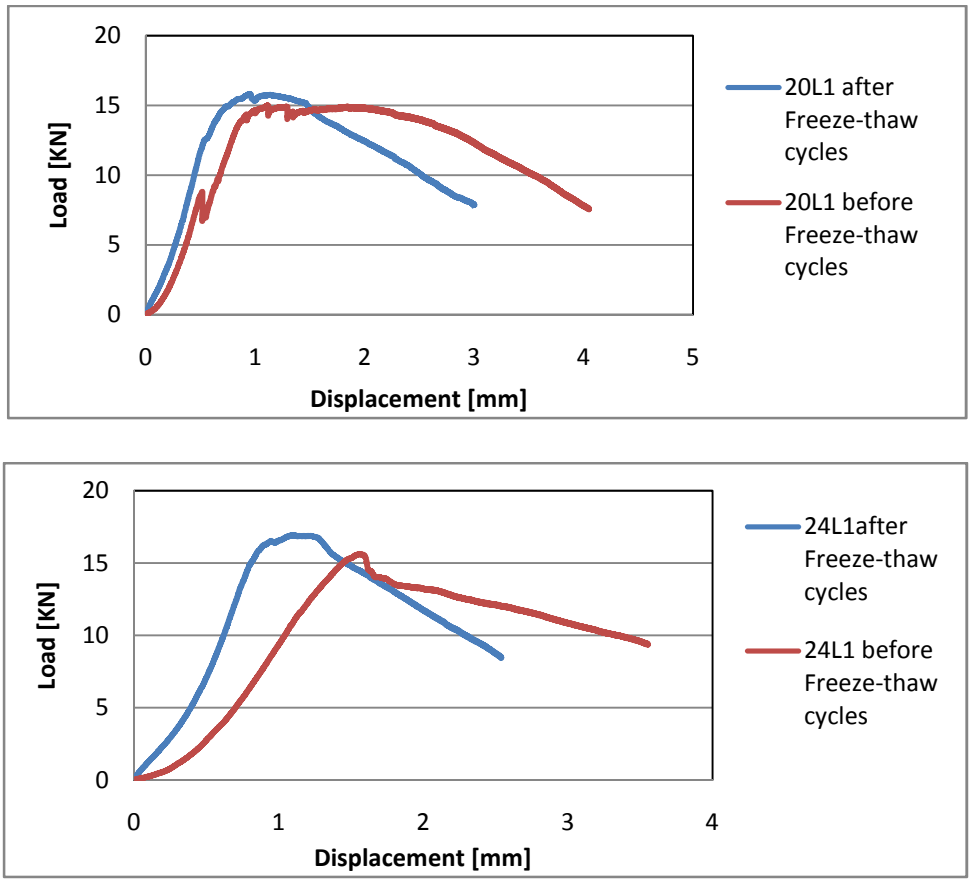

Figure B.2: Load deflection graphs before and after Freeze-thaw cycles showing comparison between same amounts of fiber volume fraction for concrete mixtures with short steel fibers.

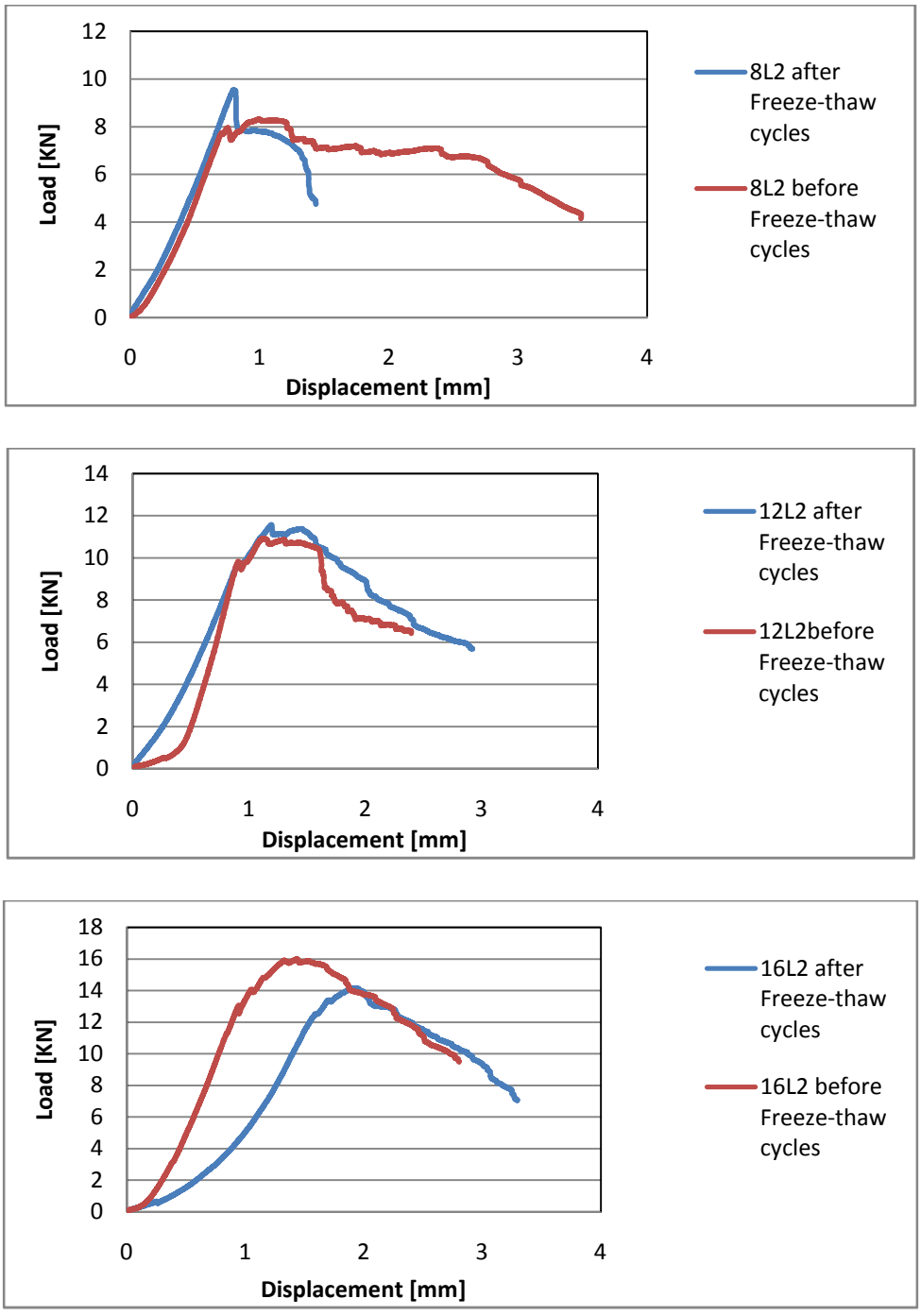

Figure B.3: Load deflection graphs before and after Freeze-thaw cycles showing comparison between same amounts of fiber volume fraction for concrete mixtures with long steel fibers.

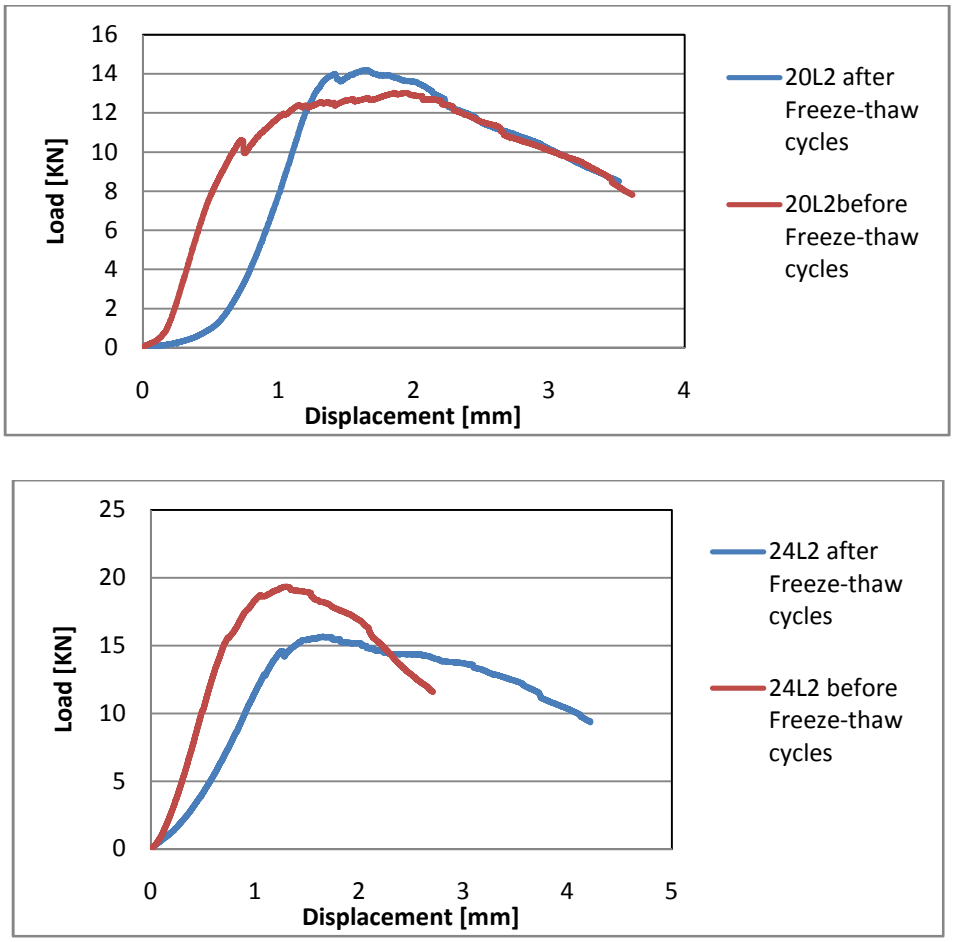

Figure B.4: Load deflection graphs before and after Freeze-thaw cycles showing comparison between same amounts of fiber volume fraction for concrete mixtures with short steel fibers.

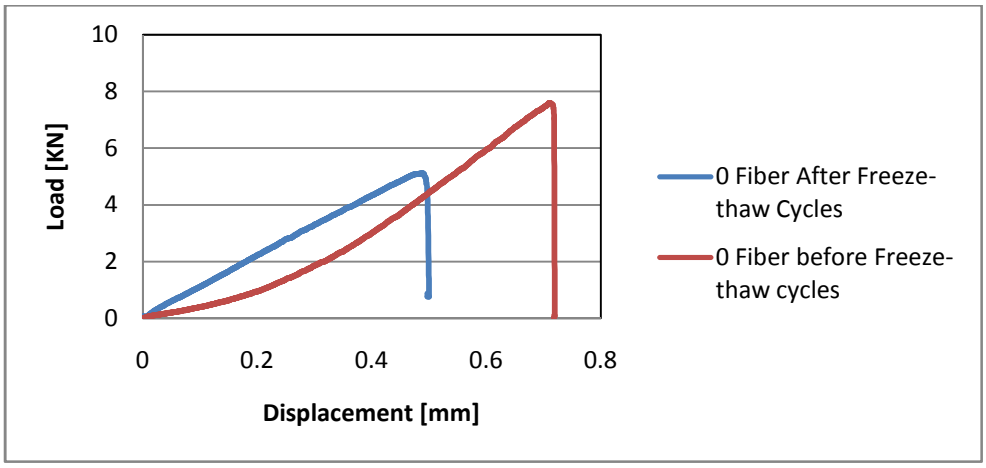

Figure B.5: Load deflection graph before and after Freeze-thaw cycles for control mixture.

References

Abrishami, H., & Mitchell, D. (1992). Simulation of Uniform Bond Stress. *ACI Material Journal , 89* (2), 161-168.

ACI Committe 237R-07. (2007). *Self-Consolidating Concrete.* American Concrete Institute, Farmington Hills.

ACI Committe 318-08. (2008). *Building Code Requirements for Structural Concrete (ACI318-08) and Commentary.* American Concrete Institute, Farmington Hills.

ACI Committe 544.4R-88. (1999). *Design Considerations for Steel Fiber Reinforced Concrete.* American Concrete Institute, Farmington Hills.

ACI Committee 544.1R-96. (2001). *State-of-the-Art Report on Fiber Reinforced Concrete.* American Concrete Institute, Farmington Hills.

Almeida Filho, F., De Nardin, S., & El Debs, A. (2005). Evaluation of the Bond Strength of Self-Compacting Concrete in Pull-out Tests. *4th International RILEM Symposium on Self-Compacting Concrete.* Chicago-U.S.A: RILEM Publication s.a.r.l.

Almusallam, A. A., Al-Gahtani, A. S., Aziz, A. R., & Rasheeduzzafart. (1996). Effect of Reinforcement Corrosion on Bond Strength. *Construction and Building Materials , 10* (2), 123-129.

Ashtiani, M. S., Scott, A., & Dhakal, R. (2011). Mechanical properties of high-strength self-compacting concrete. London: Taylor 7 Francis Group.

ASTM A820-06. (2006). *Standard Specification for Steel Fibers for Fiber-Reinforced Concrete.* American Society for Testing and Materials, Philadelphia, PA.

ASTM C1018-97. (1997). *Standard Test Method for Flexural Toughness and First Crack Strength of Fiber-Reinforced Concrete (Using Beam with Third-Point Loading).* American Society of Testing and Materials, Philadelphia, PA.

ASTM C1202-10. (2010). *Standard Test Method for Electrical Indication of Concrete's Ability to Resist Chloride Ion Penetration.* American society for Testing and Material, Philadelphia, PA.

ASTM C125-11a. (2011). *Standard Terminology Relating to Concrete and Concrete Aggregate.* American Society for Testing and Material, Philadelphia, PA.

ASTM C136-06. (2005). *Standard Test Method for Sieve Analysis of Fine and Coarse Aggregates.* American Society for Testing and Materials, Philadelphia, PA.

ASTM C1585-04. (2004). *Standard Test Method for Measurement of Rate of Absorption of Water by Hydraulic-Cement Concretes.* American society for Testing and Material, Philadelphia,PA.

ASTM C1612. (2009). *Standard Test Method for Passing Ability of Self-Consolidating Concrete by J-ring.* American Society for Testing and Material, Phiuladelphia,PA.

ASTM C39-10. (2010). *Standard Test Method for Compressive Strength of Cylindrical Concrete Specimens.* American Society for Testing and Materials, Philadelphia, PA.

ASTM C617-10. (2010). *Standard Practice for Capping Cylindrical Concrete Specimens.* American Society for Testing and Materials, Philadelphia, PA.

ASTM C666-03. (2008). *Standard Test Method for Resistance of Concrete to Rapid Freezing and Thawing.* American Society of Testing and Materials, Philadelphia, PA.

ASTM C78-10. (2009). *Standard Test Method for Flexural Strength of Concrete (Using Simple Beam with Third-Point Loading).* American Society for Testing and Material, Philadelphia, PA.

ASTM C948-81. (2009). *Standard Test Method for Dry and Wet Bulk Density, Water Absorption, and Apparent Porosity of Thin Sections of Glass-Fiber Reinforced Concrete.* American Society of Testing and Materials, Philadelphia, PA.

Atis, C. D., & Karahan, O. (2009). Properties of Steel Fiber Reinforced Fly Ash Concrete. *Construction and Building Materials , 23* (1), 392-399.

Balaguru, P., Narahari, R., & Patel, M. (1992). Flexural Toughness of Steel Fiber Reinforced Concrete. *ACI Material Journal , 89* (6), 541-546.

Banthia, N. (1994). *Fiber Reinforced Concrete.* Retrieved August 15, 2011, from watancon.com: www.watancon.com

Banthia, N., & Sappakittipakorn, M. (2007). Toughness Enhancement in Steel Fiber Reinforced Concrete Through Fiber Hybridization. *Cement and Concrete Research , 37*, 1366-1372.

Bhargava, K., Ghosh, A., Mori, Y., & Ramanujam, S. (2007). Models for Corrosion-Induced Bond Strength Degradation in Reinforced Concrete. *ACI Materials Journal , 104* (6), 594-603.

Billberg, P. (2010). The Use of Powders to Control SCC Properties. *6th International RILEM Symposium on Self-Compacting Concrete and 4th North American Conference on the Design and Use of SCC, September 26-29*, *2*, pp. 93-105. Montereal.

Boukendakdji, O., Kenai, S., Kadri, E., & Rouis, F. (2009). Effect of Slag on the Rheology of Fresh Self-Compacting Concrete. *Construction and Building Materials , 23* (7), 2593-2598.

Bouzoubaa, N., & Lachemi, M. (2001). Self-Compacting Concrete Incorporating High Volumes of Class F Fly Ash: Preliminary Results. *Cement and Concrete Research , 31* (3), 413-420.

Brzev, S., & Pao, J. (2009). *Reinforced Concrete Design: A Practical Approach.* Toronto: Pearson Education Canada.

Chao, S.-H., Naaman, A. E., & Parra-Montesinos, G. (2006). Bond Behavior of Strand Embedded in Fiber Reinforced Cementious Composities. *PCI Journal , 51* (6), 56-71.

Corinaldesi, V., & Morconi, G. (2011). Characterization of Self-compacting Concretes Prepared with Different Fibers and Mineral Additions. *Cement & Concrete Composites , 33* (5), 596-601.

"Correspondence with MBT (Singapore) pvt .Ltd". (1993). Tayweed Engineering Limited, Australia.

Dhonde, H. B., Mo, Y., Hsu, T. T., & Vogel, J. (2007). Fresh and Hardened Properties of Self-Consolidating Fiber Reinforced Concrete. *ACI Materials Journal , 104* (5), 491-500.

Domone, P. (2006). Self-compacting Concrete: An Analysis of 11 Years of Case Studies. *Cement & Concrete Composites , 28* (2), 197-208.

Edgington, J., Hannant, D., & Williams, R. (1978). *Steel Fiber Reinforced concrete Fiber Reinforced Materials.* Lancaster: Construction Press.

EFNARC. (2002, February). Retrieved 07 14, 2011, from Specification and Guidelines for Self-Compacting Concrete: http://www.efnarc.org

El-Dieb, A. S. (2009). Mechanical, Durability and Microstructural Characteristics of Ultra-high-strength Self-compacting Concrete Incorporating Steel Fibers. *Materials and Design , 30* (10), 4286-4292.

European SCC Guidelines. (2005, May). *The European Guidelines for Self-compacting Concrete, Specification, Production and Use*. Retrieved May 1, 2011, from www.efca.info

Fa-ming, L., & Chuan-qing, F. (2011). *Influence of Freeze-thaw Cycle on SFRC With Different Fly Ash Mixing*. Retrieved 01 10, 2012, from IEEEXplore: www.ieeexplore.ieee.org

Felekoglu, B., Turkel, S., & Altuntas, Y. (2007). Effect of Steel Fiber Reinforcement on Surface Wear Resistance of Self-Compacting Repair Mortars. *Cement and Concrete Compoosites , 29* (5), 391-396.

Goodier, C. I. (2003). Development of self-compacting Concrete. *Structure & Buildings , 156* (SB4), 405-414.

Grace Canada,Inc. (2006, 10 25). Retrieved 07 13, 2011, from W.R. Grace Material Shefty Date Sheet: http://www.civil.umaine.edu/cie111/concrete/ADVACast530msds.pdf

Granju, J.-L., & Balouch, S. U. (2005). Corrosion of Steel Fiber Reinforced Concrete From The Cracks. *Cement and Concrete Research , 35* (3), 572-577.

Grdic, Z. J., Topliocic-Curcic, G. A., Despotovic, I. M., & Ristic, N. S. (2010). Properties of Self-Compacting Concrete Prepared with Coarse Recycled Concrete Aggregate. *Construction and Building Materials , 24* (7), 1129-1133.

Greenough, T., & Nehdi, M. (2008). Shear Behavior of Fiber-Reinforced Self-Consolidating Concrete Slender Beams. *ACI Materials Journal , 105* (5), 468-477.

Grunewald, S. (2004). *Performance-based Design of Self-compacting fiber reinforced concrete.* MG Delft, Netherland: Delft University Press (DUP).

Grunewald, S., & Walraven, J. C. (2001). Parameter-study on the Influence of Steel Fibers and Coarse Aggregate Content on the Fresh Properties of Self-consolidating Concrete. *Cement and Concrete Research , 31* (12), 1793-1798.

Guetti, P. d., Ribeiro, G. O., & Serna, P. (2010). Experimental Study of the Post-Cracking Behaviour of Steel Fiber-Reinforced Self -Compacting Concrete. *Proceeding of the sixth International RILEM Symposium on Self-Compacting Concrete,September 26-29*, (pp. 1261-1271). Montereal.

Hassan, A. A.A., Hossain, K. M.A., & Lachemi, M. (2009). Corrosion Resistance of Self-Consolidating concrete in full-scale reinforced beams. *Cement & Concrete Composites , 31* (1), 29-38.

Hossain, K.M.A., & Lachemi, M. (2008). Bond Behaviour of Self-Consolidating Concrete with Mineral and Chemical Admixture. *Journal of Material in Civil Engineering, ASCE , 20* (9), 608-616.

Ijsseling, F. (1986). Application of Electrochemical Methods of Corrosion Rate Determination to System Involving Corrosion Product Layers. *British Corrosion Journal , 21* (2), 95-101.

Johnston, C. D. (2001). *Advance in Concrete Technology* (Vol. 3). (V. Malhotra, Ed.) Ottawa, Ontario, Canada: International Cenre for Sustainable Development of Cement and Concrete [ICON].

Joorabchian, S. M. (2005). *Durability of Concrete Exposed to Sulfuric Acid Attack.* Toronto, Canada: A theis submitted to the Faculty of Civil Engineering Department in partial fulfillment of the requirements for the degree of Master of Applied Science, Ryerson University.

JSCE SF-4. (1984). *Method of Test for Flexural Strength and Flexural Toughness of Fiber Reinforced Concrete.* Japan Society of Civil Engineers, Tokyo.

Keer, J. (1984). *Concrete Technology and Design: New Reinforced Concretes* (Vol. 2). (R. Swamy, Ed.) London: Surrey University Press.

Khaloo, A., & Molaee, A. (2003). Freeze and Thaw, and Abrasion Resistance of Steel Fiber Reinforced Concrete (SFRC). *Journal of Civil Engineering , 1* (2), 72-81.

Khatib, J. (2008). Performance of Self-compacting Concrete Containing Fly Ash. *Construction and Building Materials , 22* (9), 1963-1971.

Khayat, K. (1999). Working, Testing and Performance of Self-Consolidated Concrete. *ACI Material Journal , 96* (3), 346-353.

Khayat, K., & Roussel, Y. (2000). Testing and Performance of Fiber-reinforced, Self Consolidating Concrete. *Material & Structure , 33* (6), 391-397.

Krstulovic-Opara, N., Watson, K., & LaFave, J. (1994). Effect of Increased Tensile Strength and Toughness on Reinforcing-bar Bond Behavior. *Cement & Concrete Composite , 16* (2), 129-141.

Lachemi, M., Hossain, K.M.A., & Lambros, V. (2005). Shear Resistance of Self-consolidating Concrete Beams - Experimental Investigation. *Canadian Journal of Civil Engineering , 32* (6), 1103-1113.

Lachemi, M., Hossain, K.M.A., Lambros, V., Nikinamubanzi, P.-C., & Bouzoubaa, N. (2004). Self-consolidating Concrete Incorporating New Viscosity Modifying Admixture. *Cement and Concrete Research , 34* (6), 917-926.

Lanier, M., Badman, C., Bareno, J., Baur, K., Boster, C., Calvert, C., et al. (2003). *Interim Guidelines for the Use of Self-Consolidating Concrete in PCI Members Plants.* Chicago,IL: Precast/Prestressed Concrete Institute.

Lankard, D. R. (1986). *Steel Fiber Concrete.* (S. P. Shah, & A. Skarendahl, Eds.) London, England: Elsevier Applied Science Publication LTD.

Liao, W.-c., Chao, S.-H., Park, S.-y., & Naaman, A. E. (2006). *Self-Consolidating High Performance Fiber Reinforced Concrete (SCHPFRC)-Preliminary Investigation.* University of Michigan, Department of Civil and Environmental Engineering, Ann Arbor, MI.

Liu, M. (2010). Self-compacting Concrete with Different Levels of Pulverized Fly Ash. *Construction and Building Materials , 24* (7), 1245-1252.

Mangat, P., & Gurusamy, K. (1988). Corrosion Resistance of Steel Fibers in Concrete Under Marine Exposure. *Cement and Concrete Research , 18* (1), 44-54.

Mehta, P. K., & Monteiro, P. J. (2006). *Concrete-Microstructure, Properties and Materials.* New York: McGraw Hill Companies Inc.

Mihashi, H., Ahmed, S. F., & Kobayakawa, A. (2011). Corroion of Reinforcing Steel in Fiber Reinforced Cementitious Composites. *Journal of Advanced Concrete Technology , 9* (2), 159-167.

Miloud, B. (2005). Permeability and Porosity Characteristics of Steel Fiber Reinforced Concrete. *Asian Journal of Civil Engineering (Building and Housing) , 6* (4), 317-330.

Mindess, S., Young, J. F., & Darwin, D. (2003). *Concrete:Second Edition.* Upper Saddle River, NJ: Pearson Education, Inc.

Nagataki, S., Kawai, T., & Fyjiwara, H. (2010). State of the Art Report on SCC in Japan. *Proceedings of the 6th International RILEM Symposium on Self-Compacting concrete and 4th North American Conference on the Design and use of SCC, September 26-29*, *2*, pp. 3-23. Montreal.

Nataraja, M., Dhang, N., & Gupta, A. (2000). Toughness Characterization of Steel Fiber-reinforced Concrete by JSCE Approach. *Cement and Concrete Research , 30* (4), 593-597.

Nawy, E. G. (1997). *Concrete construction engineering hand book.* New York, Boca Raton: CRC Press.

Nawy, E. G. (2008). *Concrete Construction Engineering Hand Book* (second ed.). Boca Raton, FL, U.S: Taylor & Francis Group.

NYCON CORPORATION. (2010). Retrieved from NYCON REINFORCING FIBERS: http://www.nycon.com/About_Us.php

Oh, S., Noguchi, T., & Tomosawa, F. (1999). Toward Mix Design for Rhelogy of Self-compacting Concrete. In A. Skarendahl, & O. Petersson (Ed.), *Proceeding of the First International RILEM Symposium.* RILEM Publication s.a.r.l.

Okamura, H., & Ouchi, M. (2003). Self-compacting Concrete. *Journal of Advance Concrete Technology, Japan Concrete Institute , 1* (1), 5-15.

Ozawa, K., Sakata, N., & Okamura, H. (1994). Evaluation of Self-Compatibility of Fresh Concrete Using the Funnel Test. *Concrete Library of JSCE , 23* (490), 59-75.

Ozbay, E., Cassagnebere, F., & Lachemi, M. (2010). Effect of Fiber Types on the Fresh and Rhelogical Properties of Self-Compacting Concretes. In K. H. Khayat, & D. Feys (Ed.), *6th International RILEM Symposium of Self-Compacting Concrete and 4th North American Conference on the Design and use of SCC, September 26-29*, *2*, pp. 435-443. Monteral.

Papworth, F. (1997). *Use of Sgteel Fibres In Concrete.* Papworth's Pty Ltd.

Pereira, E., Barros, J., Cunha, V., & Santos, S. (2005). *Compression and Bending Behavior of Steel Fiber Reinforced Self-Compacting Concrete.* University of Minho, Portugal, Department of Civil Engineering.

Ramadoss, P., & Nagamani, K. (2008). Tensile Strenth and Durability Characteristics of High-Performance Fiber Reinforced Concrete. *The Arabian Journal for Science and Engineering , 33* (2B), 307-319.

RILEM Technical Committe 174-SCC. (2000). State-of-the-Art report of RILEM Technical Committe 174-SCC Self-compacting Concrete. In A. Skarendahl, & O. Petersson (Ed.), *RILEM Report 23.* RILEM Publications s.a.r.l.

RILEM Technical Committe TC 145-WSM. (2002). *Workability and Rheology of Fresh Concrete: Compendium Tests.* (P. Bartos, M. Sonebi, & A. Tamimi, Eds.) Cachan, France: RILEM Publications s.a.r.l.

Saak, A., Jennings, H., & Shah, S. (2002). New Methodology for Designing Self-Compacting Concrete. *ACI Materials Journal , 99* (5), 509-512.

Sabir, B., Wild, S., & O'Farrell, M. (1998). A Water Sorptivity Test for Mortar and Concrete. *Materials ans Structures , 31* (8), 568-574.

Sahmaran, M., Yurtseven, A., & Yaman, O. (2005). Workability of Hybrid Fiber Reinforced Self-compacting Concrete. *Building and Environment , 40* (12), 1672-1677.

Sammour, M. M. (2008). *Rheology, Fresh and Hardened Properties Self-consolidating Concrete Utilizing Metal and PVA Polymer Fibers.* Ryerson University, A thesis submitted to the Faculty of Civil Engineering , Toronto, Canada.

Schutter, G. D., & Audenaert, K. (2004). Evaluation of Water Absorption of Concrete as a Measure for Resistance Against Carbonation and Chloride Migration. *Materials and Structures , 37* (9), 591-596.

Schutter, G. D., Bartos, P. J., Domone, P., & Gibbs, J. (2008). *Self Compating Concrete.* Dunbeath, Caithness, Scotland, UK: Whittles Publishing.

Shah, A. A., & Ribakov, Y. (2011). Recent trends in steel fibered high-strength concrete. *Materials and Design , 32* (8-9), 4122-4151.

Shah, S., Ferrara, L., & Kwon, S. (2010). Recent Research on Self-Consolidating Steel Fiber-Reinforced Concrete. *American Concrete Institure, Special publication , 272* (SP272-06), 109-134.

Shutter, G. D. (2005, September). *Guidelines for Testing Fresh Self-Compacting Concretge*. Retrieved 07 14, 2011, from Testing of SCC-Self compacting Concrete: http://www2.cege.ucl.ac.uk

Singh, S., Singh, A., & Bajaj, V. (2010). Strength and Flexural Toughness of Concrete Reinforced with Steel - Polypropylene Hybrid Fibers. *Asian Journal of Civil Engineering (Building and Housing) , 11* (4), 495-507.

Someh, A. K., Saeki, N., & Notoya, T. (1997). Corrosion Protection Shield of Steel Bars, Due to Steel Fibers in Concrete. *American Concrete Institute , 171* (SP171-10), 227-248.

Song, H.-w., & Saraswathy, V. (2007). Corrosion Monitoring of Reinforced Concrete Structures-A Review. *International Journal of Electrochemical Science , 2*, 1-28.

Torrizos, M., Barragan, B., & Zerbino, R. (2008). Physical-mechanical Properties, and Mesostructure of Plain and Fiber Reinforced Self-compacting Concrete. *Construction and Building Materials , 22* (8), 1780-1788.

Tsai, C.-T., Li, L.-S., Chang, C.-C., & Hwang, C.-L. (2009). Durability Design and Application of Steel Fiber Reinforced Concrete in Taiwan. *The Arabian Journal for Science and Engineering , 34* (1B), 57-79.

Vejmelkova, E., Keppert, M., Creszczyk, S., Skalnski, B., & Cerny, R. (2011). Properties of Self-Compacting Concrete Mixtures Containing Metakaolin and Blast Furnace Slag. *Construction and Building Materials , 25* (3), 1325-1331.

Vondran, G. (1991). Application of Steel Fiber Reinforced Concrete. *Concrete International: Design & Construction , 13* (11), 44-49.

Wang, Z., Shi, Z., & Wang, J. (2011). On the Strength and Toughness Properties of SFRC Under Static-dynamic Compresion. *Composites: Part B Engineering , 42* (5), 1285-1290.

Xu, B., & Shi, H. (2009). Correlations Among Mechanical Properties of Steel Fiber Reinforced Concrete. *Construction and Building Materials , 23* (12), 3468-3474.

Yildirim, H., Tezel, O., Sengul, O., & Guner, P. (2010). Design, Production and Placement of Self-Consolidating Concrete. In K. H. Khayat, & F. Dimitri (Ed.), *6th International RIlEM Symposium on Self-Compacting Concrete, September 26-29. 2*, pp. 1333-1340. Montreal: RILEM Publicaiton s.a.r.l.

Zia, P., Nunez, R. A., & Mata, L. A. (2005). *Implementation of Self-Comsolidating Concrete For Prestressed Concrete Girders.* North Carolina State University, Department of Civil, Construction and Envrionmental Engineering , Raleigh, N.C.

Zollo, R. F. (1997). Fiber-reinforced Concrete: An Overview after 30 Years of Development. *Cement and Concrete Composite , 19* (2), 107-122.